University of Kentucky

UKnowledge

2022

PERIPHERAL AND CENTRAL GLUCOSE FLUX IN TYPE I DIABETES

Jelena Anna Juras

University of Kentucky, jjuras19@gmail.com

Author ORCID Identifier:

https://orcid.org/0000-0002-2821-9069

Digital Object Identifier: https://doi.org/10.13023/etd.2022.371

Right click to open a feedback form in a new tab to let us know how this document benefits you.

STUDENT AGREEMENT:

I represent that my thesis or dissertation and abstract are my original work. Proper attribution has been given to all outside sources. I understand that I am solely responsible for obtaining any needed copyright permissions. I have obtained needed written permission statement(s) from the owner(s) of each third-party copyrighted matter to be included in my work, allowing electronic distribution (if such use is not permitted by the fair use doctrine) which will be submitted to UKnowledge as Additional File.

I hereby grant to The University of Kentucky and its agents the irrevocable, non-exclusive, and royalty-free license to archive and make accessible my work in whole or in part in all forms of media, now or hereafter known. I agree that the document mentioned above may be made available immediately for worldwide access unless an embargo applies.

I retain all other ownership rights to the copyright of my work. I also retain the right to use in future works (such as articles or books) all or part of my work. I understand that I am free to register the copyright to my work.

REVIEW, APPROVAL AND ACCEPTANCE

The document mentioned above has been reviewed and accepted by the student's advisor, on behalf of the advisory committee, and by the Director of Graduate Studies (DGS), on behalf of the program; we verify that this is the final, approved version of the student's thesis including all changes required by the advisory committee. The undersigned agree to abide by the statements above.

Jelena Anna Juras, Student

Bret N. Smith, Major Professor

Warren J. Alilain, Director of Graduate Studies

PERIPHERAL AND CENTRAL GLUCOSE FLUX IN TYPE I DIABETES

_____

DISSERTATION
_____

A dissertation submitted in partial fulfillment of the
requirements for the degree of Doctor of Philosophy in the
College of Medicine
at the University of Kentucky

By

Jelena Anna Juras

Lexington, Kentucky

Co- Directors: Dr. Bret N Smith, Professor of Neuroscience and Physiology

and   Dr. Ramon C Sun, Assistant Professor of Neuroscience

Lexington, Kentucky

2022

ABSTRACT OF DISSERTATION

PERIPHERAL AND CENTRAL GLUCOSE FLUX IN TYPE I DIABETES

Diabetes is a complex metabolic disorder, of which high blood glucose concentration is the primary hallmark. Type I diabetes mellitus (T1DM) is characterized by the lack of insulin production, due to a poorly understood autoinflammatory cascade. In the words of historian Barnett "Diabetes may no longer be a death sentence, but for more and more people in the 21st century, it will become a life sentence", making it the focal point of many research groups. It is estimated that around 20 million individuals worldwide live with T1DM.

Effects of long-term chronically elevated blood glucose are not only seen in micro/macro-vascular diseases, retinopathy, peripheral neuropathy, and liver disease but also in the brain as people with T1DM show decreased mental speed and flexibility. Despite these clinical observations, the brain's role in hyperglycemia remains to be elucidated and could be key to identifying potential insulin-independent interventions to alleviate these effects.

In recent years, insulin-independent mechanisms involved in glucose homeostasis have been discovered, most notably the brain's capacity to regulate blood glucose. The brainstem dorsal vagal complex (DVC) is the main neuronal center responsible for parasympathetic visceral regulation and has been identified as a microcircuit that is important for the regulation of blood glucose. The present work, utilizing a designer receptor exclusively activated by the designer drug (DREADDs) system to selectively activate GABA neurons within hindbrain circuitry in vivo, demonstrates hindbrain inhibitory microcircuitry as a key mediator of whole-body glucose levels, indicating the role of the parasympathetic nervous system.

Neuronal function is affected by the brain metabolome, especially as glucose metabolism is highly heterogeneous among brain regions. To accurately capture physiological brain metabolome we developed a method utilizing a high-power focused microwave to euthanize animals, and fix and preserve metabolites. To understand how hyperglycemia modulates the central carbon metabolism of several brain regions (neocortex, hippocampus, and dorsal vagal complex) we employed gas chromatography-mass spectroscopy. Utilizing untargeted metabolomics we found that glucose concentration was significantly elevated across all regions but glycogen and glucose-6-phosphate remained unchanged with hyperglycemia only in DVC. Interestingly pyruvate and lactate were unchanged across all regions indicating that hyperglycemia does not affect anaerobic cellular respiration. Intermediates of the tricarboxylic acid (TCA) malate

and fumarate are significantly decreased with hyperglycemia only in DVC, suggesting that hyperglycemia in DVC preferentially affects TCA cycle. Furthermore, we observed a significant decrease in glutamate across all regions while glutamine and GABA were unchanged, suggesting neurotransmitter regulation disturbance. Stable isotopic tracing of uniformly labeled $^{13}C_6$ glucose was employed to assess carbon flux in different brain regions perturbed by T1DM to understand its effect on glycolysis, tricarboxylic acid cycle, and neurotransmitter synthesis. We found that hyperglycemia results in metabolic reprogramming with a significant decrease in glucose utilization and we demonstrated decrease in immunofluorescent labeling of GLUT2, a neuronal glucose transporter, as well as enzymes pyruvate dehydrogenase and pyruvate carboxylase, responsible for anaplerosis of TCA cycle intermediates, indicating glucose hypometabolism phenotype.

This work is the first of its kind to demonstrate the effects of hyperglycemia not on the brain as a whole but rather on specific regions; neocortex, hippocampus and DVC. We shown heterogeneous effects of hyperglycemia on the central carbon metabolism pathways in the brain, where TCA cycle and neurotransmitter regulation are selectively affected in the DVC. Collectively, these data demonstrate that peripheral hyperglycemia results in glucose hypometabolism in the brain and will serve as a starting point in understanding the brain's metabolic adaptations during hyperglycemia.

KEYWORDS: Type I diabetes (T1DM), hyperglycemia, glucose hypometabolism, $^{13}C_6$ glucose tracer, dorsal vagal complex, brain

Jelena Anna Juras
(Name of Student)

[08/20/2022]
Date

PERIPHERAL AND CENTRAL GLUCOSE FLUX IN TYPE I DIABETES

By
Jelena Anna Juras

Bret N Smith
Co-Director of Dissertation

Ramon C Sun
Co-Director of Dissertation

Warren J. Alilain
Director of Graduate Studies

[08/20/2022]
Date

DEDICATION

To *members of my family who walked the Earth before me. To everyone who took care of my son. To my sister Marina, brother Marinko and my parents Marija and Josip and my husband Felicien.*
Thank you,
Hvala Vam,
Asante Sana.

ACKNOWLEDGMENTS

from ordering the weirdest items to scheduling rooms, and for listening to how awesome it was to grow up in Europe.

Words cannot describe my gratitude towards my parents, Marija and Josip, my sister, Marina, brother-in-law, Zdravko, brother, Marinko, and sister-in-law, Janja. You made the biggest sacrifice of all when you let me follow my dreams and move across the world at the age of 17. For the past 13 years, our time together was always short, and suitcases were never stored away. Hopefully, the next 13 are filled with many hours of laughing and indulging in great food and drinks, with countless visits to the Croatian coast and crossing off the bucket list countries one by one.

Lastly, Felicien, you deserve an honorary Ph.D. for your dedication to me. You put your dreams on hold so that I could follow mine. You became our son's mom and dad and ran our household like a pro. You picked me up after days of failed experiments countless times and you didn't let me give up. Asante sana!

TABLE OF CONTENTS

LIST OF TABLES

LIST OF FIGURES

CHAPTER 1. INTRODUCTION

1.1   *Glucose homeostasis*

Glucose is a six-carbon monosaccharide, a simple sugar that is obtained from food sources and has two main roles: (a) a primary metabolic fuel and (b) the necessary substrate for biosynthesis of all major classes of biomolecules [1]. Glucose levels are tightly regulated and kept within a narrow physiological range. Low levels of blood sugar called hypoglycemia can quickly result in a coma and be fatal if not treated. High levels of blood glucose called hyperglycemia are not as acute of a concern but left untreated it will lead to severe complications.

Glucose homeostasis is a multi-organ task, conventionally presented as primarily orchestrated by counterbalancing the effects of two peptide hormones: insulin and glucagon. After a meal, glucose-sensing cells in the pancreas trigger the release of insulin, which results in the mobilization of insulin-dependent glucose receptors to the plasma membrane and glucose uptake into the cells. Furthermore, the rise in insulin concentration also inhibits gluconeogenesis, the endogenous glucose production by the liver. The largest reservoir of glucose in the body is in the liver and skeletal muscle in the form of glycogen. Upon a period of fasting, glucose sensing cells in the pancreas respond to low levels of circulating glucose in the bloodstream and trigger the release of glucagon, which results in glycogenolysis, the breakdown of glycogen and production of glucose from a short-term storage form.

In contrast to the canonical view of two hormones balancing glucose homeostasis in recent years, we have come to appreciate insulin-independent mechanisms involved in glucose homeostasis [2–7], most notably the brain's capacity to regulate blood glucose [8–15]. More about the brain's role will be discussed in subsequent sections.

1.2   Uptake of glucose

Glucose is an obligatory metabolite for all cells and must be up taken into the cell via facilitated diffusion or through sodium co-transport [16]. Pharmacological inhibition of glucose transporters results in a decrease of glucose in the brain to less than a 5% of pre-drug treatment values, suggesting that glucose transporters are responsible for more than 95% of all glucose transfer across the blood-brain barrier (BBB) [17]. Furthermore, the importance of glucose transporters in the brain is highlighted by conditions like glucose transporter 1 (GLUT1) deficiency syndrome which leads to severe deterioration of brain metabolism in addition to seizures and delayed development [18].

Human and canine experiments show that upon ingestion of an oral glucose load under normal conditions about 1/3 is extracted by the liver, 1/3 by muscle and fat and 1/3 by red blood cells and the brain [19]. Glucose transporters play a crucial role in supplying glucose to the brain. The demand for glucose in the brain is not constant and it changes in response to brain activity [20]. In order to enter the brain, glucose must be translocated across the BBB. That is accomplished by the high-affinity GLUT1 transporter expressed in endothelial cells. The main driving force for GLUT1-mediated glucose uptake is the concentration gradient, plasma glucose concentration is about 4-6mM, while brain interstitial glucose concentration is 1-2 mM as measured by microdialysis [21]. In addition to GLUT1-mediated glucose uptake in the brain, there are other GLUT transporters, but we will only focus on GLUT1 and three other GLUT transporters. GLUT2 is a low-affinity glucose transporter found in hepatocytes, the pancreas, and the brain. It has been shown that GLUT2 together with glucokinase (GCK) serves as a glucose sensor [22]. In the brain, GLUT2 has been shown to be localized across multiple brain cell types, including neurons and glia [23–27]. GLUT3 is expressed in the brain and predominantly in neurons [16]. GLUT4 is an insulin-sensitive glucose transporter, meaning its insertion onto the plasma

membrane is regulated by insulin concentration and plays a vital role in glucose homeostasis. GLUT4 is most abundantly expressed in adipose tissue, skeletal muscle, and the heart, but its presence has also been shown in the brain [16].

1.3   *Central Carbon Metabolism*

Glucose is crucial in many cellular processes, including adenosine 5'-triphosphate (ATP) production, oxidative stress management, and synthesis of neurotransmitters and neuromodulators. Catabolism of glucose through the process of glycolysis, tricarboxylic acid cycle (TCA), and subsequent oxidative phosphorylation results in the generation of ATP, the cell's energy currency. The major energy demand in the brain is for neuronal signaling, including resting membrane potential, action potential generation, and glutamate cycling to name a few [28]. The other major role of glucose is in terms of anabolism and being a building block. Therefore, the simplest way to define central carbon metabolism would be as a series of reactions that transforms carbon, including glycolysis, gluconeogenesis, the pentose pathway and the TCA cycle (Fig 1.1).
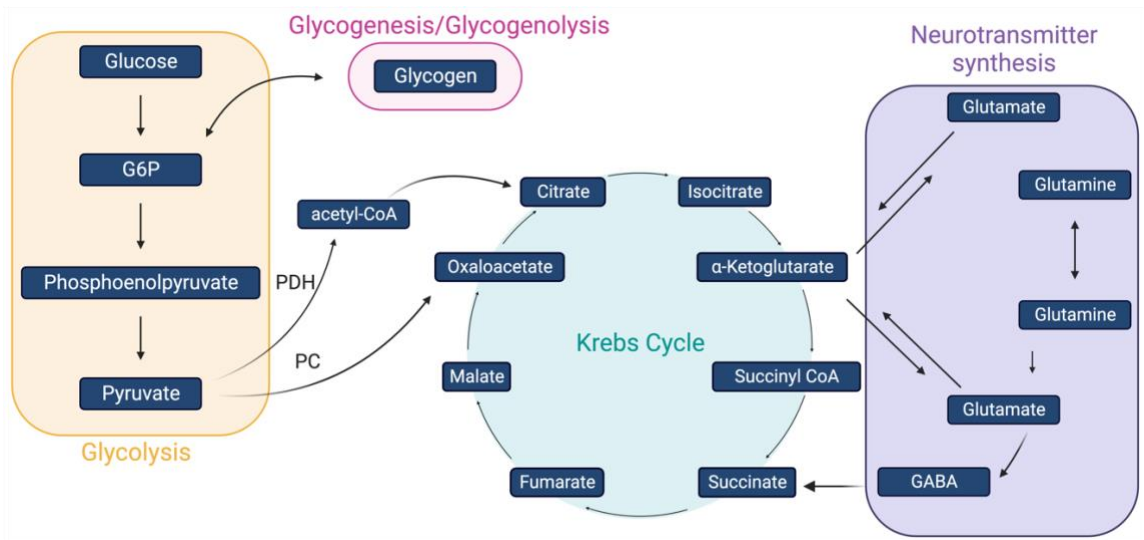
Figure 1.1 Schematic of central carbon metabolism

1.3.1 Glycolysis, TCA cycle and neurotransmitters

After uptake of glucose into the brain via GLUT transporter, glucose phosphorylation into glucose-6-phosphate (G6P) is the first irreversible step of glycolysis, trapping the glucose inside of the cell [29]. G6P is the central hub for carbohydrate metabolism as it has many possible fates (progression through glycolysis, entry into pentose phosphate pathway, glycogen synthesis, hexosamine pathway, or glucose production) [30]. The main end product of glucose oxidation through glycolysis is pyruvate, which then enters into the TCA cycle.

The product of glycolysis, pyruvate is first converted to acetyl coenzyme A (acetyl-CoA), and then it enters into the TCA cycle. Through several steps and by utilizing enzymes, the TCA cycle not only oxidizes carbohydrates, proteins and fats buy also produces several intermediates which play a central role in processes like gluconeogenesis, lipolysis, and neurotransmitter synthesis [31]. Carbons from glucose are metabolized to acetyl-CoA via pyruvate dehydrogenase (PDH) or to oxaloacetate via

pyruvate carboxylase (PC) [32], which are the two main ways for replenishment of TCA cycle intermediates.

Neurotransmitters are responsible for the transfer of signals between neurons and other cells. Glucose-derived neurotransmitters include acetylcholine, glutamate, and GABA [28].

1.3.2   Key enzymes

1.3.2.1   Pyruvate Dehydrogenase (PDH)

Upon release of pyruvate from glycolysis, PDH is responsible for its conversion into acetyl-CoA. The PDH-catalyzed reaction is necessary for oxidation of glucose, and generation of ATP [33].

1.3.2.2   Pyruvate Carboxylase (PC)

Oxaloacetate is generated from pyruvate via PC. Early work on cell culture showed that PC is expressed exclusively in astrocytes and not neurons [34–36], however, Hassel and Brathe have shown that neuron pyruvate carboxylation occurs at a substantial rate [37]. PC is critical for anaplerosis of the TCA cycle intermediates and therefore gluconeogenesis and fatty acid synthesis.

1.4   Diabetes

Diabetes is a complex metabolic disorder, of which high blood glucose concentration or hyperglycemia is the primary hallmark. The American Diabetes Association characterizes Type I diabetes mellitus (T1DM) by a lack of insulin, while type II (T2DM) is characterized by resistance to insulin [38]. T1DM is a result of loss in beta cells (β-cells) of the pancreas. The cause of the autoinflammatory cascades that destroy pancreatic beta cells remains to be fully understood (for a complete review of the current

understanding of autoimmune cascades that result in loss of insulin producing β-cells see [39]). T1DM is considered one of the most common disorders occurring affecting children [39]. In the words of historian Barnett "Diabetes may no longer be a death sentence, but for more and more people in the 21st century, it will become a life sentence", making it the focal point of many research groups [40]. It is estimated that around 1.2 million people under the age of 20 worldwide live with T1DM [41].

The first mentions of the disease with symptoms of frequent urination and a sweet taste of urine are as old as 2000BC. Before modern capacities of metabolomics, ancient Chinese doctors described utilizing ants to evaluate the urine with high content of glucose, as ants were attracted to sweet urine [42–44]. Today, diabetes is diagnosed when fasting blood glucose levels are above 125 mg/dL, or if levels are above 200mg/dL at any point in the day [45].

1.4.1 Effects of Hyperglycemia on Peripheral Tissue

1.4.1.1 Liver

The liver is the metabolic hub of the human body and is exposed to higher nutrient levels than any other peripheral tissue [46]. Its role is vital in metabolism due to its unique task as the gatekeeper of glucose storage, release, and redistribution, keeping the levels of glucose between fed and fasted states in a narrow range. Entry of glucose into the portal vein stimulates net hepatic glucose uptake and hepatic glycogen synthesis but not whole-body glucose clearance [47–49].

As mentioned earlier, in healthy individuals, intake of food will result in modest hyperglycemia and an increase in glycogen production in the liver. In individuals with poorly controlled T1DM intake of food results in drastic hyperglycemia and impaired hepatic glycogen accumulation [50–53]. Furthermore, patients with T1DM and T2DM as

6

well as animal models show increased hepatic glucose production [54–57]. It has been shown that without glucose stimulation, glucokinase (GCK) sequesters in the nucleus of hepatocytes where it is bound to a regulatory protein. Upon stimulation, GCK dissociates from the regulatory protein, enters the cytosol, and catalyzes the phosphorylation of glucose in hepatocytes [58,59]. Furthermore, data shows GCK suppression by 60% in diabetics patients [60]. Other groups have shown decreases in animal models in GCK, phosphofructokinase and pyruvate kinase activity [61]. T1DM also results in impaired hepatic glycogenolysis, the breakdown of glycogen [53,62]. Hepatic glycolytic activity is greatly affected by hyperglycemia as hepatic glycolytic flux is only 40% of the vehicle-treated hepatocytes, and glucose cycling is twice the rate of that in vehicle-treated hepatocytes [63]. Hepatic pyruvate metabolism in diabetes is also disturbed as pyruvate is being utilized for gluconeogenesis rather than energy generation through ATP and oxidative phosphorylation; thus the TCA cycle is greatly affected [64].

1.4.1.2 Skeletal Muscle

In a healthy individual, excess glucose after digestion is uptaken by liver which results in inhibition of muscle glucose uptake [19]. Patient biopsy and [3-^{3}H] glucose infusion suggests accumulation of free glucose in the muscle [68]. Furthermore, it has been shown that hyperglycemia increases the expression and activity of glutamine synthetase, leading to accelerated glutamine production in skeletal muscle [69]. Because insulin is necessary for muscle protein turnover [65,66], insulin deficiency results in profound changes in mitochondrial function as measured by proteomics, specifically mitochondrial uncoupling, lower ATP production, compromised cellular energy status, and greater ROS emission in the muscle [67]. While insulin deficiency results in increased protein synthesis in the splenic region, insulin deficiency does not affect protein synthesis levels in muscle [66]. Metabolomic study of skeletal muscle in patients revealed profound

effects of T1DM on several key metabolic pathways like glycolysis and gluconeogenesis, Krebs cycle, lipid metabolism and immune response [70].

1.4.2 Effects of Hyperglycemia on the Brain

Glucose is the preferred energy substrate of the brain [20]. To prevent possible toxicity of glucose, the brain's glucose levels are kept at about 20% of that of plasma. Glucose availability in the brain is critical for the proper function of neurons, as glucose demand increases following neuronal signaling [71].

Effects of chronically elevated blood glucose are not only seen in micro/macro-vascular diseases, retinopathy, peripheral neuropathy, and liver disease but also in the brain, as people with T1DM show decreased mental speed and flexibility [39,72,73]. Given those results, neuroanatomical studies were carried out utilizing structural magnetic resonance to investigate how hyperglycemia affects the brain, and it was found that in children, hyperglycemia regionally alters gray matter volume, where decreased gray matter volume was reported in bilateral occipital and cerebellar regions, while increased gray matter volume was found in inferior prefrontal, insula, and temporal pole regions [74]. However, brainstem regions were not studied.

Regarding glucose uptake/transport, the experiments using radiatively labeled glucose in animal models have divergent results; therefore, it is ambiguous whether glucose transport across the BBB is affected by hyperglycemia. The difference in results could be due to differences in methodology (i.e. length of hyperglycemia and measurement in conscious vs. unconscious animals). Some groups reported a decrease in glucose transport with hyperglycemia [75–78], while others reported no change [79,80].

1.5 Brain Glucose Regulation

As described by Stubbs et al., the first evidence of brain glucose regulation was presented by Dr. Claude Bernard in 1854 when he reported that a lesion in the floor of the fourth ventricle in rabbits altered blood glucose levels [81]. As mentioned earlier, diabetes decreases glucose clearance and induces insulin resistance in the muscle tissue, but that only accounts for about 10% of the dysfunctional glucose clearance observed in diabetes in muscle [83,84]. Therefore, decreased glucose clearance seems to be the culprit of failed central metabolism. Since the 19th century, the body of knowledge about the brain's glucoregulatory role has steadily increased. Several lines of evidence have emerged suggesting the brain has two main roles in glucose regulation; 1) coordinate the magnitude and timing of insulin response [85] and 2) coordinate insulin-independent mechanisms to reduce glucose production [86–92]. Insulin-independent mechanisms are responsible for about 50% of glucose disposal [88]. Especially important evidence comes from experiments where insulin or glucose were injected into the hypothalamus and resulted in decreased peripheral glucose levels and increased insulin sensitivity [10,11]. Furthermore, deletion of insulin or leptin receptors in hypothalamus results in glucose intolerance and insulin resistance [14,93].

The brainstem dorsal vagal complex (DVC) is the main neuronal center responsible for parasympathetic visceral regulation and includes the nucleus tractus solitarius (NTS), dorsal motor nucleus of the vagus (DMV), and area postrema (Fig 1.2). Within the DVC, the NTS receives viscero-sensory information, integrates the information with signals from other brain areas, and projects to preganglionic parasympathetic motor neurons in the DMV to control visceral functions [94,95]. Previous members of Smith Lab have shown that the DVC plays a key role in regulating peripheral glucose concentration, as injection of fibroblast growth factor 19 (FGF19) into the DVC of hyperglycemic mice

9

significantly lowers blood glucose levels while increasing the activity of GABAergic neurons in normoglycemic mice significantly increases peripheral glucose metabolism [15,96,97]. It is unknown how the alteration of GABAergic neurons in hyperglycemia affects the peripheral blood glucose levels, which is the body of work presented in Chapter 3.
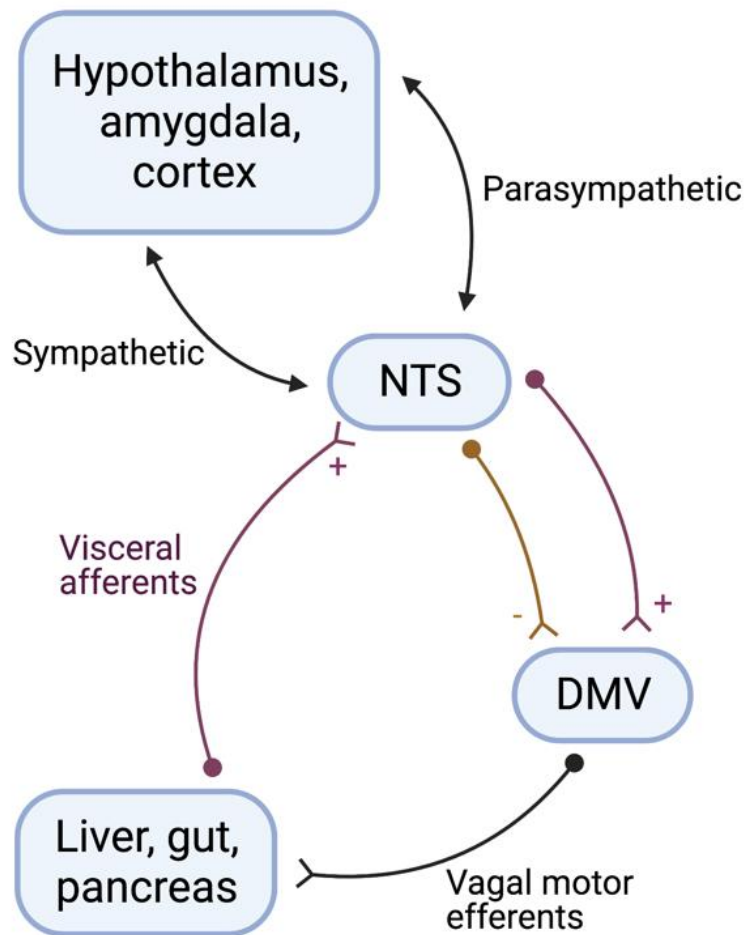
Figure 1.2 Schematic of dorsal vagal complex's (DVC) key regulatory position.
The NTS receives visceral afferent input and then projects both glutamatergic (+) and GABAergic (-) interneurons to the DMV, regulating vagal motor output to viscera. In addition, NTS is reciprocally connected with several autonomic regulatory centers.

1.6 Metabolomics and Metabolome

Metabolism plays a central role in health and diseases. Understanding how disturbances in metabolism affect disease progression and outcome is vital as new drugs and strategies are developed. Metabolomics is defined as a large-scale study of small molecules called metabolites, while the interactions of metabolites are defined as metabolomes. The state of the cell or organism can be deduced from metabolomic studies as they show the biochemical activity of the cell/tissue or organism studied. The metabolome includes amino acids, fatty acids, carbohydrates, vitamins, lipids, and other molecules and is constantly changing because of a multitude of reactions occurring [98,99]. Gas chromatography-mass spectrometry (GCMS), liquid chromatography-mass spectrometry (LCMS), or nuclear magnetic resonance spectroscopy (NMR) techniques are used to study the metabolome [100]. Two main approaches in the study of metabolomics are employed: targeted or untargeted metabolomics, the main differences are summarized in the table below (adapted from Sas et al.) [100–102].

Table 1.1 Comparison of targeted and untargeted metabolomics approaches

Feature	Targeted	Untargeted
Number of metabolites detected	Specific subset (less than 25/run)	Typically about 500 reproducible known compounds
Identification	Individual standards	Library and software based
Quantitative	Yes	No
Data Analysis time	Minimal (n = 10/group and 20 analytes takes 2-3 days)	Significant (n=10/group takes 4-6 weeks)

1.6.1 Metabolomics and diabetes

T1DM and T2DM plasma and urine levels have been extensively studied using metabolomics techniques [42,70,101–106], but regional brain metabolomics during hyperglycemia is mainly unknown. Arguably the most notable discovery is the identification of amino acids as predictors of diabetes. Elevated levels of branched chain amino acids such isoleucine, leucine and valine, were able to predict risk up to 12 years prior to onset of diabetes [107]. Metabolomics has also been extensively used to study secondary effects of diabetes such as nephropathy, chronic kidney disease and atherosclerosis [101].

1.6.2 Stable Isotopic Tracing

Understanding the metabolite abundance does not paint a whole picture and is insufficient in understanding the effects a disease has on the cell or tissue. Therefore, measurement of not only metabolite abundance but also the change of abundance over time, or metabolic flux, is necessary to understand the changes in metabolome [108]. Isotopic tracing is a powerful tool as it can detect relative pathway and nutrient contributions, in addition to the changes in the flux of metabolites [109]. Changes in metabolic flux can be the result of a change in production (biosynthesis/anabolism) or a change in consumption (degradation/catabolism). However, flux cannot be measured by simply utilizing the mass spectrometer. The assessment of metabolic flux requires non-radioactive stable isotope tracers [110]. Stable isotopic tracing is achieved by giving animals labeled metabolite, for example $^{13}C_6$ glucose, and detecting the incorporation of heavy isotopes into specific metabolites [111,112]. The mass shift due to the heavy isotope is detected using GCMS or LCMS (Figure 1.3). Data are corrected for the natural abundance of heavy isotopes, and then presented as fractional enrichment. Stable isotopic tracing has been used in cell culture, animal models and humans [101].
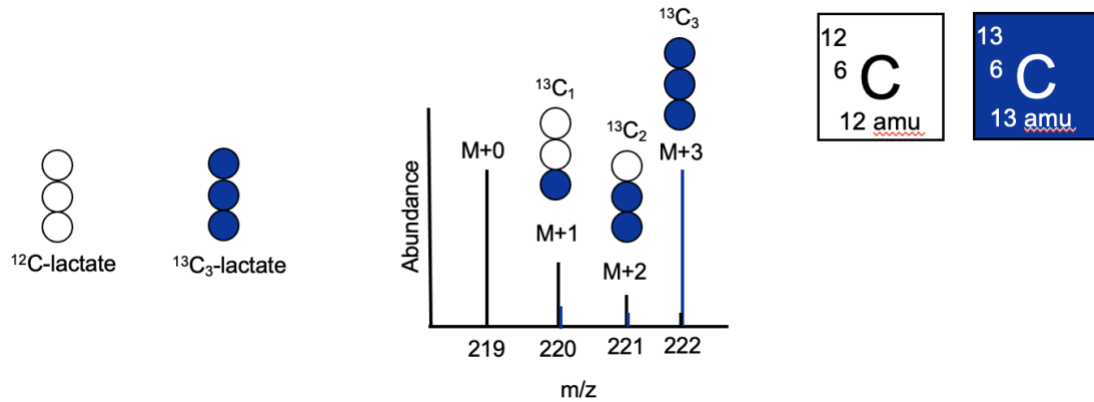
Figure 1.3 Detection of labeled metabolite using GCMS or LCMS.

Labeled metabolite lactate has detectable variation in neutron count and mass. m/z of unlabeled ^{12}C lactate is 219, and fully labeled ^{13}C$_3$ lactate is 222.

Patterns of enrichment of labeled carbons in stable isotopic tracing can be used to assess the enzymes pyruvate carboxylase and pyruvate dehydrogenase based on isotopologues enrichment percentage. For example M+2 label of TCA cycle intermediates is used to analyze pyruvate dehydrogenase while M+3 is used to analyze pyruvate carboxylase (Figure 1.4).
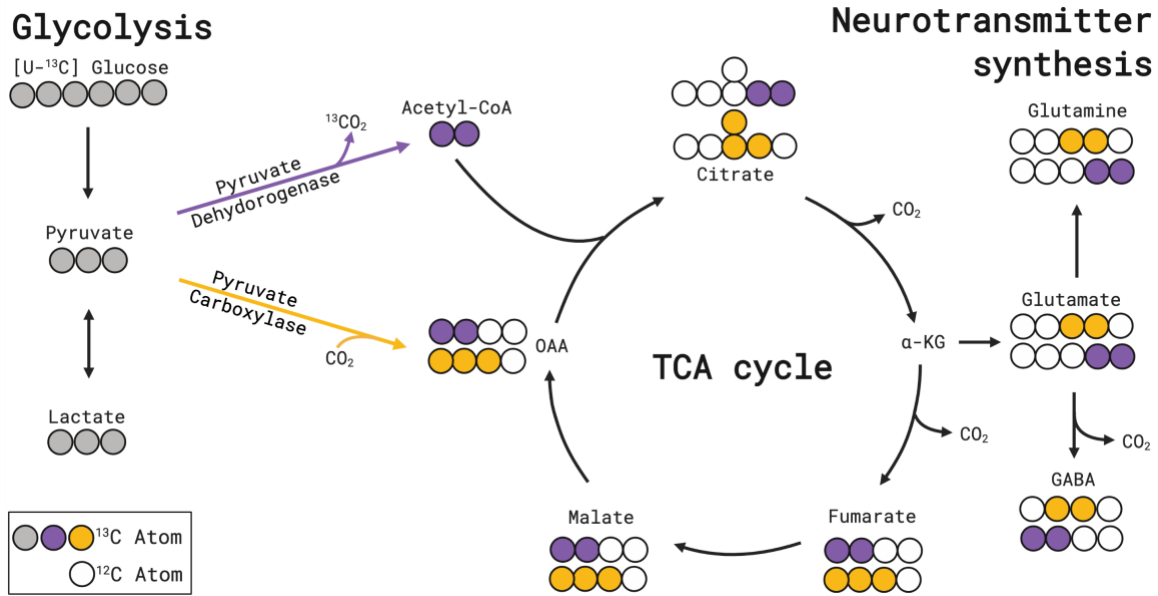
Figure 1.4 Analysis of pyruvate dehydrogenase and pyruvate carboxylase using stable isotopic tracing.

Fully labeled glucose, after turning into pyruvate, has two main entryways into TCA cycle; pyruvate dehydrogenase (M+2) and pyruvate carboxylase (M+3).

1.7   Overall goals of the dissertation

There are three main goals of the dissertation, 1) to define DVC's role in whole-body glucose regulation during hyperglycemia, 2) to develop and implement a protocol for studying the brain metabolome by utilizing high power focused microwave fixation, and 3) to understand the effects of hyperglycemia on central carbon metabolism within different brain regions as well as peripheral organs.

In Chapter 2, we present a STAR protocol developed for studying the brain metabolome utilizing high power focused microwave fixation. In Chapter 3 we establish a

central role for the DVC in peripheral glucose homeostasis, mediated through the parasympathetic nervous system. In Chapter 4 we investigate hyperglycemia effects on central carbon metabolism in the neocortex, hippocampus, and DVC given that glucose is the main source for *de novo* production of neurotransmitters glutamate and GABA, whose signaling is altered during T1DM. In chapter 5, we summarize the results presented and discuss its implication and importance.

CHAPTER 2. HIGH-POWERED FOCUSED MICROWAVE FIXATION TO STUDY BRAIN METABOLOME

2.1 Preface

The following Chapter describes a STAR protocol prepared for publication (Parts 2.5-2.8) and methods verification results that is a part of separate publication. The development of the STAR protocol was designed by Jelena Anna Juras, Lyndsay Young and Ramon Sun. The manuscript was written and edited by Jelena Anna Juras, Lyndsay Young and Ramon Sun. Jelena Anna Juras and Lyndsay Young contributed equally to the STAR protocol, as every part of it was done together. Data in 2.2-2.4 was used in a separate manuscript prepared for publication. For a detailed description of this manuscript's author contribution see Chapter 4.1. For materials and methods see Chapter 4.3.

To make the chapter flow better, the full STAR protocol as prepared for publication is at the end of the chapter.

2.2   Introduction

The best techniques to accurately capture physiological brain metabolism in rodents *in vivo* rely on nuclear magnetic resonance (NMR) [113–115], wherein mice are anesthetized, and live animals are used to study metabolic parameters. Metabolites captured by *in vivo* NMR are limited, thus large-scale metabolomics studies of the brain require rapid dissection of brain regions post-mortem followed by cryopreservation and mass spectrometry detection of metabolites [116–118]. Post-mortem surgical removal of the brain ranges from 90 seconds to several minutes depending on the individual performing the resection. It is well documented that metabolism changes postmortem [119,120] and the rates of metabolic flux through glycolysis and the TCA cycle occur in seconds [121–123]. Furthermore, artificial tissue hypoxia has been reported in mice following cervical dislocation [124], decapitation [125], and CO_2 euthanasia [126]. Brain tissue collection through conventional routes results in glycogen degradation and changes in global protein phosphorylation status [127,128]. A deeper understanding of neuronal function hinges on expanded metabolic pathway coverage, creating a critical need to establish an accurate baseline brain metabolome that excludes residual non-physiological metabolism that occurs during post-mortem brain resection.

Microwave fixation of mammalian tissues use the vibration of water molecules to produce heat [129], resulting in heat-inactivated protein denaturation and, in principle, stopping all metabolic processes [130]. Indeed, microwave fixation is frequently used in pathology laboratories to preserve mammalian tissues for histopathological analyses [131]. For direct *in situ* tissue fixation of whole animals, a focused microwave system has been developed for the rapid inactivation of brain proteins and shown to preserve global protein phosphorylation through enzyme inactivation, however, they did not look at the metabolome of brain regions [128]. Similarly, our model places the mouse in a holder and

in the microwave in a way where the focused beam targets the brain, more specifically bregma (A-P 0). The peripheral organs are not in the direct path of the radiation beam. We hypothesize that enzymatic inactivation through microwave fixation would preserve the brain metabolome. Herein, we compared *in situ* microwave fixation (0.6 seconds) to the conventional decapitation, rapid dissection, and cryo-preservation of wild-type C57Bl/6 brain tissues, where enzyme inactivation takes about 90 seconds. We observed a drastic degradation of free glucose and glycogen for lactate production during the 90 seconds of enzyme inactivation (traditional cryo-preservation tissue harvesting), which was not seen with focused microwave where enzyme inactivation took 0.6 seconds.

2.3   Results

2.3.1   *In situ* microwave fixation preserves brain metabolome

Cellular metabolism continues post-mortem for rodents, with signs of hypoxia driven metabolic reprogramming [120]. This metabolic reprogramming is especially true for the brain and capturing an accurate snapshot of the brain metabolome remains a critical challenge in the field. In this study, we utilized the high-powered focused microwave specifically designed for the rapid fixation of rodent brain tissue to prevent postmortem metabolic changes during brain resection. To test the application of microwave fixation, we designed an experiment to compare the impact of decapitation, followed by rapid dissection of the brain and cryo-preservation by LN_2 where enzyme inactivation took around 90 seconds (n=3), to the microwave fixation, where enzyme inactivation took about 0.6 seconds (n=3), (Fig. 2.1A). Brain and other tissues from both cohorts of animals were cryomilled and prepared for pooled metabolomics analysis by gas chromatography mass spectrometry (GCMS) for both polar metabolites and biomass [132–134]. For this study, instead of doing a whole brain analysis, we dissected the brain into regions, neocortex, hippocampus, and the dorsal vagal complex (DVC), which can be

reliably separated during the brain dissection. GCMS metabolomics analyses between 90 seconds and 0.6 seconds needed for enzyme inactivation displayed clear separation by Partial Least Squares-Discriminant Analysis (PLS-DA) (Fig. 2.1B), and metabolic pathway enrichment analysis identified glycolysis, gluconeogenesis, TCA cycle, and amino acid in all three brain regions as key pathways differing between two enzyme inactivation times (Fig 2.1C). Targeted metabolite analysis of the central carbon pathway revealed a significant increase in glycogen, glucose, citrate, and a significant decrease in lactate, malate, and fumarate with HPFM (Fig 2.1D). Since the microwave beam does not have peripheral organs in its path, we included GCMS analysis of the lung, liver, and muscle as controls. We only observed changes in glucose and glucose-6-phosphate in liver and the muscle, but not other metabolites (Figure 2.2). Further, microwave fixation shows improved variance within groups showing reduced coefficient of variance (CoV) among multiple metabolites (Fig. 2.1E), indicating that focused microwave with 0.6 seconds time interval to inactivate enzymes is an improved method over traditional decapitation with cryo-preservation where enzyme inactivation takes around 90 seconds.
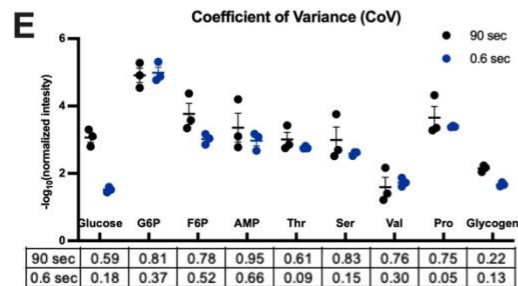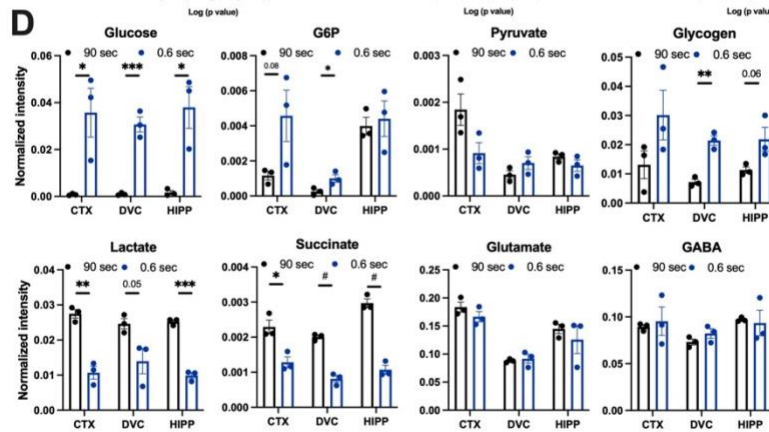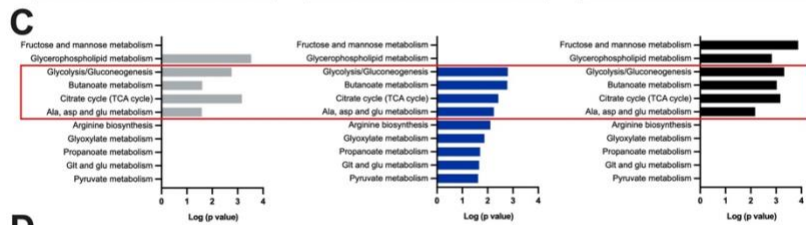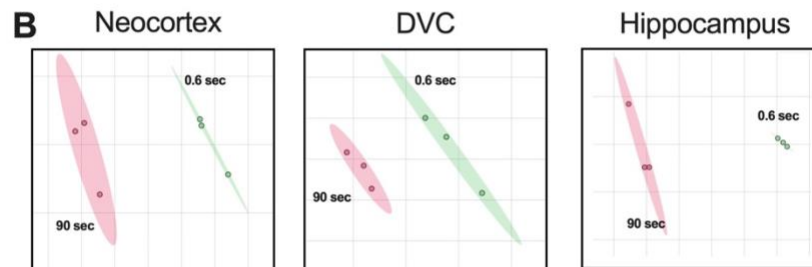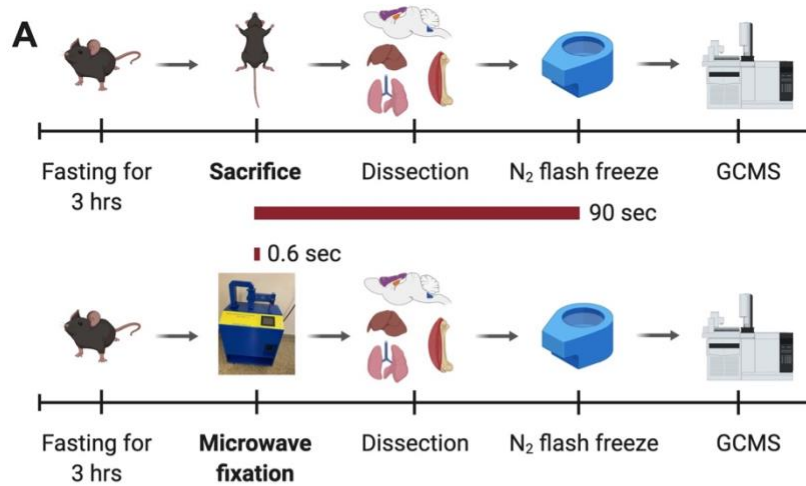
Figure 2.1 In situ high-power focused microwave fixation (HPFM) preserves brain metabolome.

(A) Schematic of the experimental design. 6-week-old mice were fasted for 3 hours, and euthanized by decapitation (top) or microwave fixation (bottom). Brain regions were then dissected, flash-frozen, and analyzed by GCMS. (B) Partial Least Squares-Discriminant Analysis (PLS-DA) of neocortex (CTX), dorsal vagal complex (DVC), and hippocampus (HIPP) metabolites showing distinct separation between 90 seconds and 0.6 seconds enzyme inactivation. (C) Pathway analysis comparing 90 seconds and 0.6 seconds enzyme inactivation (performed by Metaboanalyst) in CTX, DVC, and HIPP brain regions. (D) Representatives metabolite levels from glycogen metabolism, glycolysis, and TCA cycle between 90 seconds and 0.6 seconds. Values are presented as mean $\pm$ SEM (n=3 biological replicates), *p<0.05, **p<0.01, ***p<0.001, #p<0.0001, analyzed by student t-test. (E) Coefficient of variance (CoV) analysis of representative metabolites in B. G6P: glucose 6-phosphate, F6P: fructose 6-phospahte, AMP: adenosine phosphate, Thr: Threonine, Ser: Serine, Val: Valine, Pro: Proline.
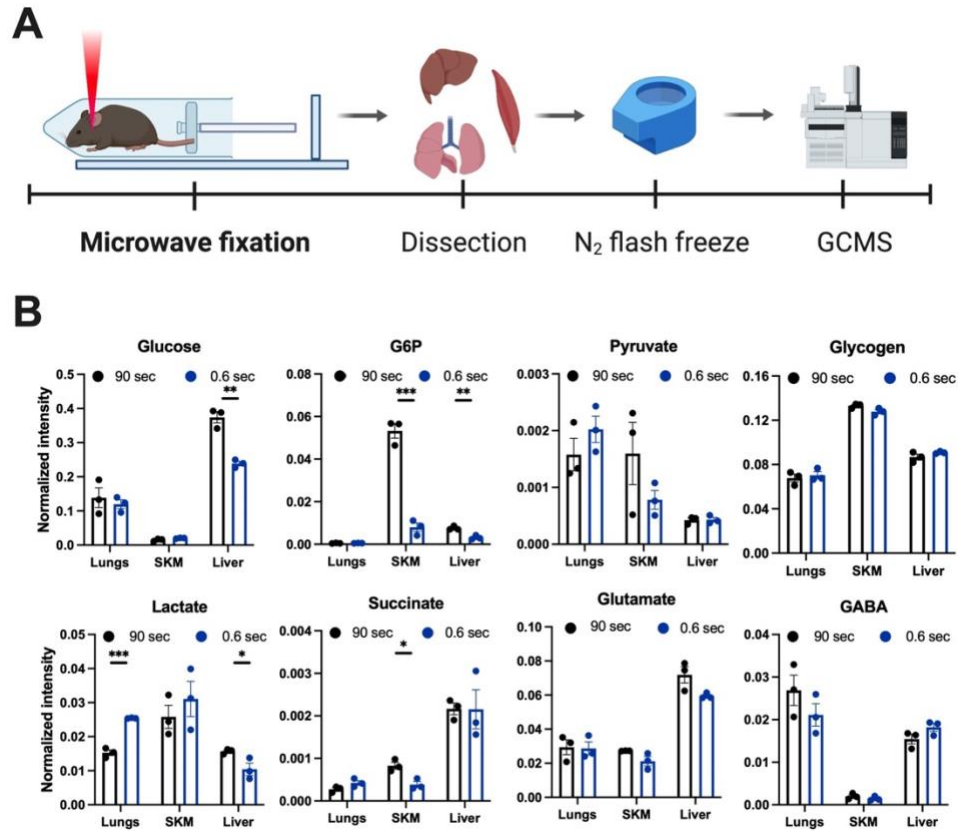
Figure 2.2. *In situ* **high power focused microwave fixation (HPFM) to study metabolome in peripheral organs.**

(**A**) Schematic of the HPFM showing the energy beam hitting the brain but not peripheral organs. (**B**) Representative metabolite levels from glycogen metabolism, glycolysis, and TCA cycle between 90 seconds and 0.6 seconds enzyme inactivation. Values are presented as mean $\pm$ SEM (n=3 biological replicates), *p<0.05, **p<0.01, ***p<0.001, analyzed by student t-test. G6P: glucose 6-phosphate.

2.3.2 *In situ* microwave fixation is compatible with stable isotope tracing

Stable isotopic tracing is invaluable for delineating substrate metabolism and interrogating enzymatic activities [135,136]. To test whether focused microwave fixation is compatible with stable isotope tracing, we performed oral gavage delivery of ^{13}C-glucose using a method previously described [133] and performed 0.6 seconds and 90 seconds enzyme inactivation methods to interrogate isotopic enrichment of central carbon metabolites between the two different brain fixative strategies (n=3) (Fig 2.3A). We identified significantly increased enrichment of ^{13}C in glycogen and glycolytic metabolites, including glucose, DHAP, and PEP in the neocortex between 0.6 seconds and 90 seconds of enzyme inactivation strategies (Fig 2.3B-C). However, lactate, citrate, fumarate, malate, and amino acids such as glutamate, glutamine, serine, and GABA were not different between 0.6 and 90 seconds (Fig. 2.3C). It is likely that even though total pooled metabolites were changed during 90 seconds of inactivation, both ^{13}C-enriched and ^{12}C in TCA cycle and amino acid metabolism were either consumed or synthesized at the same rate during 90 seconds fixation interval, as compared to 0.6 seconds enzyme inactivation interval. Similarly, we did not observe major changes in ^{13}C-enrichment between 90 seconds and 0.6 seconds enzyme inactivation periods in the lung, liver, and SKM (Fig. 2.4). Collectively, these data suggest 1) glycogen and glucose are utilized to supply glycolysis during the 90 seconds of tissue resection (Fig. 2.3D), and 2) stable isotope tracing could be a better strategy then untargeted metabolomics to study brain metabolism when the focused microwave is not available to prevent conclusions made on data that is not physiologically relevant.
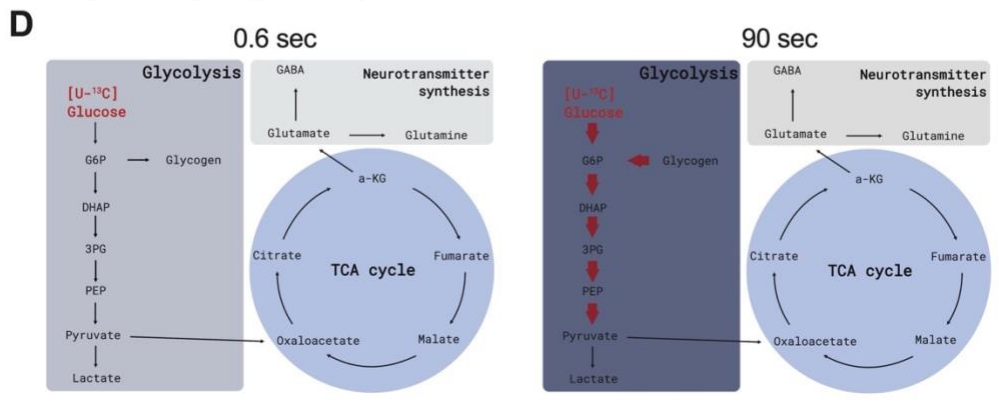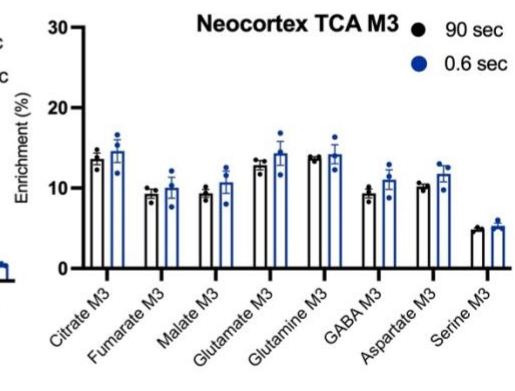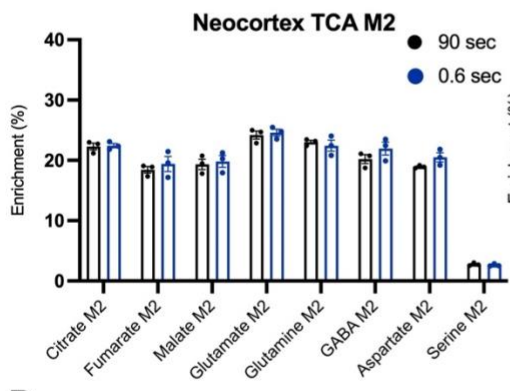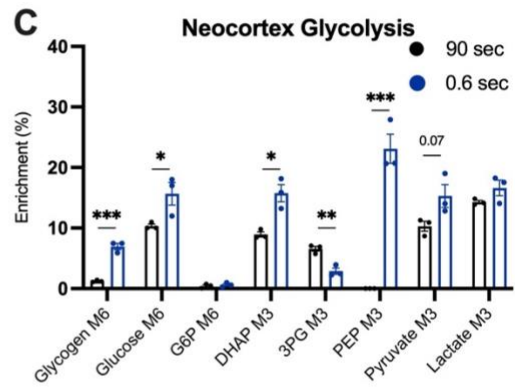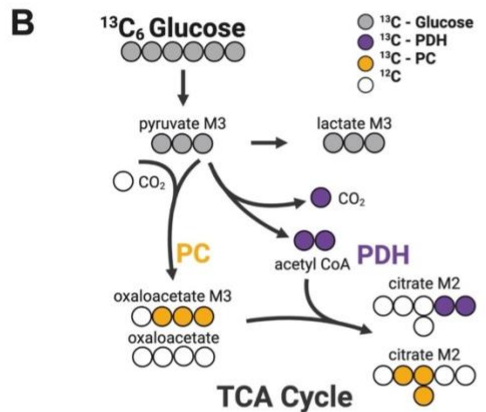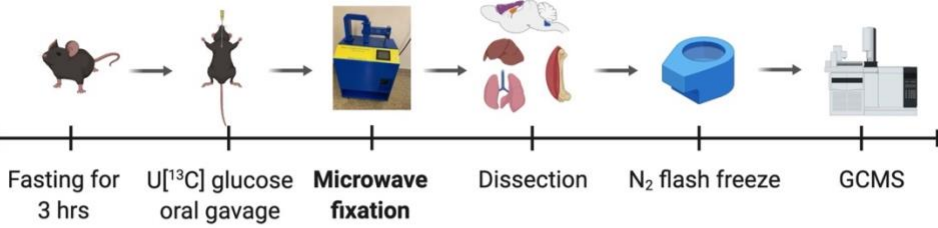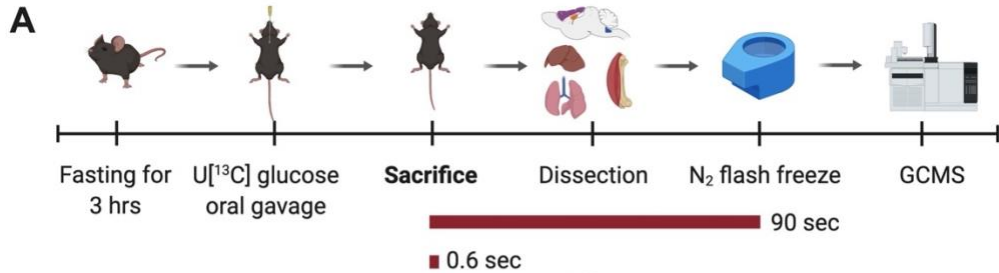
Figure 2.3 In situ high power focused microwave fixation (HPFM) is compatible with stable isotope labeling.

(**A**) Schematic of the experimental design. In a parallel experiment, as shown in **Figure 2.3A**, 6-week-old mice were fasted for 3 hours, gavaged with $^{13}C_6$-glucose, and euthanized by decapitation (*top*) or microwave fixation (*bottom*), brain regions were then dissected, flash-frozen, and analyzed by GCMS. (**B**) Schematic showing the stable isotope tracing glucose in glycolysis and TCA cycle and subsequent interpretations. (**C**) Representative isotopologue for M6 of glycogen, glucose, and G6P, M2 of citrate, fumarate, malate, glutamate, glutamine, GABA, aspartate, and serine, M3 of DHAP, 3PG, PEP, pyruvate, lactate, citrate, fumarate, malate, glutamate, glutamine, GABA, aspartate and serine within the prefrontal cortex regions of mice subjected to enzyme inactivation at 90 seconds and 0.6 seconds. Values are presented as mean $\pm$ SEM (n=3 biological replicates), *$p < 0.05$, **$p < 0.01$, ***$p < 0.001$, #$p < 0.0001$, analyzed by student t-test. (**D**) Model of changes in glucose utilization within cortex between enzyme inactivation at 90 seconds or 0.6 seconds. Bolded red arrows represent overutilized pathways during 09 seconds enzyme inactivation. G6P: glucose 6-phosphate, DHAP: dihydroxyacetone phosphate, 3PG:3-phosphoglyceric acid, PEP: phosphoenolpyruvate, CTX: neocortex.
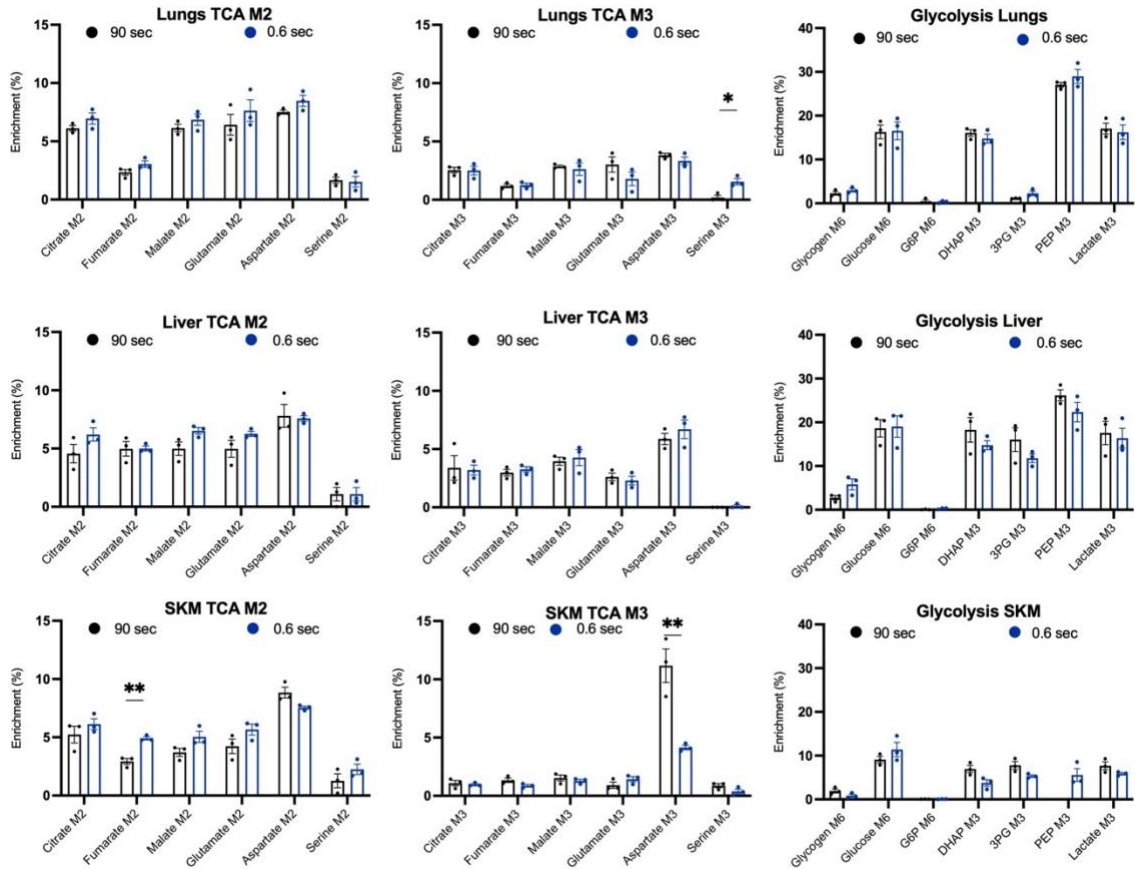
Figure 2.4 $^{13}C_6$ glucose isotope tracing does not alter in the lung, liver, or skeletal muscle (SKM) with high power focused microwave fixation (HPFM).

Representative isotopologue for M6 of glycogen, glucose, and G6P, M2 of citrate, fumarate, malate, glutamate, aspartate, and serine, M3 of DHAP, 3PG, PEP, lactate, citrate, fumarate, malate, glutamate, aspartate and serine between mice subjected to 90 seconds or 0.6 seconds enzyme inactivation. Values are presented as mean $\pm$ SEM (n=3 biological replicates), *p<0.05, **p<0.01, analyzed by student t-test.

2.4 Discussion

There is a major scientific interest in deepening our understanding of the brain metabolome [137,138], as many speculate it will aid in our understanding of brain physiology and could be key to understanding neurological disease pathology. Brain metabolism is a highly heterogeneous and rapid cycling series of events; therefore capturing an accurate snapshot of the brain metabolome is technologically challenging. In this study, we employed a focused microwave to create a snapshot of the brain metabolome through *in situ* heat inactivation and fixation of metabolic enzymes. By comparing focused microwave, which takes 0.6 seconds and conventional decapitation with cryopreservation which takes around 90 seconds to preserve metabolites, we found that focused microwave significantly retained total pools of glycogen, glucose, and citrate, but decreased levels of lactate, malate, and succinate as compared decapitation with cryo-preservation. Our study highlighted the importance of capturing the accurate brain metabolome and supports the use of a focused microwave to study brain metabolism. When a focused microwave is not available, data interpretation should be carefully examined with the assumption that non-physiological metabolism occurs during cryopreservation. The effect of non-physiological metabolism is the most extensive for glucose, glycogen, and lactate.

Currently, strategies to study brain metabolism include total pooled metabolomics analyses for large-scale pathway coverage [116] and, in certain cases, stable isotope tracing to study metabolic flux or enzyme activity [114,139]. We observed a number of interesting changes between enzyme inactivation at 0.6 seconds (focused microwave) and 90 seconds (cryo-preservation) in total pooled metabolomics analysis. Primarily, fixation of brain with focused microwave resulted in significantly increased levels of glycogen, glucose, citrate, aKG compared to cryo-preservation. In addition, microwave

fixation resulted in a significant decrease in lactate, succinate, and malate as compared to cryo-preservation. These data suggest increased utilization of glycogen and glucose for glycolysis and lactate production during the 90 seconds interval to preserve metabolites. Interestingly, the metabolic shift toward lactate production is often observed during hypoxia [140] and occurs frequently during cancer metabolism [141]. One possible explanation of this metabolic phenotype is that after euthanasia, the lack of circulation supplying the brain creates a hypoxic environment for the metabolically active brain cells, resulting in a shift towards a hypoxic metabolic phenotype. It is worth noting we did not observe a change in amino acid abundances between the two time intervals of fixation (0.6 seconds and 90 seconds). Amino acids such as glutamate, glutamine, aspartate, or GABA were comparable between the two different brain harvest strategies. Our GCMS settings includes heating the column to a maximum temperature of 280°C, allowing us only to study heat resistant metabolites. In addition, if microwaving produced heat related artifacts, due to high temperature of the column, the artifacts would not make it to the detector.

Stable isotope tracing is a powerful technique to study metabolic flux and enzyme activity in vivo and is frequently used to study brain metabolism [114,139]. We performed isotopic tracing experiment using an *in vivo* oral delivery method developed previously [133] to test the effects of *in situ* fixation by focused microwave on stable isotope enrichment of central carbon metabolites. In line with pooled metabolomics analysis, 90 seconds of enzyme inactivation as compared to 0.6 seconds resulted in a significant increase in glucose and glycogen utilization, as demonstrated by decrease in the enrichment of M6 isotopologue of glucose and glycogen, and an increase in enrichment of M3 isotopologue of 3-PG. To our surprise, we did not observe major changes between 0.6 seconds and 90 seconds intervals in isotopic enrichment of TCA cycle metabolites.

28

M2 and M3 isotopologues of citrate, fumarate, and malate were consistent between the two time intervals. These data imply that although the total pool of metabolites was changing during 90 seconds of cryo-preservation, it did not affect the isotopic ratios or enrichment. Further, both labeled and unlabeled ^{13}C fractions were either produced or consumed at the same rate. Based on these data, we recommend the use of stable isotope tracing to study brain metabolism when focused microwave is not available.

The method development presented here is the first step of creating an accurate snapshot of the brain metabolome without influence from post-mortem brain resection. We would like to highlight that rodent brain metabolism is highly sensitive to stimuli such as handling and stress [142], anesthesia [143], and time post-euthanasia [120]. Additional steps will be needed to control these factors in the future to truly capture the brain metabolome. Future studies should focus on isolating single cell types through fluoresce-activated cell sorting (FACS) or magnetic separation methodologies post focused microwave to define the cell type specific brain metabolism in healthy and diseased tissue. It would also be of interest to test whether focused microwave is compatible with new single-cell technologies such as matrix-assisted laser desorption ionization MALDI mass spectrometry imaging [144], single cell RNAseq [145], and spatial proteomics analyses [146,147].

2.5   Summary

Metabolism does not stop immediately postmortem, when rodents are decapitated. Rather it undergoes substantive change induced by post-mortem dissection and the onset of hypoxia, thus presenting a challenge to capture physiological changes in the metabolism induced by disease. Enzymes can be stopped almost instantaneously by denaturation, therefore we employed high-power focused microwave (HPFM) fixation to stop all metabolic changes in 0.6 seconds. This workflow details the step-by-step high-power focused microwave fixation protocol for the untargeted and stable isotopic tracing metabolome study in various tissues.

2.6   Graphical Abstract
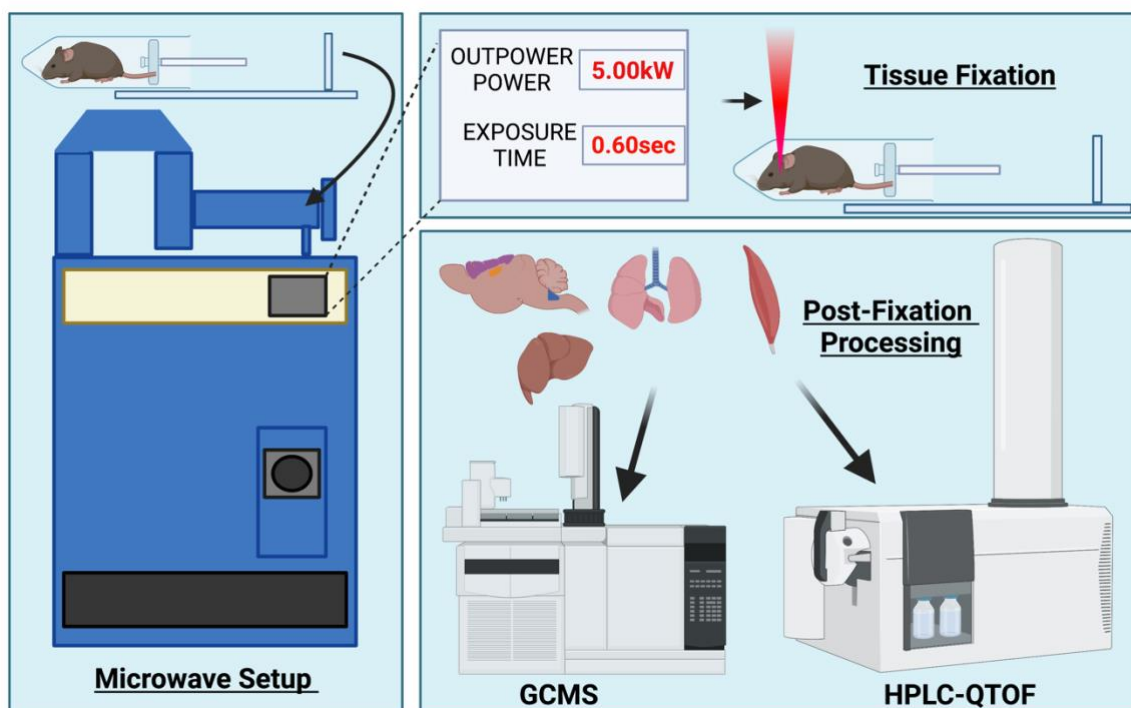
Figure 2.5 Graphical abstract of the protocol.

In short, mice were placed in a mouse holder, secured with silicon rods, and placed in the microwave apparatus. The microwave was run at 5.00 kW for 0.6sec. Utilizing the high-

power microwave results in euthanasia of animals and tissue fixation. Regions of the brain as well as peripheral organs were then dissected. We employed GCMS and HPLC-QTOF to analyze the metabolome.

2.7   Preparation of the high-powered focused microwave

Microwave Specifications - For proper microwave fixation, machine outlets will need to be configured to meet power requirements of 190-240V 3-A 3 Phase or 380-440V 20A 3 Phase prior to operation.

Timing: 30 min

The microwave has a warm-up time before use. Turn the microwave (Figure 2.6.) on and leave it for 30 minutes. Set the power of the microwave to 5kW and time to 0.65 seconds.

Figure 2.6 Muromachi Kikai Company High Power Focused Microwave.

2.7.1 Preparation of animal holder

Choose the appropriate size of the animal holder (Figure 2.7). Fill the animal holder with DI water carefully, ensuring that no bubbles are trapped in the holder. This is extremely important as the water is used to dissipate the heat during the fixation process. Water must be replaced after each animal.
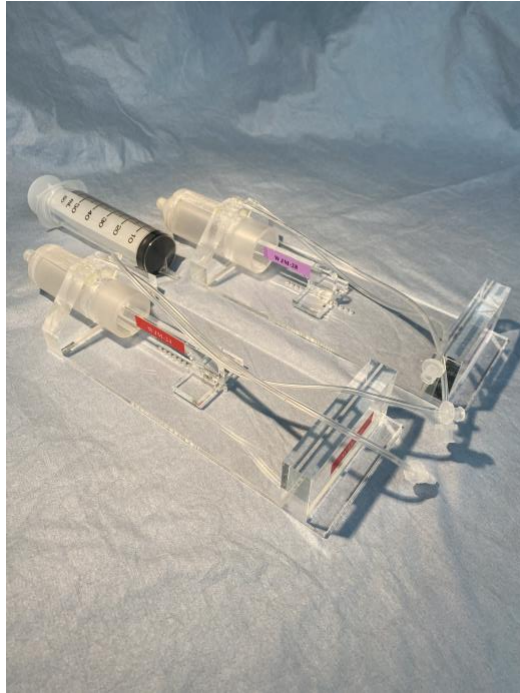
Figure 2.7 Animal holder for HPFM

2.7.2 Key Resources Table

Table 2.1 Key resources needed to run high power focused microwave

REAGENT or RESOURCE	SOURCE	IDENTIFIER
Chemicals, Peptides, and Recombinant Proteins		
Ethanol	Decon Labs	CAS#: 64-17-5
Other		
High power-focused microwave	Muromachi Kikai Company	MMW-05
Animal Holder, TAW-174P	Muromachi Kikai Company	WJM-24 for 15-20g Mouse, WJM-28 for 20-40g Mouse, WJM-30 for 40-50g Mouse
60 mL syringe only, luer lock tip	BD Sciences	BD 309653
Over the head ear muffs	Fisher Scientific	19-130-1978
Safety Glasses	Fisher Scientific	19-181-514
N95 mask	Fisher Scientific	18-999-473

2.7.3 Step-by-step method details

2.7.3.1 Placing the animal into the holder

Timing: 1 min

The animal must be secured in the holder properly.

Restrain the animal

Guide the animal's snout into the animal holder

Secure the animal in the apparatus with the holder plunger. Make sure the animal is not too tight or too loose.

2.7.3.2   Place the animal into the high-power focused microwave

Timing: 1 min

Placement of the animal holder within the microwave is crucially important for proper fixation. Misplacement will result in under or over fixation of the tissue of interest.

Following the markings on the interior of the microwave, place the animal holder inside of the microwave (Figure 2.8).

Close the metal door on the microwave.

Run the microwave.

Carefully remove the animal from the holder.

Caution: Both animal and the holder are hot after exposure to microwave. Leave the animal to sit on RT for 4 min before dissection.

Figure 2.8. Placement of animal holder in high-power focused microwave

2.7.3.3 Microwave re-charging

Timing: 2 min

The microwave needs 2 min between the animals in order to recharge to the appropriate power.

For consistency between animals, we found 10 min was sufficient for fixation of all (n=3) animals in the studies.

2.7.3.4 Cleaning the animal holder between animals

Timing: 2 min

The animal holder must be cleaned and prepared for next animal.

Cleaning should be done by using 70% Ethanol, spraying, and wiping down the animal holder.

Replace the current water in the animal holder with fresh DI water.

2.8 Expected outcomes

In our experimental protocol, we describe a detailed method for preserving metabolites in the brain and other tissues. Post-extraction tissue was run on GCMS and LCMS. Other groups have reported Western Bloot analysis for protein glycosylation after microwave fixation [128].

2.8.1 Limitations

The described protocol works well when tissue barriers in an animal are intact. In other words, animals do not have craniotomy or other major procedures that would compromise the structural integrity of the tissue and result in overheating or underheating the tissue.

2.8.2   Troubleshooting

Problem 1: Tissue is under or over-fixed. Tissue will be in liquid form if under fixated, or extremely fragile if overfixated.

Potential solution: Animal's weight, genotype, and water content will greatly influence the quality of the tissue. Before each study, it is necessary to perform optimization for genotype and body weight.

CHAPTER 3. SYSTEMIC GLUCOSE REGULATION BY AN INHIBITORY BRAINSTEM CIRCUIT IN A MOUSE MODEL OF TYPE I DIABETES

3.1   Preface

The following chapter is a part of a manuscript prepared for publication. The manuscript comprises of two separate sets of experiments: in vivo blood glucose measurements and electrophysiological experiments. The study design and interpretation of the results for the in vivo blood glucose measurements were conducted by Jelena Anna Juras and Bret Smith. Surgery procedures, tissue processing, animal handling, blood glucose data collection, analysis, and statistics for in vivo blood glucose measurements were conducted by Jelena Anna Juras. Given that study design and interpretation of electrophysiological experiments were conducted by Sole Pitra and Bret Smith these data are not shown in the thesis. Abstract below is the same as in the manuscript to offer a general understanding of the manuscript. The manuscript was written and edited by Jelena Anna Juras, Sole Pitra and Bret Smith.

3.2   Abstract

Previous work showed that modulating the electrical activity of inhibitory neurons of the dorsal vagal complex (DVC) is sufficient to alter whole-body glucose concentration in normoglycemic mice. Here we tested the hypothesis that deactivating GABAergic neurons in the dorsal hindbrain of hyperglycemic mice decreases synaptic inhibition of parasympathetic motor neurons in the dorsal motor nucleus of the vagus (DMV) and decreases systemic glucose levels. Chemogenetic activation of GABAergic NTS neurons in normoglycemic mice increased their action potential firing, resulting in increased inhibitory synaptic input to DMV motor neurons and elevated blood glucose concentration. Deactivation of GABAergic DVC neurons in normoglycemic mice altered their electrical activity but did not alter systemic glucose levels. Conversely, stimulation of GABAergic

DVC neurons in hyperglycemic mice changed their electrical activity but did not alter whole-body glucose concentration, while deactivation of this inhibitory circuit decreased circulating glucose concentration. Peripheral administration of a brain impermanent muscarinic acetylcholine receptor antagonist abolished these effects. This inhibitory brainstem circuit emerges as a key parasympathetic regulator of whole-body glucose homeostasis that undergoes functional plasticity in hyperglycemic conditions.

3.3   Introduction

Blood glucose concentration is modulated through peripheral actions of the hormones insulin and glucagon, which interact with various organ systems to impact glucose storage, release, and cellular utilization. Relatively recently, insulin-independent glucose homeostatic mechanisms have been identified [2–7], and the regulatory role of the brain has gained acceptance [88]. Early investigation focused on hypothalamic nuclei, into which injection of insulin, glucose, or leptin decreases systemic blood glucose levels [10,148,149], while deletion of insulin or leptin receptors decreases glucose tolerance and results in insulin resistance [14,93]. However, there is not a direct connection between the hypothalamus and viscera. Rather, these effects are mediated largely by connections with brainstem vagal circuits [3,148,150].

The brainstem dorsal vagal complex (DVC) has been shown to play a role in glucose and energy homeostasis [15,97,151–155]. The DVC is the main neuronal region responsible for parasympathetic visceral regulation and includes the nucleus tractus solitarius (NTS), dorsal motor nucleus of the vagus (DMV), and area postrema (AP). Within the DVC, the NTS receives viscerosensory vagal afferent information, integrates the information with signals from other brain areas, and projects to preganglionic parasympathetic motor neurons in the DMV to control visceral functions. Furthermore, the

blood-brain barrier in the NTS and AP is permeable due to fenestrated capillaries[156], and may allow central access to circulating chemicals. Neurons in the DVC, and particularly the GABAergic NTS neurons, are sensitive to multiple circulating chemicals, including glucose and metabolic signaling hormones [157–164], making the DVC uniquely positioned as a potential central omphalos for modulating peripheral glucose metabolism.

Type I diabetes causes a sustained increase in glutamate release and postsynaptic GABA signaling in the DMV [165–171]. In normoglycemic mice, chemogenetic, designer receptor exclusively activated by designer drugs (DREADDs) mediated activation of GABAergic neurons in the dorsal hindbrain results in an insulin-independent increase in blood glucose mediated by the vagus nerve, while deactivation of the same neuron group has no glucoregulatory effect [97]. Because of the increased GABA release and receptor function in the DVC of chronically hyperglycemic mice, we employed a similar approach to investigate how selective activation (or deactivation) of inhibitory, GABAergic neurons in the dorsal hindbrain modulates whole-body glucose levels in diabetic mice. We hypothesized that, contrary to what occurs under normoglycemic conditions, deactivating GABAergic neurons in the DVC of hyperglycemic mice would disinhibit DMV motor neurons and increase their activity, resulting in decreased whole-body blood glucose levels.

3.4   Materials and Methods

3.4.1   Animals

All experiments were performed on male and female Vgat-ires-Cre knock-in mice (Slc32a1tm2(cre)lowl/J, 016962, The Jackson Laboratory, Bar Harbor, ME). Mice were housed and cared for in the University of Kentucky Division of Laboratory Animal Resources facilities under normal 14:10 light-dark condition with food (Tekad 2018,

Envigo, Indianapolis, IN) and water available ad libitum, except where noted and according to protocols approved by the University of Kentucky Animal Care and Use Committee.

3.4.2 Stereotaxic DREADDs construct injections

At seven weeks of age (± 3 days), mice were anesthetized using isoflurane (5% induction, 3% maintenance) and placed on a heating pad in a stereotaxic frame (Kopf Instruments, Tujunga, CA). The skull was exposed using a midline incision, and an approximately 1.5 mm craniotomy was made at the following stereotaxic coordinates from bregma: AP = 7.15 mm, ML = 0.25 mm, DV = 3.30 mm, targeting the NTS region. 150 nl of floxed DREADDs constructs, pAAV8-hSyn-DIO-hM3D(Gq)-mCherry (plasmid #44361, Addgene, Cambridge, MA), pAAV8-hSyn-DIO-hM4D(Gi)-mCherry (plasmid #44362, Addgene), or blank plasmid was injected using a 5 μl syringe equipped with a 32 gauge blunt-tipped needle (Hamilton, Reno, NV) over a period of 10 minutes, at a rate of 15 nl/minute. The needle was kept in place for 10 minutes before withdrawing. Mice were allowed to recover for 72 h following surgery and then were acclimated to handling for 3 weeks. Acclimation included daily handling, changing the home cage, puncture of lateral tail vein, and intraperitoneal (i.p.) injection of 0.1 ml of saline (Figure 3.1).
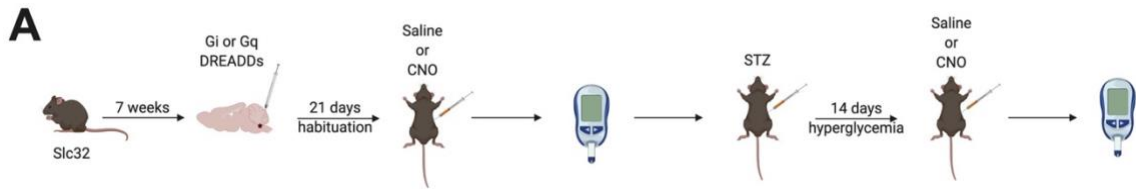
Figure 3.1. Experimental design for in vivo experiments.

Seven-week-old male and female mice were injected with either Gi or Gq virus. After recovery, mice were acclimated to handling for 21 days. Blood glucose was then tested upon administration of CNO or saline, the opposite treatment was administered three days later. Half the mice then received STZ, resulting in hyperglycemia within approximately 48 h. Mice were hyperglycemic for 14 days and blood glucose was measured again upon administration of CNO or saline in balanced cohorts. A subset of mice was pre-treated with methyl-scopolomine to block peripheral muscarinic receptors prior to CNO treatment.

3.4.3 In vivo glucose assessments

Three weeks after viral delivery, mice were randomly selected to receive either vehicle (0.9% saline + 0.1% DMSO) or clozapine-N-oxide (CNO, 1 mg/kg). All mice, across all cohorts started fasting between 8 - 9 am. Mice were fasted for three hours before receiving an i.p. injection of either vehicle or CNO. Initial lateral tail vein puncture was performed at the time of fasting and subsequent measures were performed by removing the scab to allow for free-flowing blood. Blood glucose levels were measured by handheld glucometer (Nova Max Plus, Nova Biomedical, Waltham, MA). Animals remained fasted and blood glucose was measured every 30 min for 5 h after injection of vehicle or CNO. The following day mice were fasted again and a 24 h measurement was taken. Each animal received the opposite treatment 3 days later to provide a counter-balanced design. One cohort of normoglycemic mice (n = 6) received 2 injections of CNO 72 hours apart to verify similar response to repeated CNO application.

Following the 24 h measurement after the second testing, mice were injected with streptozotocin (STZ, 200 mg/kg, i.p., Sigma-Aldrich, St. Louis, MO) or citric acid (CA, 0.1 M), after a 6 h fast. Mice were monitored daily for weight and blood glucose levels. Mice with blood glucose concentration $\geq$ 300mg/dL were considered hyperglycemic. After at least 14 days (14-16 days) of hyperglycemia, mice were tested again with CNO and vehicle, as above. One cohort of diabetic mice (n = 6) received a third CNO test after being pre-treated with methylscopolamine (MSA, 1 mg/kg, i.p.) 30 min prior to CNO injection, and blood glucose was measured for 5 h and at 24 h post-CNO injection. A separate cohort of normoglycemic mice that did not receive DREADDs viral constructs was tested for potential off-target or systemic effects of CNO or its metabolite, clozapine at 1 mg/kg and 10 mg/kg [172]. Data are expressed as the change in blood glucose measured immediately prior to injection (t = 0).

To verify DREADDs construct location, mice were anesthetized with isoflurane inhalation to effect and perfused transcardially with heparinized saline (10 units/mL), followed by 4% paraformaldehyde (PFA) in 0.1 M phosphate-buffered saline (PBS). The brain was removed and postfixed for 1 h in 4% PFA. The brainstem was then blocked at the rostral edge of the cerebellum and immersed in 30% sucrose in 0.1 M PBS overnight until equilibration. Sections were cut at 30 μm on a cryostat, mounted on slides, visualized with epifluorescence optics (Olympus BX40, Center Valley, PA), and imaged using a SPOT RT camera (Diagnostic Instruments, Sterling Heights, MI).

3.4.4 Data Analysis

In vivo glucose measurements are reported as mean ± standard error of the mean (SEM). Repeated-measures ANOVA with Tukey's post hoc was used to determine if CNO injection significantly changed blood glucose concentration. Animals in which mCherry was expressed in the NTS (i.e., indicating DREADDs transfection) were used in the analysis, blood glucose did not change in mice in which the NTS exhibited no mCherry labeling (n = 11) or when the label was identified mainly outside the DVC (i.e., off-target injections, n = 5), and these mice were not further analyzed. Animals in which blank plasmid was injected (n = 5) showed no blood glucose change. Unless otherwise stated, statistical significance for all measures was set at $p < 0.05$.

3.5 Results

The present study involved *in vivo* chemogenetic modulation of cre-recombinase-expressing GABAergic neurons in the dorsal hindbrain, centered on the caudal NTS. Stereotaxic injection of cre-recombinase-inducible adeno-associated viruses expressing the DREADDs with mCherry as the fluorescent marker allowed the activation or inhibition

of this neuronal population to study circulating glucose levels under normal physiological conditions and in a model of type 1 diabetes.

3.5.1 Chemogenetic activation of GABAergic NTS neurons

To assess the effects of GABAergic activation on whole-body glucose levels, normoglycemic mice were subjected to CNO (1 mg/kg) or vehicle (0.9% saline and + 0.1% DMSO) 3 weeks after viral inoculation with the excitatory hM3D(Gq) DREADDs construct. There was no difference in baseline blood glucose levels before receiving saline (144 $\pm$ 11 mg/dL) or CNO injection (143 $\pm$ 13 mg/dL). As shown in Figure 3.2C, CNO injection in normoglycemic mice (n = 10) resulted in an elevation of blood glucose concentration within 15 min, which was significantly different than after vehicle injection by 30 minutes (p<0.05), and continued to be significantly elevated 2 hours post-injection. The response to CNO was not different between mice that received CNO as a first or second injection, preliminary studies in six mice transfected with excitatory hM3D(Gq) DREADDs showed no decrement in response with repeated CNO treatments at three-day intervals (not shown).

A subset of the same mice was then subjected to a single injection of STZ (200 mg/kg) and maintained in a hyperglycemic state for 14 days before either vehicle or CNO injection. There was no difference in baseline blood glucose level before receiving saline (403 $\pm$ 53 mg/dL) or CNO injection (397 $\pm$ 37 mg/dL, p>0.05). Activation of dorsal hindbrain GABA neurons with CNO injection in hyperglycemic mice (n = 7) had no effect on blood glucose levels at any time point after injection (p>0.05, Fig 3.2D). Thus, whereas excitatory DREADDs activation in GABAergic neurons of the dorsal hindbrain led to increased blood glucose concentration in normoglycemic mice, activating the same neurons after two weeks of hyperglycemia had no effect on blood glucose.
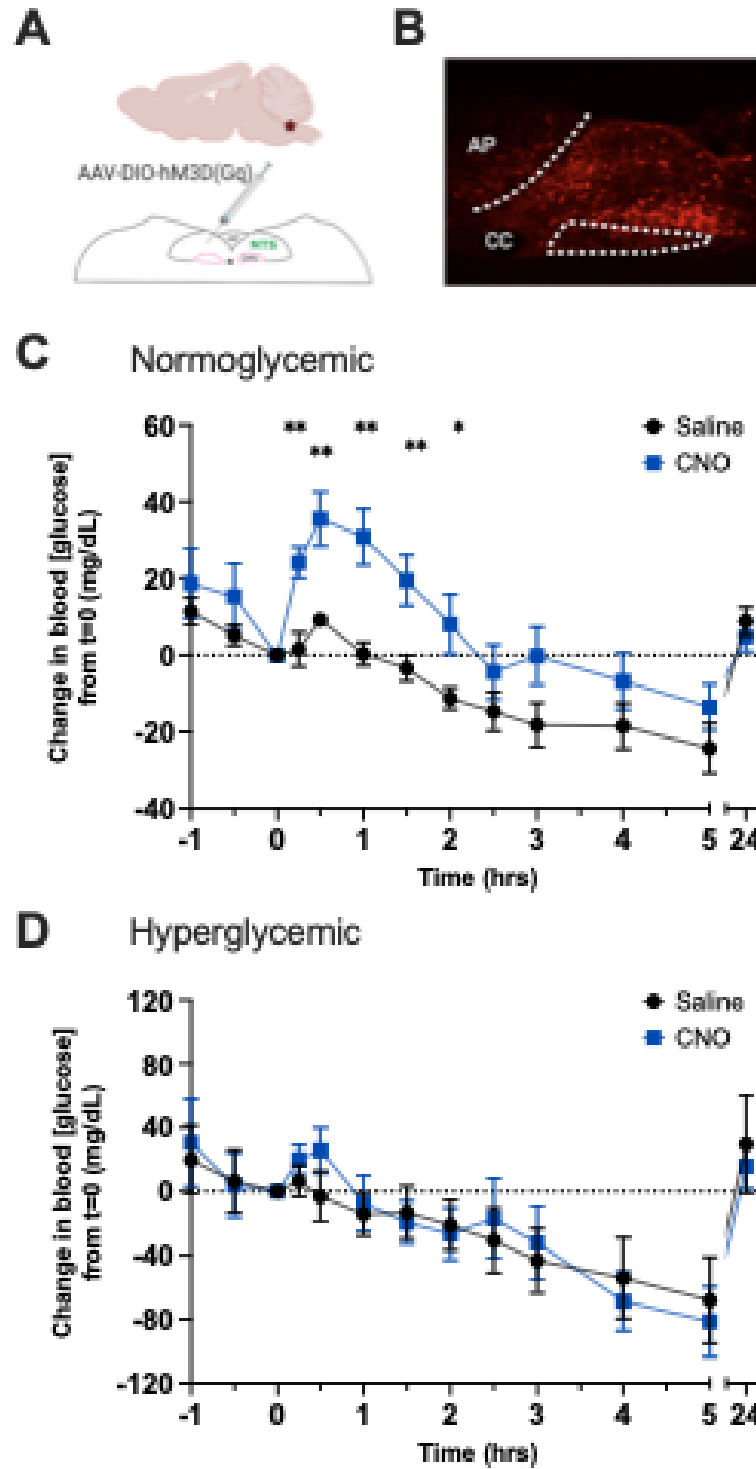
Figure 3.2. Chemogenetic activation of GABAergic neurons of the NTS increases whole-body glucose levels in normoglycemic but not hyperglycemic mice.

A, Schematic representation of the location of stereotaxic microinjection of pAAV-hSyn-DIO-hM3D(Gq) into the dorsal vagal complex. B, Representative image of DREADDs expression 6 weeks after inoculation. C, Blood glucose contraction after i.p. administration of CNO (1 mg/kg) or vehicle (0.9% saline + 0.5% DMSO) in normoglycemic mice (n = 10). D, Blood glucose contraction after i.p. administration of CNO (1 mg/kg) or vehicle (0.9% saline + 0.1% DMSO) in hyperglycemic mice (n = 7). Bars, SEM, * $p < 0.05$, ** $p < 0.01$. AP – area postrema, CC – central canal.

3.5.2   Chemogenetic inhibition of GABAergic NTS neruons.

To evaluate the effects of inhibiting GABAergic neurons in the dorsal hindbrain on blood glucose levels, normoglycemic mice were subjected to CNO (1 mg/kg) or vehicle (0.9% saline and + 0.5% DMSO) 3 weeks after viral inoculation with the inhibitory hM4D(Gi) DREADD construct. There was no difference in baseline blood glucose levels before receiving saline (145 $\pm$ 13 mg/dL) or CNO injection (152 $\pm$ 7 mg/dL). Similar to previous results[97], injection of CNO in normoglycemic mice resulted in no change in blood glucose concentration (n = 6, Fig. 3.3).

The same mice were then subjected to a single injection of STZ (200 mg/kg) and maintained in a hyperglycemic state for 14 days. Injecting CNO in hyperglycemic mice resulted in a significant decrease in blood glucose concentration starting 30 min post-injection ($p < 0.05$) and continuing for 2.5 hours (n = 6). Pre-treatment of 6 mice with methylscopolamine (MSA, 1 mg/kg) 30 minutes before administration of CNO prevented the effect of DREADDs mediated inhibition of GABAergic dorsal hindbrain neurons on blood glucose concentration ($p > 0.05$, Fig 3.3). There was no difference in baseline blood glucose levels before receiving saline (417 $\pm$ 29 mg/dL), CNO (442 $\pm$ 32 mg/dL) or methylscopolamine injection (433 $\pm$ 21 mg/dL).

A Normoglycemic
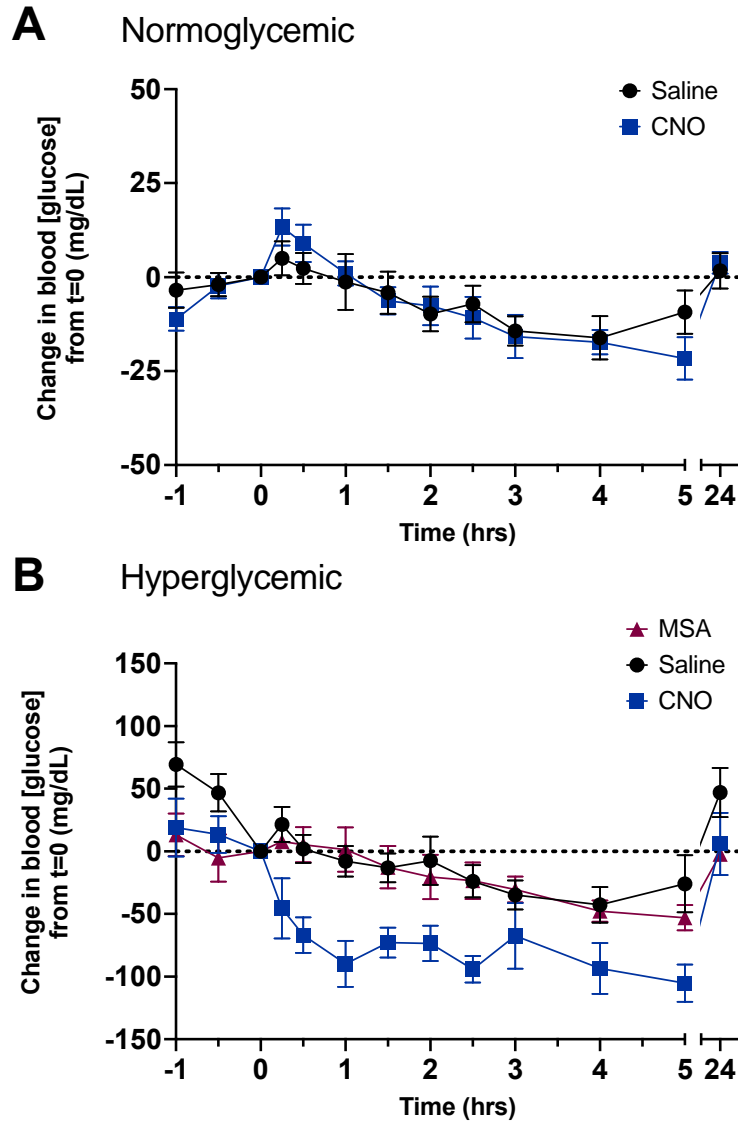
B Hyperglycemic

Figure 3.3. Chemogenetic deactivation of GABAergic neurons of the NTS decreases whole-body glucose levels in hyperglycemic, but not normoglycemic mice.

A, Blood glucose contraction after i.p. administration of CNO (1 mg/kg), vehicle (0.9% saline + 0.5% DMSO) in normoglycemic mice (n = 6). B, Blood glucose contraction after i.p. administration of CNO (1 mg/kg), vehicle (0.9% saline + 0.5% DMSO) or methylscopolamine (MSA, 1 mg/kg) in hyperglycemic mice (n = 6). Bars, SEM, * $p < 0.05$, ** $p < 0.01$.

3.6   Discussion

The concept of brain-centered whole-body glucose regulation has been gaining appreciation over the past two decades, but the role of the parasympathetic nervous system in regulating systemic blood glucose levels remains unclear, especially after periods of sustained diabetic hyperglycemia. Synaptic and extra-synaptic GABAergic inhibition has been shown to be a key modulator of parasympathetic drive to subdiaphragmatic viscera [159,173–175], and both synaptic and extra-synaptic GABA signaling in DMV neurons is upregulated in hyperglycemic mice [166,167]. Therefore, we investigated how GABAergic neurons within the dorsal hindbrain contribute to systemic blood glucose regulation after several days of hyperglycemia. In this study, we utilized DREADDs constructs to selectively activate or deactivate GABAergic neurons in the dorsal hindbrain, particularly the NTS, in both normoglycemic and hyperglycemic mice and measured whole-body glucose levels. As previously described our results confirmed that remote chemogenetic activation of GABAergic NTS neurons in normoglycemic mice is sufficient to increase blood glucose concentration, while deactivation of these neurons failed to alter blood glucose levels [97]. Conversely, deactivation of GABAergic hindbrain neurons resulted in a decrease in blood glucose levels in hyperglycemic mice. The CNO-driven decrease in blood glucose concentration was abolished upon administration of methylscopolamine, a muscarinic acetylcholine receptor antagonist that does not access the brain, consistent with a vagally mediated change in peripheral glucose metabolism.

Neurons in the DVC are capable of glucosensing [176–178], and changes in nutrient concentration can lead to modification of DVC circuitry, including sustained changes in synaptic and intrinsic neuronal properties that affect the function of the system [162,167,171,179,180]. Activation of excitatory DREADDs in GABAergic NTS neurons produced a significant change in blood glucose levels mediated by the vagus nerve and

produced through an increase in glucagon release and hepatic gluconeogenesis [97]. Even though cellular and synaptic effects of inhibitory DREADDs in the DVC were evident, systemic effects in terms of altered glucose levels were not detected[97]. These findings, which were replicated here (electrophysiological data not shown), suggest that disinhibition of DMV motor activity alone is not sufficient to induce hypoglycemia normally. However, since the effect of GABA release in the DMV is upregulated after periods of sustained hyperglycemia due to increased tonic GABA current density [165,167], and increased inhibition of DMV neurons tends to increase blood glucose concentration [91,181], we hypothesized that suppression of inhibition in hyperglycemic mice would have a greater systemic effect than in normoglycemic mice. There was no glycemia related difference in the effect of CNO on action potentials in GABAergic NTS neurons or on synaptic currents in downstream DMV neurons (electrophysiological data not shown). After sustained hyperglycemia, however, tonic GABA currents mediated by extrasynaptic receptors are upregulated in the DMV[166], implying a greater effect of reduced GABA release in DMV motor neurons from hyperglycemic mice. The specific contribution of tonic GABA currents in DMV neurons in regulating blood glucose remains to be clarified. Alternatively, the elevated glucose levels in STZ-treated mice could result in a ceiling effect due to the already elevated glucose and saturation of downstream visceral mediators of glucose regulation. This is consistent with the finding that DREADDs-mediated excitation of DMV motor neurons blunted the peak response during a glucose tolerance test [181].

To address concerns that the DREADDs system causes off-target effects [172], several control experiments were performed. Blood glucose concentration was measured post-CNO administration in mice that received blank viral construct, mice that received no

viral construct, mice that had off-target transfection, and mice that had no visible transfection. There were no effects of CNO injection in any of these control experiments.

Finally, inhibiting GABAergic neurons was sufficient to lower blood glucose levels in a hyperglycemic model in which insulin is significantly depleted, suggesting that the response was likely insulin independent. We speculate, based on Boychuck *et al.* [97], that these results are due to decreased gluconeogenesis, but the peripheral mechanism beyond involvement of parasympathetic output remains to be determined. These results further establish the link between the dorsal hindbrain and systemic glucose metabolism and highlight the need to continue investigating the role of GABAergic brainstem neurons in whole-body blood glucose regulation.

CHAPTER 4. HYPERGLYCEMIA DRIVEN METABOLIC REPROGRAMMING IN THE BRAIN

4.1   Preface

Parts of the following chapter comprises a manuscript prepared for publication. The study design and interpretation of the results were conducted by Jelena Anna Juras, Bret Smith and Ramon Sun. Induction of diabetes, handling of animals, daily measurement weights/blood glucose concentration, oral gavage of $^{13}C_6$ glucose, derivatization of samples, perfusion of mice, slicing of tissue, free-floating immunofluorescence, image acquisition and data analysis was done by Jelena Anna Juras. Madison Webb helped with the development of IF protocols, the development of image acquisition protocols and the analysis of IF staining. Lyndsay Young helped with animal euthanasia and GCMS method development. Kia Markussen and Ron Bruntz helped with developing methods for data analysis and helped with the verification of data. Michael Bouoncristiani, Kayli Bolton, Peyton Colbrun, Meredith Williams and William Sanders helped with tissue homogenization, daily blood glucose measurements, and data input. Chi Wang ran power analysis of GCMS data. The manuscript was written by Jelena Anna Juras and Ramon Sun, and edited by Jelena Anna Juras, Kia Markussen, Lyndsay Young, Lindsey Conroy, Tara Hawkinson, Mathew Gentry, Bret Smith and Ramon Sun.

4.2   Introduction

The brain consumes 20% of circulating glucose [182] and although debated, neurons are proposed to be the major glucose-consuming cells of the brain [71,183]. The major energy demand in the brain is for neuronal signaling and cellular processes needed to support healthy transmission of neuronal signals. Glucose is crucial in many cellular processes and glucose metabolism of the brain can be subdivided into catabolic or anabolic processes. Catabolic processes involve the breakdown of glucose for energy production via glycolysis, the Tricarboxylic acid cycle (TCA) and electron transport chain [184]. The anabolic processes entail glucose as a building block of many molecules, including lipids [185], and complex carbohydrates such as glycans [186], chondroitin [187] and heparin sulfate biopolymers [188], all of which are critical biomass and structural components of the brain. Furthermore, neurotransmitters such as GABA and glutamate can be synthesized *de novo* from glucose carbons [189]. Given that brain glucose participates in a numerous of metabolic processes from bioenergetics to neurotransmitter and biomass production, it is difficult to decipher which downstream processes are perturbed from alterations in availability or concentration of glucose.

Type I diabetes mellitus (T1DM) is a complex metabolic disorder resulting from autoimmune loss of pancreatic β-cells, affecting more than 20 million people worldwide. Effects of chronically elevated blood glucose are not only seen in peripheral organs but also in the brain. It has been shown that people with T1DM have decreased mental speed and flexibility [39,72,73]. Glucose homeostasis is modulated through the actions of two hormones: insulin and glucagon. In recent years it has been shown that beyond islet-centric glucose regulation, various brain nuclei, most notably in hypothalamus and brainstem, are involved in insulin-independent glucose homeostasis [2–4,87,148,149]. The dorsal vagal complex (DVC) is a brainstem nucleus that has been shown to participate

in glucose and energy homeostasis [15,97,151–154]. The DVC is the hub of parasympathetic visceral regulation as it receives sensory information from the viscera through afferent vagal branches and can modulate visceral functions through parasympathetic motor neurons. T1DM results in a sustained increase in glutamate and glutamate-induced GABA release in the DVC [165,168,169] and, as shown in Chapter 3, modulation of GABAergic neurons in the DVC alters peripheral glucose concentration via the parasympathetic nervous system.

Given the importance of glucose as a precursor for various macromolecules, the central role that the DVC plays in insulin-independent glucose homeostasis and the effects of hyperglycemia on mental flexibility, we investigated the effects of hyperglycemia on metabolome and glucose flux in several brain regions: neocortex, hippocampus and DVC, as well as peripheral organs. We hypothesized that hyperglycemia would lead to glucose hypometabolism in the brain in the neocortex and hippocampus but not the DVC. Utilizing untargeted metabolomics we found that glucose concentration was significantly elevated across all regions but glycogen and glucose-6-phosphate remained unchanged with hyperglycemia only in DVC. Interestingly pyruvate and lactate were unchanged across all regions indicating that hyperglycemia does not affect anaerobic cellular respiration. Intermediates of the tricarboxylic acid (TCA) malate and fumarate are significantly decreased with hyperglycemia only in DVC, suggesting that hyperglycemia in DVC preferentially affects TCA cycle. Furthermore, we observed a significant decrease in glutamate across all regions while glutamine and GABA were unchanged, suggesting neurotransmitter regulation disturbance. Stable isotopic tracing of uniformly labeled $^{13}C_6$ glucose was employed to assess carbon flux in different brain regions perturbed by T1DM to understand its effect on glycolysis, tricarboxylic acid cycle, and neurotransmitter synthesis. We found that hyperglycemia results in metabolic reprogramming with a

significant decrease in glucose utilization and we demonstrated decrease in immunofluorescent labeling of GLUT2, a neuronal glucose transporter, as well as enzymes pyruvate dehydrogenase and pyruvate carboxylase, responsible for anaplerosis of TCA cycle intermediates, indicating glucose hypometabolism phenotype.

4.3   Materials and Methods

4.3.1   Chemicals and Reagents

HPLC grade methanol (34860-4X4L-R) and methoxyamine hydrochloride (226904-25G) were purchased from Sigma Aldrich (Burlington, MA, USA). Silylation Reagents, MSTFA + 1% TMCS Reagent (TS-48915) and pyridine (TS-27530) were purchased from Thermo Fisher Scientific (Waltham, MA, USA). Amber vials (5184-3554), blue screw caps (5182-0717) were purchased from Agilent Technologies (Santa Clara, CA, USA). Streptozotocin (572201) PBS (P3813) , Triton X (X100), Tween 20 (P1379) were purchased from Sigma-Aldrich (St. Louis MO). Sodium citrate dihydrate (BP327), Citric acid anhydrous (A940), normal goat serum (31873) and OCT compound (23-730-571), 2-methylbutane (019387AP), and ProlongGlass (P36984) were purchased from Thermo Fisher Scientific. [U-^{13}C] Glucose was obtained from Cambridge Isotope Laboratories (Tewksbury, MA, USA).

4.3.2   Animals

All experiments were performed on either male Vgat-ires-Cre knock-in mice (Slc32a1tm2(cre)lowl/J, 016962, The Jackson Laboratory, Bar Harbor, ME) or C57BL6 mice (000664, The Jackson Laboratory). Mice were housed and cared for in the University of Kentucky Division of Laboratory Animal Resources facilities under normal 14:10 light-dark conditions with food (Tekad 2018, Indianapolis, IN) and water available ad libitum,

except where noted and accordaning to protocols approved by the University of Kentucky Animal Care and Use Committee.

4.3.3 Induction of hyperglycemia and in vivo glucose assessment

At 6 weeks of age, mice were injected with streptozotocin (STZ, 200mg/kg, i.p., Sigma-Aldrich, St. Louis, MO) in citric acid (CA, 0.1M), after a 6 hour fast. Mice were monitored daily for weight and blood glucose levels. Blood glucose levels were measured by handheld glucometer (Nova Max Plus, received from American Diabetes Wholesale, Pompano Beach, FL), using $0.3\mu L$ of blood from the tail vein. Nova Max glucose test strips were used (#8548043523, ADW Diabetes, Pompano Beach, FL). Levels above 300mg/dL were considered hyperglycemic. Mice were used for experiments after at least 14 days (14-16 days) of hyperglycemia.

4.3.4 Gavage of [U-^{13}C] glucose

[U-^{13}C] Glucose was dissolved in ddH$_2$O (Millipore Milli-Q, Bedford, MA, USA) based on the average mouse cohort bodyweight (2 g [U-^{13}C] glucose/kg bodyweight). After a 3 hour fast, 250 µL of glucose solution was administered via oral gavage. Tissues were collected at 30 minutes and 2 hours post-gavage. Blood glucose levels were measured before fasting, at tracer delivery and before microwave was used.

4.3.5 Microwave fixation

Mice were euthanized by microwave fixation at 5kHz for 0.6 seconds (MMW-05, Muromachi Kikai Company, Japan). Brain regions (hippocampus, neocortex, DVC), as well as muscle and liver, were dissected postmortem.

4.3.6 Immunofluorescence

Separate cohort of mice were briefly exposed to anesthesia until sedated and transcardially perfused with Heparin-PBS (10 units/mL), followed by 4% PFA. Tissue was

post-fixed for 24 hours in 4%PFA and then cryoprotected with 30% sucrose in 0.01M PBS. The tissue was frozen with isopentanes and cut at 20μm with a sliding microtome. Staining was done free-floating in 24-well plates without inserts. Three sections of the brain and 4 sections of brainstem tissue, serially cut into 8 wells was rinsed with 0.01M PBS, incubated for 1 hour in 5% normal goat serum in 0.3% Triton X-100 in PBS. The tissue was then incubated at room temperature in the primary antibody (table 4.1) diluted in 1% normal goat serum, followed by 3 x 15 minutes rinses in 0.05% Tween-20 in PBS. Tissue was then incubated for 1 hour in secondary antibody diluted in 1% normal goat serum in PBS. For multiple labeling, primary antibodies were incubated for 2 hours, and secondary antibodies for 1 hour. Tissue was then exposed to DAPI for 5 minutes, mounted on the slides and cover slipped with Prolong Glass.

Digital images were acquired through the Zeiss Axio Scan Z.7 digital slide scanner at 20X magnification and 12 Z-stacks. Figures were captured using HALO software (v3.3.2541.345, Indica Labs, Albuquerque, NM). Analysis was done by outlining the regions of interest in the HALO software and quantifying the positive pixels. Regions of interest included cortex, retro-splenial cortex hippocampus, CA1, CA2 and CA3 and DVC, and were defined by using Allen Mouse Brain Reference Atlas.

Table 4.1. Primary Antibodies

Primary antibodies	Host	Company and catalog #	Dilution	Conditions
GLUT1	Rabbit	Abcam ab115730	1:200	Overnight, RT
GLUT2	Rabbit	Novus NBP2-22218	1:200	Overnight, RT
GLUT3	Rabbit	Alomone AGT-023	1:200	Overnight, RT
Pyruvate Carboxylase	Rabbit	GeneTex GTX121987	1:200	Overnight, RT
Pyruvate Dehydrogenase (ser 293)	Rabbit	EMD Milipore AP1062	1:200	Overnight, RT
NeuN	Mouse	Abcam ab279295	1:1000	1 hrs, RT
NeuN	Rabbit	Abcam ab236870	1:1000	1 hrs, RT
GFAP	Chicken	GeneTex GTX85454	1:2000	2 hrs, RT
DAPI		Novus NBP2-31156	1:5000	5 min, RT

Table 4.2. Secondary Antibodies

Secondary antibodies	Fluorophore	Company and catalog #	Dilution	Conditions
Goat anti-chicken	Alexa 594	A-11042	1:400	1hr, RT
Goat anti-rabbit	Alexa 488	A-11034	1:400	1hr, RT
Goat anti-mouse IgG	Alexa 647	A-21236	1:400	1hr, RT

4.3.7   Metabolomics Sample Preparation

Brains were removed aftrer microwave fixation, separated into regions of interest (neocortex, hippocampus, DVC), and washed once with PBS, twice with diH_2O, blotted dry, and snap frozen in Liquid nitrogen. The frozen tissues were pulverized to 10 µm particles in liquid N_2 using a Freezer/Mill Cryogenic Grinder (SPEX SamplePrep). Brain regions were extracted with 1ml of 50% methanol in the grinder, while for muscle and liver twenty milligrams of each pulverized tissue were extracted in 1ml of 50% methanol and separated into polar (aqueous layer), and protein/DNA/RNA/glycogen pellet. The polar fraction was dried at 10^{-3} mBar using a SpeedVac (Thermo) followed by derivatization.

4.3.8 Pellet Hydrolysis

Hydrolysis of the protein/DNA/RNA/glycogen pellet was performed by first resuspending the dried pellet in diH$_2$O followed by the addition of equal parts 2N HCl. Samples were vortexed thoroughly and incubated at 95°C for 2 hours. The reaction was quenched with 100% methanol with 40μM L-norvaline (as an internal control). The sample was incubated on ice for 30 minutes and the supernatant was collected by centrifugation at 15,000rpm at 4°C for 10 minutes. The collected supernatant was subsequently dried for 4 hours by vacuum centrifuge at 10^{-3} mBar.

4.3.9 Sample Derivatization

Dried polar and glycogen samples were derivatized by the addition of 20mg/ml methoxyamine hydrochloride in pyridine and sequential addition of N-methyl-trimethylsilyl-trifluoroacetamide (MSTFA). Both reactions were incubated for 60 minutes at 60°C with thorough mixing in between addition of solvents. The mixture was then transferred to a v-shaped amber glass chromatography vial and analyzed by GCMS.

4.3.10 GCMS Quantification

GCMS protocols were similar to those described previously [190,191], except a modified temperature gradient was used for GC: Initial temperature was 130°C, held for 4 minutes, rising at 6°C/minutes to 243°C, rising at 60°C/minutes to 280°C, held for 2 minutes. The electron ionization (EI) energy was set to 70 eV. Scan (m/z:50-800) and full scan mode were used for metabolomics analysis. Automated Mass Spectral Deconvolution and Identification System (AMDIS) software in combination with FiehnLib metabolomics library was utilized to translate mass spectra into relative metabolite abundance. Metabolites were matched for retention time and fragmentation pattern with a confidence score of > 80 [192–194]. Data was further analyzed using the Data Extraction for Stable Isotope-labelled Metabolites (DEXSI) software package [195]. Untargeted

metabolomics data was normalized to total ion chromatogram and performed as described in Young et al [196]. For glucose tracer raw data was exported and corrected for natural abundance was done in IsoCorrectoR [197]. Fractional enrichment of each metabolite was calculated as the relative abundance of each isotopologue relative to the sum of all other isotopologues. Mean enrichment was calculated as sum of fractional enrichment of labeled isotopologues (m+1, m+2, m+3…). For principal component analysis and pathway impact analysis the online tool Metaboanlyst was used (https://www.metaboanalyst.ca/). Data was was auto-scaled and log transformed.

4.3.11 Statistics

Statistical analyses were carried out using GraphPad Prism, student t-test. All numerical data are presented as mean ± SEM. A P-value less than 0.05 was considered statistically significant.

4.4   Results

4.4.1   Pooled metabolomics analysis of brain regions in a mouse model of T1DM

T1DM is a peripheral disease that is characterized by the lack of insulin production and persistent high circulating blood glucose. To study the impact of T1DM on brain glucose metabolism, we utilized the STZ model of insulin impairment and hyperglycemia in mice and performed untargeted analysis of metabolite pools using GCMS. Mice were randomly assigned to two groups (n=8), one that was injected intraperitoneally (IP) with vehicle (citric acid, CA), and another with a single dose of STZ (200mg/kg) to induce artificial hyperglycemia for 14 days to mimic T1DM (Fig 4.1A-B). Both cohorts of mice were euthanized and fixed by microwave fixation followed by surgical resection of multiple brain

regions (DVC, hippocampus, and neocortex) as well as peripheral organs (muscle and liver). We observed increases only in glucose and leucine across all brain regions.

To understand the difference or similarities in our large data set we first carried out an unsupervised principal component analysis (PCA). The role of PCA is to reduce the number of variables of a data set while preserving as much information as possible. It is a statistical tool to allow us to look at difference and similarities of large data sets. Each dot represents a biological replicate for the particular group, with shading indicating the 95% confidence interval of the data set. Overlap in the data sets indicates metabolic similarity, while distance indicates metabolic diversity. Our data shows that DVC is metabolically different from the other brain regions, and T1DM drives metabolic reprogramming differently (Fig 4.1).
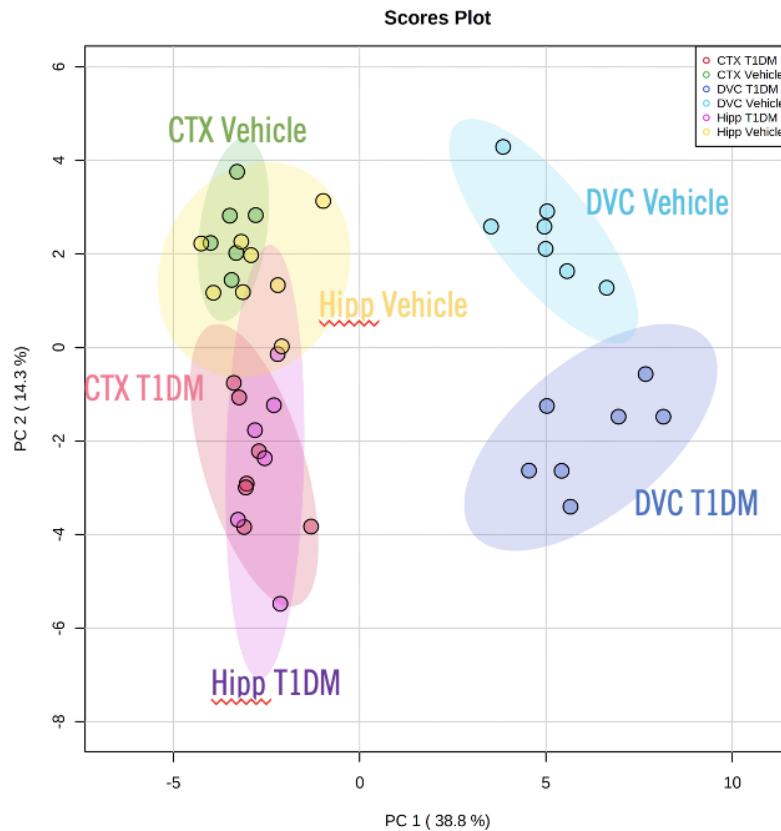
Figure 4.1 PCA of mouse brain regions from a model of T1DM.

To understand which metabolites, drive the metabolomic reprogramming across the regions, we evaluated changes in each metabolite and changes within pathways. Utilizing untargeted metabolomics we found that glucose concentration was significantly elevated across all regions but glycogen and glucose-6-phosphate remained unchanged with hyperglycemia only in DVC (Fig. 4.2C-D). Interestingly, pyruvate and lactate were unchanged across all regions indicating that hyperglycemia does not affect anaerobic cellular respiration. Intermediates of the tricarboxylic acid (TCA) malate and fumarate are significantly decreased with hyperglycemia only in DVC, suggesting that hyperglycemia in DVC preferentially affects TCA cycle. Furthermore, we observed a significant decrease in glutamate across all regions while glutamine and GABA were unchanged, suggesting neurotransmitter regulation disturbance (Fig. 4.2C-D). We observed changes in multiple glycolytic and TCA cycle metabolites in the liver, but not in muscle, where the only major difference was that T1DM increased glucose and leucine while decreasing lactate and pyruvate (Fig. 4.3). Collectively, our data suggest that the DVC has a unique metabolomic profile and that STZ-induced hyperglycemia mouse model predominately impacts TCA metabolites in the DVC.
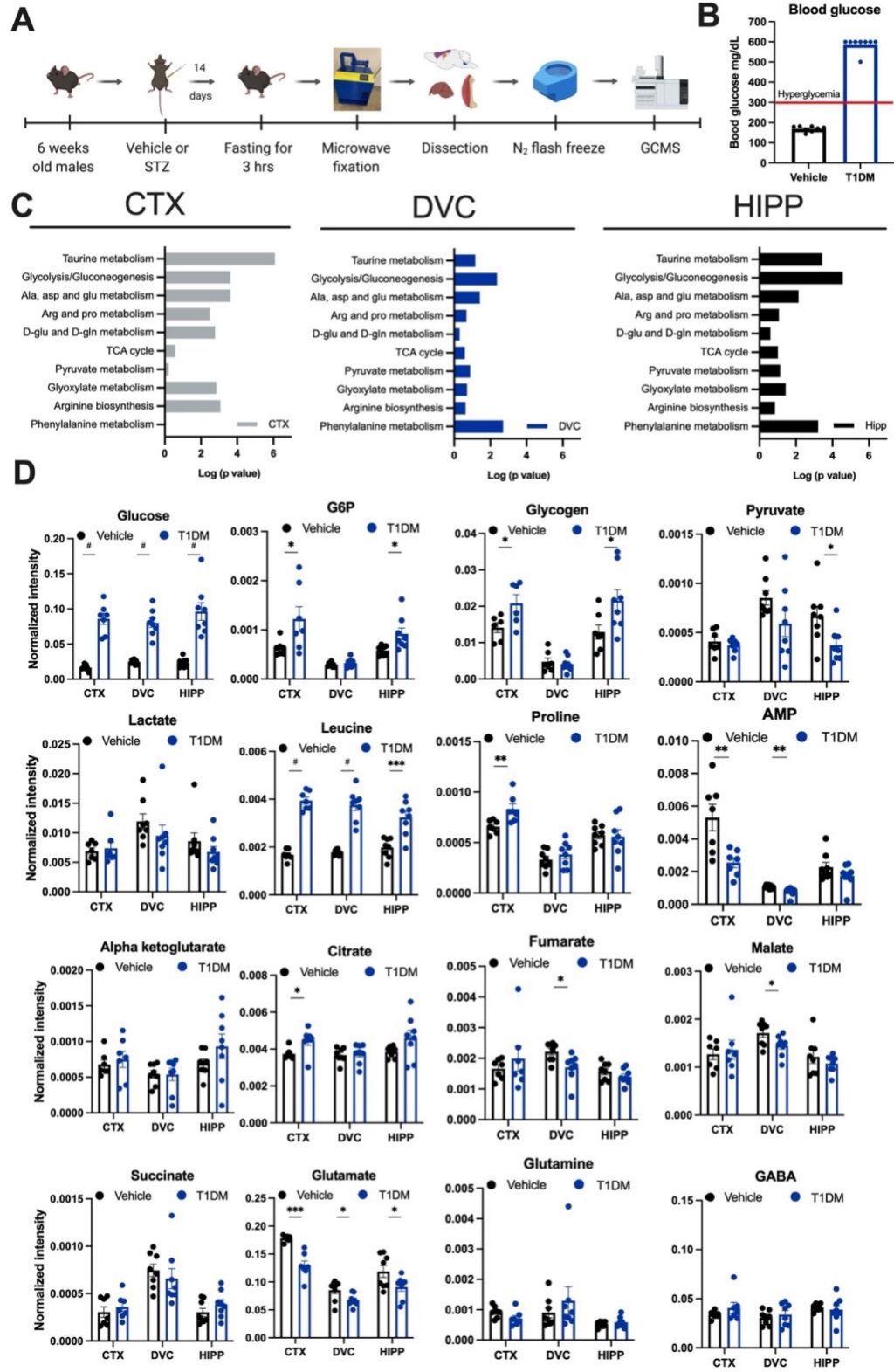
Figure 4.2 Pooled metabolomics analysis of mouse brain from a model of T1DM using high power focused microwave fixation (HPFM).

(**A**) Schematic of the experimental design. 6-week-old mice were injected with either vehicle or 200mg/kg of streptozotocin (STZ) to induce hyperglycemia. After 14 days mice were fasted for 3 hrs and euthanized by HPFM. Brain regions were then dissected, flash-frozen, and analyzed by GCMS. (**B**) Blood glucose levels measured by hand-held glucometer in vehicle and T1DM mice after 14 days of hyperglycemia (n=8 biological replicates per treatment). (**C**) Pathway analysis (performed by Metaboanalyst) of neocortex (CTX), dorsal vagal complex (DVC), and hippocampus (HIPP) brain regions between vehicle treated and T1DM mice. (**D**) Representative metabolite levels from glycogen metabolism, glycolysis, and TCA cycle between vehicle and T1DM. Values are presented as mean $\pm$ SEM (n=6-8 biological replicates), *$p<0.05$, **$p<0.01$, ***$p<0.001$, [#]$p<0.0001$, analyzed by student t-test.

A

SKM

Taurine and hypotaurine metabolism
Gluthathione metabolism
D-glu and D-gln metabolism
Gly, ser, thr metabolism
TCA cycle
Ala, asp and glu metabolism
Arginine biosynthesis
Pyruvate metabolism
Glyoxylate metabolism
Arg and pro metabolism
Glycolysis/Gluconeogenesis

SKM

Log (p value)
0 2 4 6 8 10

Liver

Taurine and hypotaurine metabolism
Gluthathione metabolism
D-glu and D-gln metabolism
Gly, ser, thr metabolism
TCA cycle
Ala, asp and glu metabolism
Arginine biosynthesis
Pyruvate metabolism
Glyoxylate metabolism
Arg and pro metabolism
Glycolysis/Gluconeogenesis

Liver

Log (p value)
0 2 4 6 8 10

B

Vehicle

T1DM

Vehicle

T1DM

C

65

Figure 4.3 Pooled metabolomics analysis of skeletal muscle (SKM) and liver from a model of T1DM using high power focused microwave fixation (HPFM).

(**A**) Pathway analysis (performed by Metaboanalyst) of SKM and liver between vehicle and T1DM. (**B**) Partial Least Squares-Discriminant Analysis (PLS-DA) of SKM and liver metabolites between vehicle and T1DM animals (n=6-8). (**C**) Representative metabolite levels from glycogen metabolism, glycolysis, and TCA cycle between vehicle and T1DM. Values are presented as mean $\pm$ SEM (n=6-8 biological replicates), *$p<0.05$, **$p<0.01$, ***$p<0.001$, #$p<0.0001$, analyzed by student t-test. G6P: glucose 6-phosphate, PEP: phosphoenolpyruvate, AMP: adenosine phosphate

4.4.2 Tracing $^{13}C_6$-glucose metabolism in the brain of a mouse model of T1DM

Metabolic pathways are interconnected within a cell and metabolite pools can be replenished through different metabolic substrates [186]. The TCA cycle metabolite pools can be replenished from glucose, glutamine, and fatty acid metabolism. Therefore, pooled metabolomics analysis does not fully illuminate unique substrate metabolism such as glucose. T1DM is primarily a disease of hyperglycemia; therefore it is crucial to define the glucose contribution to different metabolite pools. To assess whether there are differences in glucose metabolism between vehicle and STZ treated mice we performed an additional animal experiment with vehicle (citric acid) and STZ. Stable isotope tracing was performed by delivery of $^{13}C_6$-glucose through oral gavage and collection of brain regions (neocortex, hippocampus and DVC) as well as muscle and liver at either 30 min or 2 hours post gavage (Fig 4.4A-B). Similar to above, all cohorts of mice were euthanized and fixed in situ with focused microwave and followed by brain regional dissection and peripheral organ extraction. We observed significant decreases in glucose enrichment in central carbon metabolites and *de novo* synthesized amino acids. This phenotype was consistent across the neocortex, hippocampus, and the DVC for both time points (Fig. 4.4C-E, Fig. 4.5) as well as in peripheral organs (Fig. 4.6). Further, M2 and M3 isotopologues of citrate, malate, fumarate, glutamine, glutamate, and aspartate all exhibit a decrease with hyperglycemia compared to the vehicle at both time points (Fig. 4.4C-E, Fig. 4.5). This suggests down-regulation of pyruvate dehydrogenase and pyruvate carboxylase activity in STZ-induced hyperglycemia (T1DM) in multiple brain regions.
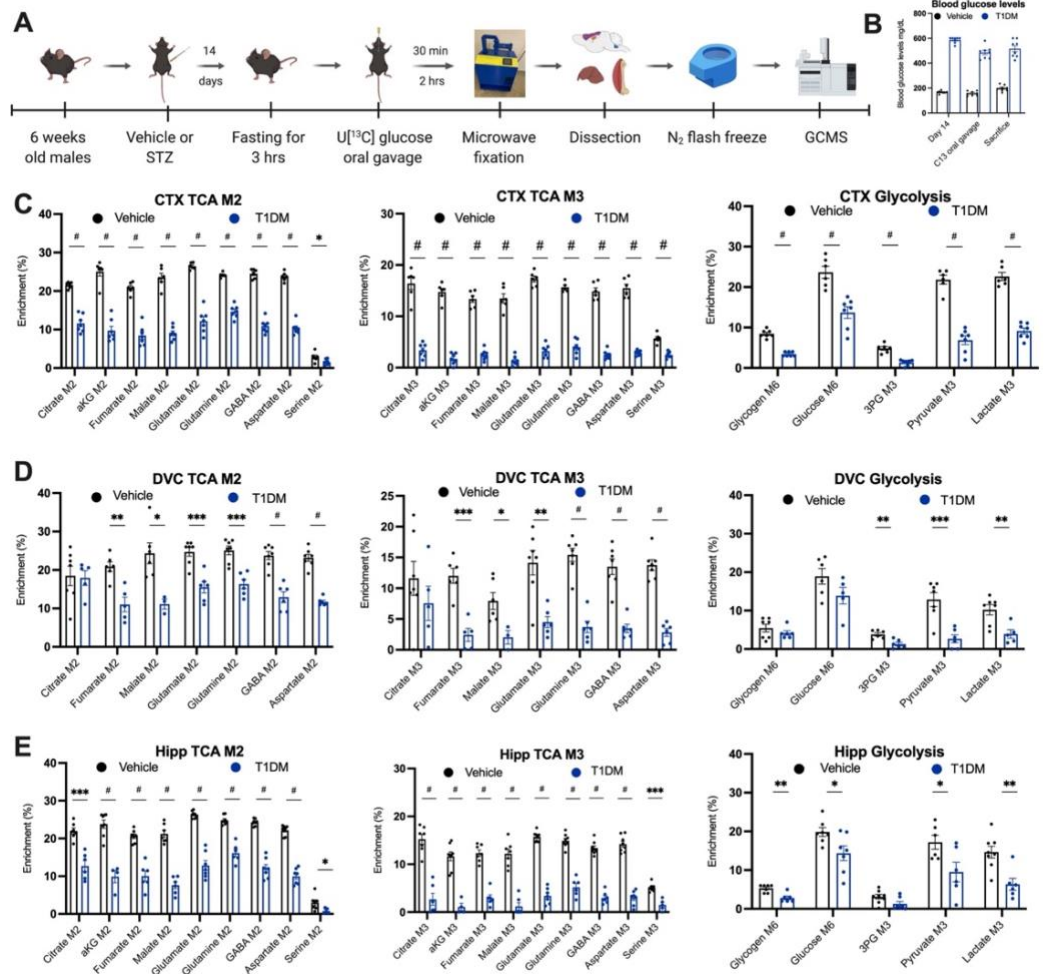
Figure 4.4 Stable isotope labeling in the brain of a mouse model of T1DM at 2 hrs.

(**A**) Schematic of the experimental design. 6-week-old mice were injected with either vehicle or 200mg/kg of streptozotocin (STZ) to induce hyperglycemia. After 14 days mice were fasted for 3 hours, gavaged with $^{13}C_6$-glucose and euthanized by high power fixation microwave (HPFM). Brain regions were then dissected, flash-frozen, and analyzed by GCMS. (**B**) Blood glucose levels were measured by hand-held glucometer before fasting, before tracer gavage delivery, and before microwave fixation (n=8). (**C-E**) Representative isotopologue for M6 of glycogen, glucose, and, M2 of citrate, aKG fumarate, malate, glutamate, glutamine, GABA, aspartate and serine, and M3 of 3PG, pyruvate, lactate, citrate, aKG, fumarate, malate, glutamate, glutamine, GABA, aspartate and serine for

three brain regions, neocortex (CTX) (**C**), dorsal vagal complex (DVC) (**D**), and hippocampus (Hipp) (**E**) of T1DM animals. Values are presented as mean $\pm$ SEM (n=6-8 biological replicates), *p<0.05, **p<0.01, ***p<0.001, [#]p<0.0001, analyzed by student t-test. 3PG:3-phosphoglyceric acid, aKG: alpha-ketoglutarate.
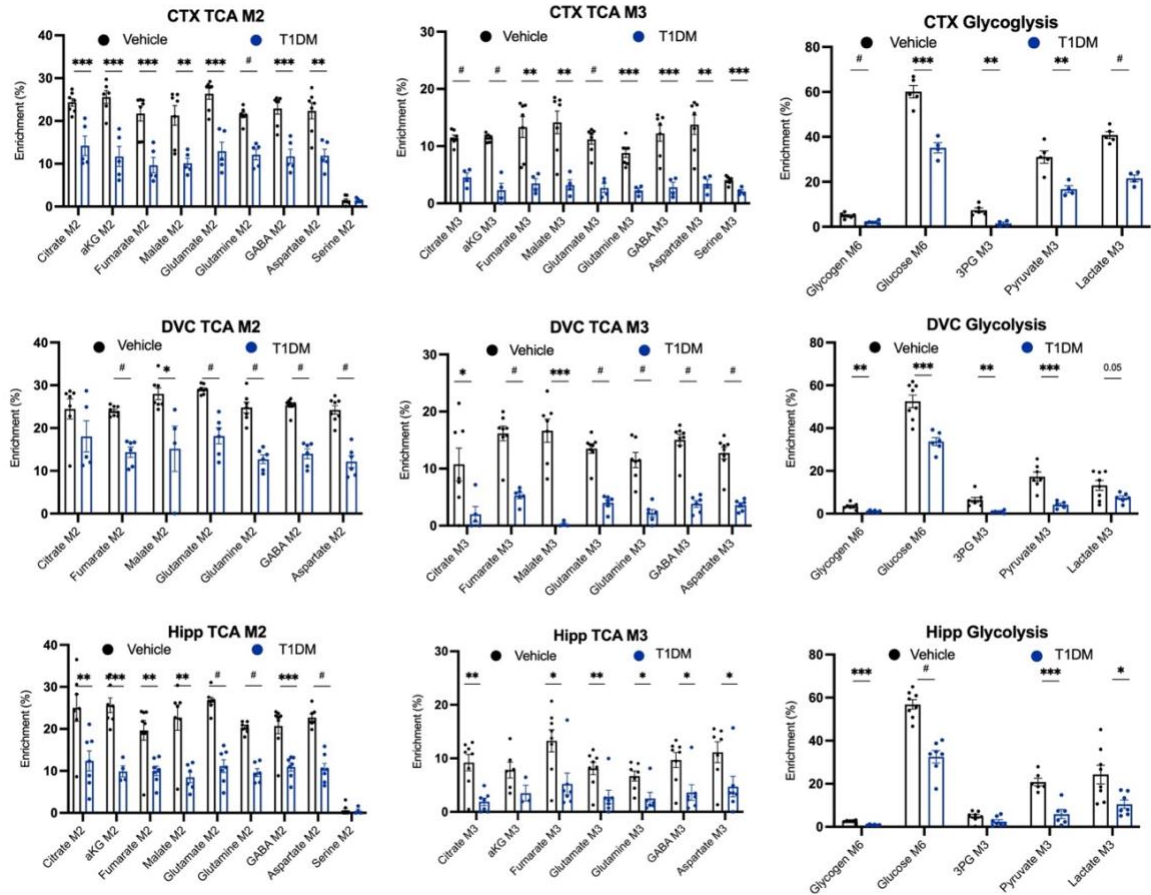
Figure 4.5 Stable isotope labeling in the brain of a mouse model of T1DM using HPFM at 30 min.

Representative isotopologue for M6 of glycogen, glucose, and, M2 of citrate, aKG, fumarate, malate, glutamate, glutamine, GABA, aspartate and serine, and M3 of 3PG, pyruvate, lactate, citrate, aKG, fumarate, malate, glutamate, glutamine, GABA, aspartate and serine for three brain regions, neocortex (CTX), dorsal vagal complex (DVC) and hippocampus (HIPP) of T1DM animals. Values are presented as mean $\pm$ SEM (n=4-7 biological replicates), *p<0.05, **p<0.01, ***p<0.001, #p<0.0001, analyzed by student t-test. 3PG:3-phosphoglyceric acid, aKG: alpha-ketoglutarate.
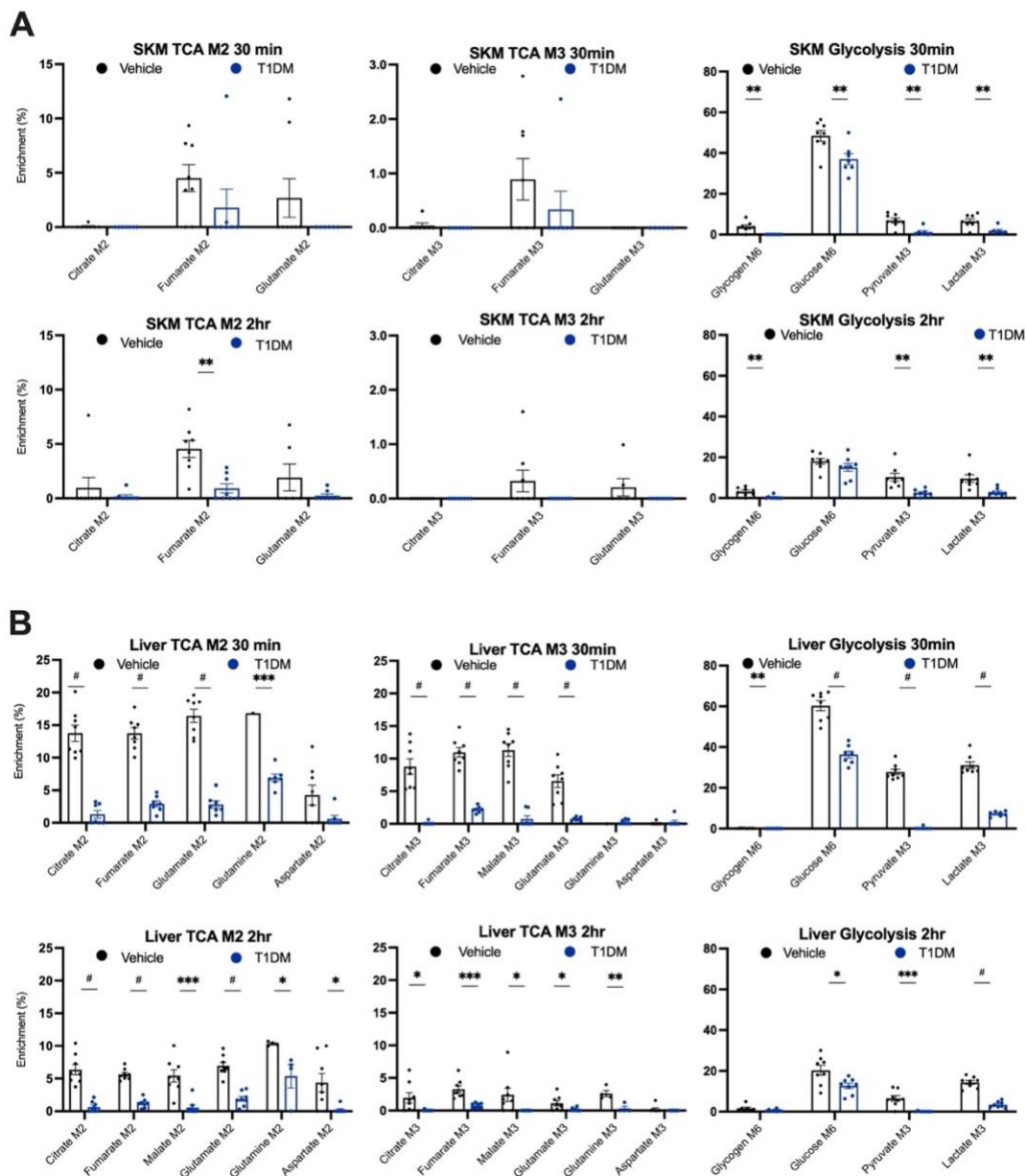
Figure 4.6 Stable isotope labeling at 30 min and 2 hrs in T1DM mice in skeletal muscle (SKM) (A) and liver (B).

Representative isotopologue for M6 of glycogen, glucose, and, M2 of citrate, fumarate, malate, glutamate, glutamine, and aspartate, and M3 of pyruvate, lactate, citrate, fumarate, malate, glutamate, glutamine, and aspartate for SKM and liver of T1DM animals. Values are presented as mean ± SEM (n=7-8 biological replicates), *p<0.05, **p<0.01, ***p<0.001, #p<0.0001, analyzed by student t-test.
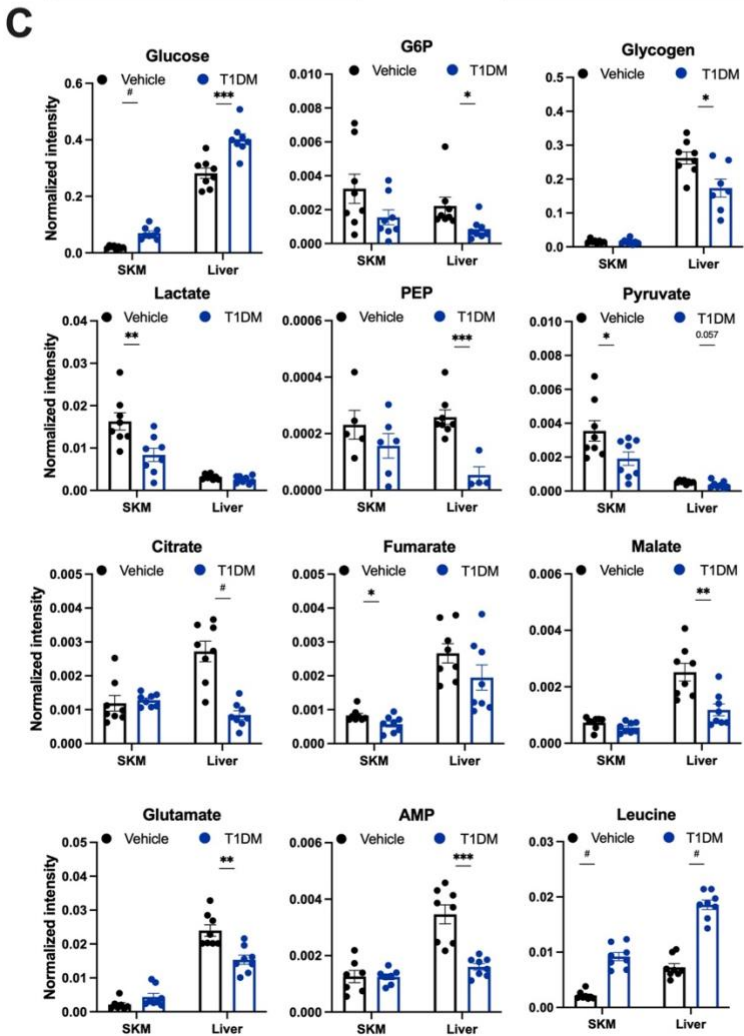
4.4.3 Downregulation of GLUT2, PDH, and PC proteins in unique neuronal cell layers.

The power of stable isotopic tracing is the direct assessment of metabolic enzyme activities, through fractional enrichment, i.e. M2 and M3 isotopologues of citrate represent PDH and PC activities, respectively. STZ-induced hyperglycemia mice show decreased glucose enrichment in central carbon metabolites and reduced M2 and M3 isotopologues of citrate (Fig 4.4). Therefore, we continued to evaluate glucose transporters, PDH, and PC protein expressions in cortical and hippocampal regions using immunofluorescence (IF). First, we performed IF on GLUT1, GLUT2, and GLUT3 glucose transporters that have been shown to be increased with hyperglycemia in peripheral tissues [198–200]. Our hypothesis was that glucose transporters would be decreased, as we have shown with stable isotopic tracing that T1DM results in hindered glucose incorporation in all regions of the brain across all central carbom metabolism pathways. We did not observe significant changes in GLUT1 and GLUT3 expression in different brain regions (Fig 4.8). However, GLUT2, a neuronal glucose transporter, showed a 15% to 70% decrease across cortical/hippocampal regionals and the DVC (Fig. 4.9D). We saw a similar decrease in PDH and PC protein by IF in cortical regions and the DVC (Figure 4.8L and Fig. 4.9H). Interestedly, CA3 neuronal layer of the hippocampus was the only sub-region affected by hyperglycemia, while CA1 and CA2 layers show no differences in protein expression between PC and PDH assessed by IF (Figure 4.8B and Fig. 4.9). Collectively, these data suggest STZ-induced hyperglycemia results in downregulation of metabolic enzymes PDH and PC at the protein level, as well as glucose transporter downregulation that correlate with glucose hypometabolism of the brain.

72
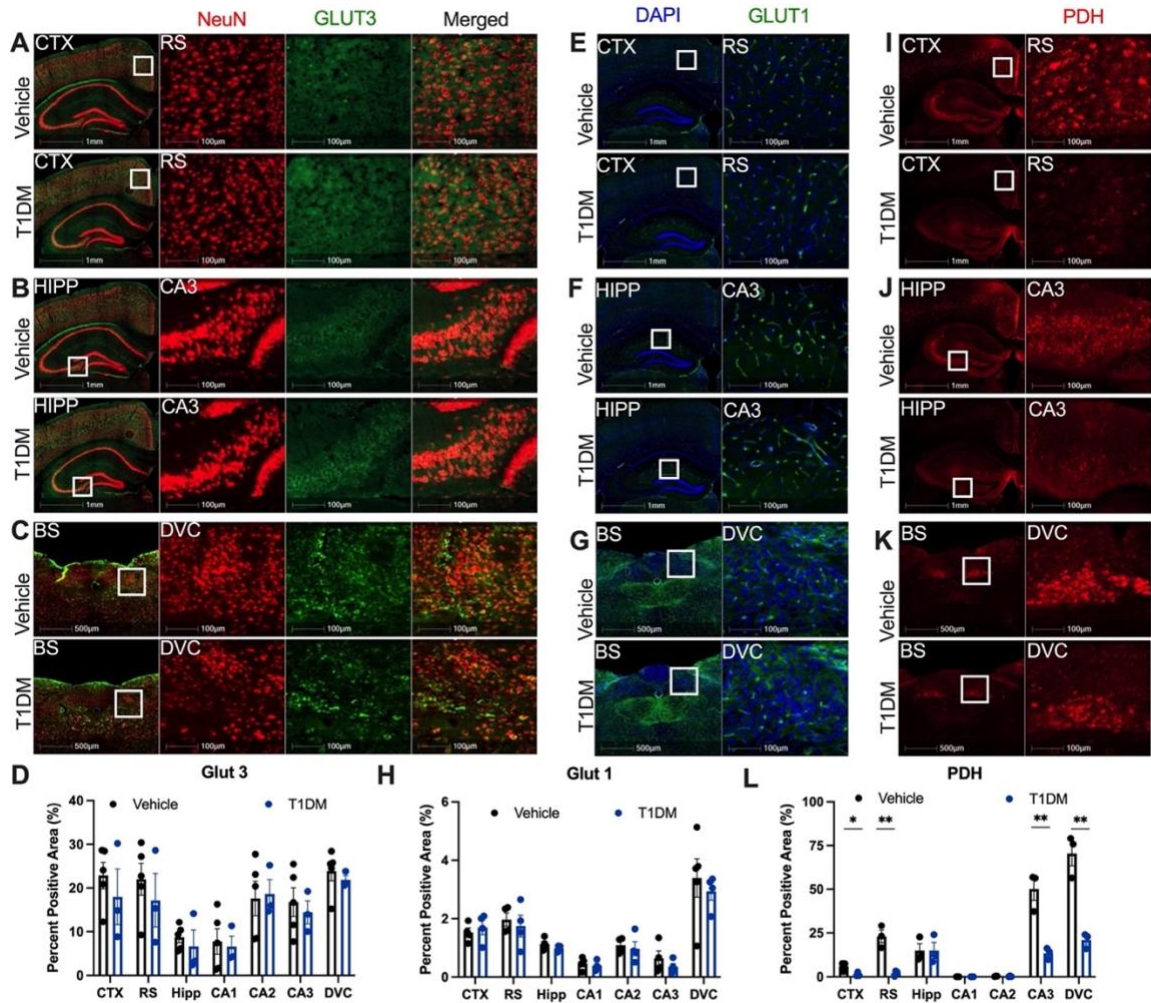
Figure 4.8 Immunofluorescent analysis of GLUT3, GLUT1 and PDH expression in neocortex (CTX), hippocampus (HIPP) and brainstem (BS) in a mouse model of T1DM.

(**A-D**) 20μm coronal sections of the mouse brain were stained with GLUT3 (green) and NeuN (red) and quantified in the CTX (**A**), HIPP (**B**), and BS (**C**). Zoomed-in images are shown for the retro-splenial cortex (RS), Cornu Ammonis 3 (CA3) of HIPP, and dorsal vagal complex (DVC) of BS. (**D**) Quantification of % positive pixels for Glut3 using HALO software, area of interest include whole cortex, RS (zoomed in), whole HIPP, CA1-CA3 (zoomed in), and DVC following mouse brain atlas, and quantification was run for positive pixels in each channel and colocalization. Values are presented as mean ± SEM (n=4

biological replicates), *p<0.05, **p<0.01, ***p<0.001, analyzed by student t-test. (**E-H**) 20μm coronal sections of the mouse brain were stained with GLUT1 (green) and DAPI (blue) and quantified in the CTX (**E**), HIPP (**F**), and BS (**G**). Zoomed-in images are shown for the RS, CA3 of HIPP, and DVC of BS. (**H**) Quantification of % positive pixels for GLUT1 using HALO software, area of interest including whole neocortex, RS (zoomed in), whole HIPP, CA1-CA3 (zoomed in), and DVC following mouse brain atlas, and quantification was run for positive pixels in each channel and colocalization. Values are presented as mean ± SEM (n=4 biological replicates), *p<0.05, **p<0.01, ***p<0.001, analyzed by student t-test. (**I-L**) 20μm coronal sections of the mouse brain were stained with PDH (red) and quantified in the CTX (**I**), HIPP (**J**), and BS (**K**). Zoomed-in images are shown for the retro-splenial cortex (RS), CA3 of HIPP, and DVC of BS. (**L**) Quantification of % positive pixels for PDH using HALO software, area of interest include whole cortex, RS (zoomed in), whole HIPP, CA1-CA3 (zoomed in), and DVC following mouse brain atlas, and quantification was run for positive pixels in each channel and colocalization. Values are presented as mean ± SEM (n=4 biological replicates), *p<0.05, **p<0.01, ***p<0.001, analyzed by student t-test. Scale bars are either 1mm, 500μm, or 100μm. GLUT1-glucose transporter 1, GLUT3-glucose transporter 3, PDH-pyruvate dehydrogenase.
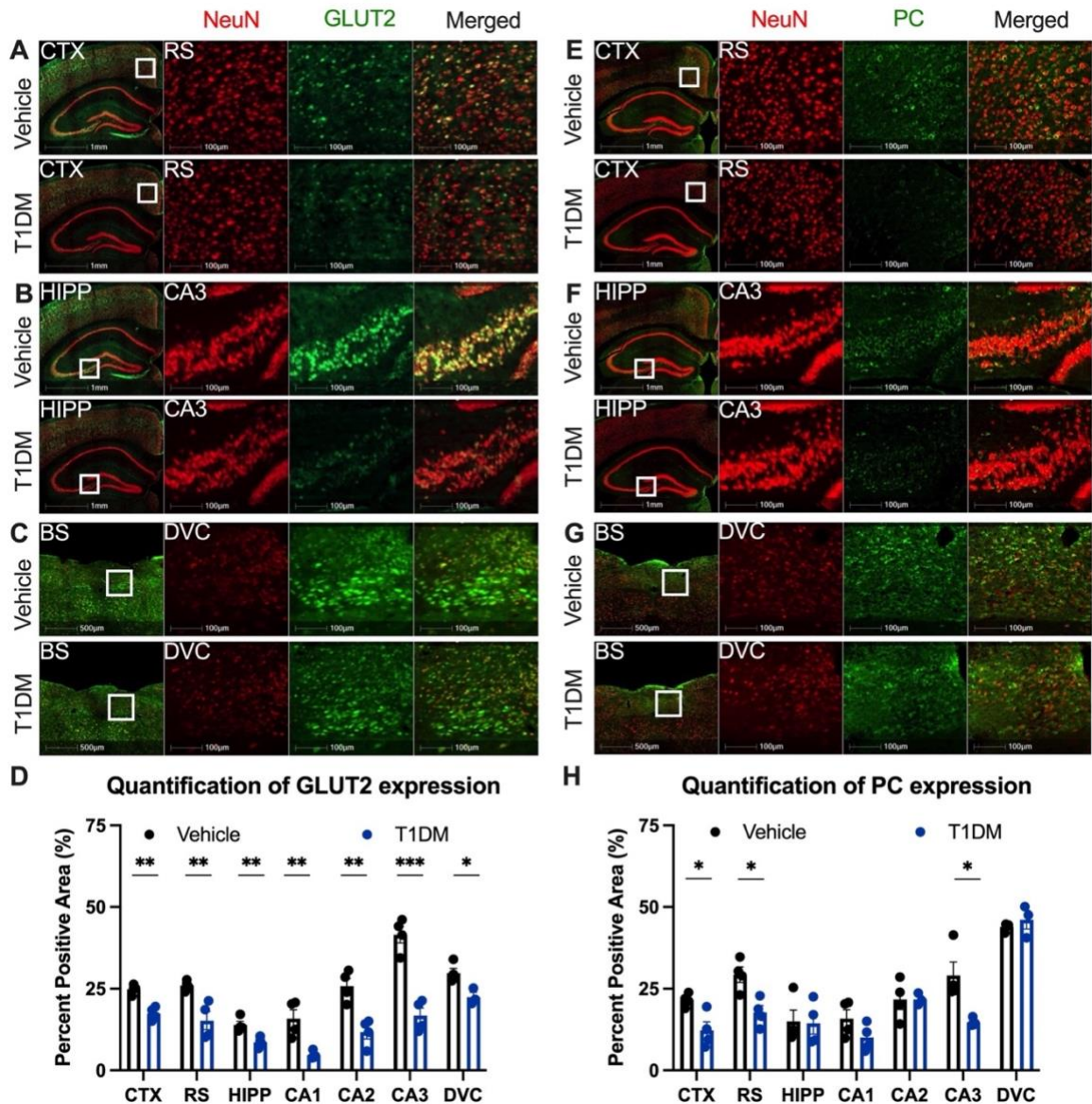
Figure 4.9 Immunofluorescent analysis of GLUT2 and PC expression in neocortex (CTX), hippocampus (HIPP) and brainstem (BS) in a mouse model of T1DM.

(A-D) 20μm coronal sections of the mouse brain were stained with GLUT2 (green) and NeuN (red) and quantified in in the CTX (A), HIPP (B), and BS (C). Zoomed-in images are shown for the retro-splenial cortex (RS), Cornu Ammonis 3(CA3) of HIPP, and dorsal vagal complex (DVC) of BS. (D) Quantification of % positive pixels for GLUT2 using HALO software, area of interest include whole cortex, RS (zoomed in), whole HIPP, CA1-CA3 (zoomed in), and DVC following mouse brain atlas, and quantification was run for positive

pixels in each channel and colocalization. Values are presented as mean ± SEM (n=4 biological replicates), *p<0.05, **p<0.01, ***p<0.001, analyzed by student t-test. (E-H) 20 μm coronal sections of the mouse brain were stained with pyruvate carboxylase (PC) (green) and NeuN (red) and quantified in in the CTX (E), HIPP (F), and BS (G). Zoomed in image are shown for the RS, CA3 of HIPP, and DVC of BS. (H) Quantification of % positive pixels for PC using HALO software, area of interest including whole neocortex, RS (zoomed in), whole HIPP, CA1-CA3 (zoomed in), and DVC following mouse brain atlas, and quantification was run for positive pixels in each channel and colocalization. Values are presented as mean ± SEM (n=4 biological replicates), *p<0.05, **p<0.01, ***p<0.001, analyzed by student t-test. Scale bars are either 1mm, 500μm, or 100μm. PC: pyruvate carboxylase, GLUT2: glucose transporter 2.

4.5   Discussion

T1DM affects about 20 million people worldwide and chronic hyperglycemia leads to micro/macro-vascular diseases, retinopathy, peripheral neuropathy, and liver disease [201]. Recent reports have highlighted the impact of T1DM on brain glucose metabolism as T1DM patients have increased risk of developing late-onset dementia [202]. Glucose hypometabolism is characterized by reduced uptake of 2-fluorodeoxyglucose (FDG), imaged by Positron Emission Tomography (PET), and is a common pathological feature shared among multiple neurological disorders such as Alzheimer's disease (AD) [205], Parkinson's disease [206], temporal lobe epilepsy [207], as well as inherited pediatric neurodegenerative diseases [208].

We interrogated the changes in pooled brain metabolome and more specifically, glucose metabolism using $^{13}C_6$-glucose isotopic tracing in the STZ mouse model of T1DM. We observe reginal changes in pooled metabolites. Glucose was increased across all regions, while glycogen and glucose-6-phosphate was increased in the neocortex and hippocampus but not in DVC. Pyruvate and lactate were unchanged across all regions indicating that hyperglycemia does not affect anaerobic cellular respiration. Intermediates of the tricarboxylic acid (TCA) malate and fumarate are significantly decreased with hyperglycemia only in DVC, suggesting that hyperglycemia in DVC preferentially affects TCA cycle. Furthermore, we observed a significant decrease in glutamate across all regions while glutamine and GABA were unchanged, suggesting neurotransmitter regulation disturbance (Fig. 4.2C-D).

We then performed ^{13}C-glucose tracing through oral gavage. We observed glucose hypometabolism in multiple regions of the brain. Decreased enrichment of glycolytic and TCA cycle isotopologues were noted in multiple regions of the brain including cortex, hippocampus, and DVC. These data are in agreement with multiple previous reports

showing brain glucose hypometabolism in T1DM patients [203], impaired hepatic glycogen accumulation [50–53], glycogenolysis [62,204], and increased hepatic glucose production [54–57].

Furthermore, while glucose metabolism is decreased with T1DM, because glycogen remained unchanged in the DVC it is suggesting alternative fuel sources are being utilized by the DVC in T1DM mice. Within the DVC, isotopic enrichment of glycogen, glucose and citrate remained unchanged. However, $^{13}C_6$ enrichment in the DVC of T1DM animals was significantly decreased in pyruvate and lactate, as well as fumarate, malalte, glutamate, glutamine, GABA and aspartate, suggesting glucose is preferentially oxidized via the TCA cycle. It is worth noting that the DVC is not enclosed within the blood-brain barrier and could have alternative metabolic controls compared to the cortex and hippocampus.

Finally, we have shown that PC and PDH are neuronally expressed enzymes in the brain and significantly downregulated with hyperglycemia. In addition, we have shown that GLUT2 is downregulated across all region (neocortex, hippocampus and DVC). Collectively, these results establish that hyperglycemia drives metabolic reprogramming in the brain and highlights the need to continue investigating how peripheral glucose concentration affects the brain metabolome.

CHAPTER 5. GENERAL DISCUSSION

5.1   Review of major findings

5.1.1   High-powered focused microwave to study brain metabolism

In Chapter 2, we showed that high-power focused microwave (HPFM) fixation preserves the glycolytic metabolome better than traditional decapitation followed by cryo-preservation of brain tissue and is compatible with stable isotopic tracing. We have also shown that HPFM does not change the isotopic enrichment, suggesting that flux was unchanged as the rate of production to utilization was the same.

5.1.2   Systemic glucose regulation by an inhibitory brainstem circuit in a mouse model of T1DM

In Chapter 3, we demonstrated that inhibiting GABAergic neurons was sufficient to lower blood glucose levels in a hyperglycemic mouse model, while activating GABAergic neurons in normoglycemic animals was sufficient to raise blood glucose levels. Interestingly, activating GABAergic neurons in hyperglycemic animals and inhibiting GABAergic neurons in normoglycemic animals resulted in no change in blood glucose levels. We also showed that observed changes in peripheral glucose concentration were mediated by the vagus nerve as administration of MSA, a muscarinic acetylcholine receptor antagonist that cannot cross the blood-brain barrier, abolished the CNO-driven change in blood glucose levels.

5.1.3   Hyperglycemia driven metabolic reprogramming in the brain

In Chapter 4, we demonstrated that T1DM increases glucose and leucine concentration across all brain regions studied. Glycogen and glucose 6-phosphate were only increased in cortex and hippocampus, but not DVC. We observed decreased concentration of glutamate across all regions of the brain but no change in glutamine or GABA levels. However, to our surprise, the vast majority of metabolites analyzed did not

change in abundance. To understand the changes in flux between different pools of metabolites we utilized $^{13}C_6$ tracing and we were able to demonstrate a glucose hypo-metabolic phenotype in the brain. Immunofluorescence labeling revealed a decrease in the expression of the GLUT2 transporter, and colocalization indicated neuronal-specific expression. Notably, both isotopic tracing and immunofluorescence showed a decrease in activity and expression of PC, and PDH enzymes, further indicating a hypometabolic phenotype.

5.2   Hyperglycemia's effect on the expression of glucose transporters in the brain

The majority of brain glucose uptake is insulin-independent [213] and relies on the concentration gradient as the major driving force across blood-brain barrier. When the concentration of glucose increases in the plasma it stands to reason that it will increase in the brain interstitium as well, and our data supports that notion. The majority of the glucose is transported across the BBB by the GLUT1 transporter and previous studies of GLUT1 protein expression have shown a decrease [78,214] or no change in GLUT1 expression in T1DM [76,215,216]. Our immunofluorescent analysis showed no change in GLUT1 between T1DM and vehicle mice in the neocortex, hippocampus, and DVC. This is not surprising given that studies that did find differences were utilizing vessel extraction and not IF. Given that the concentration of glucose within the brain regions of T1DM mice was significantly increased, we expected no change with GLUT1 transporter. Neuronal GLUT3 protein abundance has been shown to increase with STZ-induced hyperglycemia but only in hippocampus [217]. Based on our immunofluorescence analysis of GLUT3 in the brain and brainstem we have shown no changes in GLUT3 expression; however, we observed a profound decrease in GLUT2 expression in the cortex, hippocampus, and DVC. It has been reported that GLUT2 is capable of glucose sensing [161,218–220], and therefore we speculate that the decrease in GLUT2 could be an adaptive response of the body to

prevent excessive glucose uptake, as glucotoxicity could lead to apoptosis [221]. Furthermore, if GLUT2 is responsible for glucose sensing in the brain, the downregulation of the transporter could potentially trick the brain into sensing that the glucose levels are still within normal range, and therefore allow the brain to continue with normal function, despite the high levels of glucose. Lastly, GLUT2 is known to be neuronal, which we confirmed with immunofluorescence colocalization with NeuN. Therefore, the impact of hyperglycemia would be the greatest in neuronal glucose metabolism and could explain the cognitive deficits that are present with T1DM [202,222,223]. Given that DVC is not under the blood-brain barrier and has a significant decrease in GLUT2 expression with T1DM it would stand to reason that increase in peripheral glucose levels with T1DM would not affect glucose utilization during T1DM in the DVC, which is exactly what we have demonstrated with stable isotopic tracing; glucose and glycogen utilization in the DVC with T1DM remains unchanged.

5.3   Role of glucose in anabolic reactions in hyperglycemia

Metabolism can be described as a combination of two opposing processes, anabolism and catabolism. Energy harvested during catabolism is utilized in anabolic reactions. Glucose-derived neurotransmitters include acetylcholine, glutamate, and GABA [28]. We have shown that hyperglycemia results in decreased generation of glutamate and GABA in cortex, DVC and hippocampus. Therefore, one of the major ways hyperglycemia affects the production of neurotransmitters is through hypometabolism of glucose which results in lower flux of key neurotransmitters derived from glucose. Interestingly, while the total pool of glutamate was decreased with T1DM, there were no changes in GABA or glutamine, suggesting the utilization of alternative pathways for the generation of glutamate, such as glutamine or fatty acids. Furthermore, we report in Chapter 3 that the changes in peripheral blood glucose levels are driven through

glutamate-dependent GABA signaling, but we have not observed an increase in GABA with metabolomics approaches. One way to reconcile that difference is the fact that in Chapter 3 we focused on GABA as a signaling molecule and have reported hyperglycemia's effect on electrical activity of the DVC microcircuit, while metabolomics analysis does not discriminate between GABA neurotransmitter packed into vesicle ready to act onto receptor or GABA metabolite within cellular compartments.

5.4 Origin of glucose hypometabolism

Hyperglycemia results in a decrease in GCK expression in the liver [60] and in the brainstem [224,225]. It has been demonstrated that GCK is involved in glucose sensing [161,225–227]. We have shown that hyperglycemia results in increased glucose in all brain regions and increased glycogen levels in the cortex and hippocampus, but not the DVC. Of note, despite the high levels of glucose, *de novo* synthesis of TCA cycle intermediates is decreased. Glucose 6 phosphate was only increased in the cortex and hippocampus, not DVC, suggesting an increase in glucose entry just in the cortex and hippocampus but not in DVC, as the conversion of glucose into glucose 6-phosphate traps the glucose inside of the cell [228]. It could be speculated that once glucose reaches a high concentration in the DVC, GCK downregulation results in the maintenance of a relatively similar total concentration of G6P, suggesting that the origin of glucose hypometabolism in the DVC is possibly due to GCK. Furthermore, we have shown a significant decrease in the expression of PC, a key enzyme in the irreversible carboxylation of pyruvate into oxaloacetate in cortex and CA3, but not in the DVC. Given the reduction in the PC in cortex and CA3 the reduced glucose utilization as seen in isotopic tracing (significant decrease in the enrichment of $^{13}C_6$ across all TCA cycle intermediates) was expected because the PC is gate keeper in replenishing TCA cycle intermediates. However, in the DVC, PC was unchanged and glucose utilization was also

unchanged (no changes in the enrichment of $^{13}C_6$ in glucose), which was expected as well because PC is also a key enzyme in gluconeogenesis.

5.5   Glucose as a signaling molecule

Communication in the brain between different cells, as well as maintenance of overall homeostasis, is achieved by neurotransmitters and hormones. The primary role of glucose is that of an energy source and building block, but another important one is in terms of signaling [229]. Therefore, alterations in glucose concentration not only have a profound effect on metabolism and homeostasis but also on an array of processes where glucose serves as a signaling molecule both in the periphery and the brain. For example, one of the processes in the CNS where glucose plays a key signaling role is in glucose sensing in the brainstem nuclei which has been described in depth [162,176–178]. Glucose sensing is impaired with hyperglycemia. Neuronal activity is dependent on glucose concentration. Therefore, changes in the concentration of glucose, viewed in terms of energy homeostasis, can directly lead to functional changes in neuronal activity.

5.6   Role of glycogen in T1DM

Glycogen levels are very heterogenous among the tissues, with the liver having 100 times more glycogen than the brain [230]. Glycogen plays important role in brain physiology as it is involved in maintaining the proper neuronal function and is involved in learning and memory [231]. Our data shows an increase in the total pool of glycogen and a decrease in glycogen production with $^{13}C_6$ labeled glucose in the cortex and hippocampus but not in the DVC. This suggests that excess glucose that we observed with T1DM in all brain regions analyzed is not converted to a storage form of glycogen in the DVC, further suggesting a similar rate of glycogenesis in the DVC between control and T1DM animals. This is of importance for the metabolism of the DVC as we also shown no

change in pyruvate and lactate, therefore indicating that the excess glucose in the DVC is oxidized through TCA cycle.

5.7 Does T1DM drive brain glucose hypometabolism, or is the glucose hypo-metabolism driving T1DM?

Metabolome changes and metabolic stress precede the appearance of the first islet autoantibodies [42]. We here investigated the 14 days time point of T1DM, but it should be noted and considered if changes in the metabolome drive the pathophysiology of T1DM. As proposed by Schwartz et al., a more complete understanding of glucose homeostasis involves insulin-independent glucose disposal under the control of the CNS [88]. In that perspective, hyperglycemia is a result of the failure of the islet to produce insulin and lower blood glucose via insulin-dependent pathways, as well as altered activity of neuronal nuclei in the hypothalamus and brainstem, resulting in insulin-independent failure to control glucose production. DVC is the last modulation point of the CNS capable of altering hepatic glucose production. It is possible that maybe metabolites like glycogen or glucose-6-phosphate are used as signaling molecules to alter hepatic glucose production. In that case, we have shown that with T1DM in the DVC the levels of glycogen and glucose-6-phosphate are unchanged compared to other brain regions and are potentially the culprit for dysregulation of hepatic glucose. If hyperglycemia alters the CNS's capacity to regulate hepatic glucose production, then the potential therapeutic target should be restoring the glucose hypometabolism phenotype in the brain and thus restoring the CNS's capacity to regulate hepatic glucose production.

5.8 Future directions

While we demonstrated the effect of T1DM on the metabolome of different brain regions and peripheral organs and the impact of altering GABAergic neurons in the DVC

has on the whole blood glucose levels, we were unable to pinpoint whether the changes in altered activity are driven through changes in the metabolome. In addition, while we showed a glucose hypometabolic phenotype in the brain with T1DM, we were unable to pinpoint specific changes in different cell types. Future studies should focus on isolating single cell types through fluoresce-activated cell sorting (FACS) or magnetic separation methodologies after microwave fixation, to define the cell type-specific brain metabolism in healthy and diseased tissue. It would also be of interest to test whether HPFM is compatible with new single-cell technologies such as matrix-assisted laser desorption ionization (MALDI) mass spectrometry imaging [144], single cell RNAseq [145], and spatial proteomics analyses [146,147]. Furthermore, it would be of great importance to understand if hyperglycemia affects differently glutamatergic and GABAergic neurons in the brains, and especially in the DVC. This could be done by utilizing cell culture and MALDI or GCMS. Understanding how each cell type within different brain regions is affected by hyperglycemia would allow for therapeutic approaches that potentially only target a subset of cells which could restore brain metabolic homeostasis.

We choose to look at 14 days after the onset of hyperglycemia, a time point in which we have had only 5% mortality and mice consistently have elevated blood glucose (above 550mg/dL). At this time point, blood-brain barrier permeability is still intact [232], and therefore the effects seen are due to hyperglycemia and not complications with micro or macro vasculature. Given the glucose hypometabolism results, it would be of interest to conduct metabolomic experiments across different time points to identify which of the central carbon pathways is affected first and leads to the downstream effects on glucose hypometabolism.

In the future, the addition of T2DM in both sets of experiments would further our understanding of similarities/differences between T1DM and T2DM, including a cohort of

animals treated with insulin to understand which of the metabolic phenotypes we observed were rescuable. It would be of importance not only to look at insulin delivered peripherally, but to the brain (either intranasally or ICV). Insulin's role as a neurotransmitter has only started to be elucidated [213]. Also, GLUT1 staining was only performed on one isoform, the heavily glycosylated form found in endothelial cells (52kDa), and not the lightly glycosylated form found in astrocytes [233].

5.9   Final Conclusion

The combined findings of this body of work show that modulating the activity of GABAergic neurons in the DVC can alter peripheral glucose levels, and the metabolome of the DVC undergoes reprogramming with T1DM, as seen in a hypometabolism phenotype. Interestingly the utilization of glycogen and glucose in the DVC, as measured by stable isotopic tracing, remained unchanged, suggesting the possible target for intervention and connection to hepatic gluconeogenesis. In addition, these data warrant exploring therapeutic interventions beyond insulin administration for T1DM, specifically focusing on hindering hepatic gluconeogenesis. The experiments outlined in this thesis are novel in several ways. First, there are no other published studies looking at the metabolome of multiple brain regions and peripheral organs to assess the abundance as well as the metabolic flux of major metabolic pathways including glycolysis, tricarboxylic acid cycle, and neurotransmitter synthesis. Secondly, we performed an in-depth characterization of high-power focused microwave fixation, highlighting its compatibility with isotopic tracing. Next, we have shown different metabolic footprints between areas of the brain under the blood-brain barrier (cortex and hippocampus) and areas outside of the blood-brain barrier (DVC).   Lastly, we employed DREADDs approach to selectively change the activity of GABAergic neurons and show that neuronal modulation affects whole-body glucose levels. The exact role that peripheral metabolic changes play in

affecting neuronal activity and how hyperglycemia can drive those has yet to be elucidated.

REFERENCES

[1]   H.C. Towle, Glucose as a regulator of eukaryotic gene transcription, Trends in Endocrinology & Metabolism. 16 (2005) 489–494. https://doi.org/10.1016/J.TEM.2005.10.003.

[2]   T. Fujikawa, J.C. Chuang, I. Sakata, G. Ramadori, R. Coppari, Leptin therapy improves insulin-deficient type 1 diabetes by CNS-dependent mechanisms in mice, Proc Natl Acad Sci U S A. 107 (2010) 17391–17396. https://doi.org/10.1073/pnas.1008025107.

[3]   A. Pocai, S. Obici, G.J. Schwartz, L. Rossetti, A brain-liver circuit regulates glucose homeostasis, Cell Metabolism. 1 (2005) 53–61. https://doi.org/10.1016/j.cmet.2004.11.001.

[4]   S.A. Stanley, L. Kelly, K.N. Latcha, S.F. Schmidt, X. Yu, A.R. Nectow, J. Sauer, J.S. Dordick, J.M. Friedman, Hypothalamus Regulates Feeding and Metabolism, Nature. 531 (2016) 1–20. https://doi.org/10.1038/nature17183.Bidirectional.

[5]   D.M. Breen, B.A. Rasmussen, A. Kokorovic, R. Wang, G.W.C. Cheung, T.K.T. Lam, Jejunal nutrient sensing is required for duodenal-jejunal bypass surgery to rapidly lower glucose concentrations in uncontrolled diabetes, Nature Medicine. 18 (2012) 950–955. https://doi.org/10.1038/nm.2745.

[6]   J.M. Scarlett, J.M. Rojas, M.E. Matsen, K.J. Kaiyala, D. Stefanovski, R.N. Bergman, H.T. Nguyen, M.D. Dorfman, L. Lantier, D.H. Wasserman, Z. Mirzadeh, T.G. Unterman, G.J. Morton, M.W. Schwartz, Central injection of fibroblast growth factor 1 induces sustained remission of diabetic hyperglycemia in rodents, Nature Medicine. 22 (2016) 800–806. https://doi.org/10.1038/nm.4101.

[7]   J.P. German, B.E. Wisse, J.P. Thaler, S. Oh-I, D.A. Sarruf, K. Ogimoto, K.J. Kaiyala, J.D. Fischer, M.E. Matsen, G.J. Taborsky, M.W. Schwartz, G.J. Morton, Leptin deficiency causes insulin resistance induced by uncontrolled diabetes, Diabetes. 59 (2010) 1626–1634. https://doi.org/10.2337/db09-1918.

[8]   D. Sandoval, D. Cota, R.J. Seeley, The Integrative Role of CNS Fuel-Sensing Mechanisms in Energy Balance and Glucose Regulation, The Annual Review of Physiology Is Online At. 70 (2008) 513–548. https://doi.org/10.1146/annurev.physiol.70.120806.095256.

[9]   J.K. Elmquist, R. Coppari, N. Balthasar, M. Ichinose, B.B. Lowell, Identifying hypothalamic pathways controlling food intake, body weight, and glucose homeostasis, Journal of Comparative Neurology. 493 (2005) 63–71. https://doi.org/10.1002/cne.20786.

[10]   S. Obici, B.B. Zhang, G. Karkanias, L. Rossetti, Hypothalamic insulin signaling is required for inhibition of glucose production, Nature Medicine. 8 (2002) 1376–1382. https://doi.org/10.1038/nm1202-798.

[11] T.K.T. Lam, R. Gutierrez-Juarez, A. Pocai, L. Rossetti, Regulation of blood glucose by hypothalamic pyruvate metabolism, Science (1979). 309 (2005) 943–947. https://doi.org/10.1126/science.1112085.

[12] R. Coppari, M. Ichinose, C.E. Lee, A.E. Pullen, C.D. Kenny, R.A. McGovern, V. Tang, S.M. Liu, T. Ludwig, S.C. Chua, B.B. Lowell, J.K. Elmquist, The hypothalamic arcuate nucleus: A key site for mediating leptin's effects on glucose homeostasis and locomotor activity, Cell Metabolism. 1 (2005) 63–72. https://doi.org/10.1016/j.cmet.2004.12.004.

[13] G.J. Morton, R.W. Gelling, K.D. Niswender, C.D. Morrison, C.J. Rhodes, M.W. Schwartz, Leptin regulates insulin sensitivity via phosphatidylinositol-3-OH kinase signaling in mediobasal hypothalamic neurons, Cell Metabolism. 2 (2005) 411–420. https://doi.org/10.1016/j.cmet.2005.10.009.

[14] S.D. Jordan, A.C. Könner, J.C. Brüning, Sensing the fuels: Glucose and lipid signaling in the CNS controlling energy homeostasis, Cellular and Molecular Life Sciences. 67 (2010) 3255–3273. https://doi.org/10.1007/s00018-010-0414-7.

[15] J. Wean, B.N. Smith, FGF19 in the hindbrain lowers blood glucose and alters excitability of vagal motor neurons in hyperglycemic mice, Annals of Medicine. 0 (2021) 1–14. http://dx.doi.org/10.1080/07853890.2020.1840620.

[16] H. Koepsell, Glucose transporters in brain in health and disease, Pflugers Archiv European Journal of Physiology. 472 (2020) 1299–1343. https://doi.org/10.1007/s00424-020-02441-x.

[17] R. Duelli, W. Kuschinsky, Brain glucose transporters: Relationship to local energy demand, News in Physiological Sciences. 16 (2001) 71–76. https://doi.org/10.1152/physiologyonline.2001.16.2.71.

[18] M. Tang, U.R. Monani, Glut1 deficiency syndrome: New and emerging insights into a prototypical brain energy failure disorder, Neuroscience Insights. 16 (2021). https://doi.org/10.1177/26331055211011507.

[19] A.D. Cherrington, Banting Lecture 1997 Control of Glucose Uptake and Release by the Liver In Vi v o, 1198 DIABETES. 48 (1999). http://diabetesjournals.org/diabetes/article-pdf/48/5/1198/364681/10331429.pdf (accessed July 12, 2022).

[20] P. Mergenthaler, U. Lindauer, G.A. Dienel, A. Meisel, Sugar for the brain: the role of glucose in physiological and pathological brain function, Trends Neurosci. 36 (2013) 587. https://doi.org/10.1016/J.TINS.2013.07.001.

[21] S.G. Patching, Glucose Transporters at the Blood-Brain Barrier: Function, Regulation and Gateways for Drug Delivery, Molecular Neurobiology 2016 54:2. 54 (2016) 1046–1077. https://doi.org/10.1007/S12035-015-9672-6.

[22] B. Thorens, GLUT2 in pancreatic and extra-pancreatic gluco-detection (review), Mol Membr Biol. 18 (2001) 265–273. https://doi.org/10.1080/09687680110100995.

[23] M. Arluison, M. Quignon, B. Thorens, C. Leloup, L. Penicaud, Immunocytochemical localization of the glucose transporter 2 (GLUT2) in the adult rat brain. II. Electron microscopic study, Journal of Chemical Neuroanatomy. 28 (2004) 137–146. https://doi.org/10.1016/j.jchemneu.2004.06.002.

[24] M. Arluison, M. Quignon, P. Nguyen, B. Thorens, C. Leloup, L. Penicaud, Distribution and anatomical localization of the glucose transporter 2 (GLUT2) in the adult rat brain—an immunohistochemical study, Journal of Chemical Neuroanatomy. 28 (2004) 117–136. https://doi.org/10.1016/J.JCHEMNEU.2004.05.009.

[25] C. Leloup, M. Arluison, N. Lepetit, N. Cartier, P. Marfaing-Jallat, P. Ferré, L. Pénicaud, Glucose transporter 2 (GLUT 2): expression in specific brain nuclei, Brain Research. 638 (1994) 221–226. https://doi.org/10.1016/0006-8993(94)90653-X.

[26] T. Dakic, T. Jevdjovic, I. Lakic, S.F. Djurasevic, J. Djordjevic, P. Vujovic, Food For Thought: Short-Term Fasting Upregulates Glucose Transporters in Neurons and Endothelial Cells, But Not in Astrocytes, Neurochemical Research. 44 (2019) 388–399. https://doi.org/10.1007/S11064-018-2685-6/FIGURES/7.

[27] C. Ngarmukos, E.L. Baur, A.K. Kumagai, Co-localization of GLUT1 and GLUT4 in the blood-brain barrier of the rat ventromedial hypothalamus, Brain Res. 900 (2001) 1–8. https://doi.org/10.1016/S0006-8993(01)02184-9.

[28] G.A. Dienel, Brain glucose metabolism: Integration of energetics with function, Physiological Reviews. 99 (2019) 949–1045. https://doi.org/10.1152/PHYSREV.00062.2017/ASSET/IMAGES/LARGE/Z9J0011928950009.JPEG.

[29] M.C. Petersen, D.F. Vatner, G.I. Shulman, Regulation of hepatic glucose metabolism in health and disease, Nature Reviews Endocrinology. 13 (2017) 572–587. https://doi.org/10.1038/NRENDO.2017.80.

[30] F. Rajas, A. Gautier-Stein, G. Mithieux, Glucose-6 Phosphate, a Central Hub for Liver Carbohydrate Metabolism, Metabolites. 9 (2019). https://doi.org/10.3390/METABO9120282.

[31] D.A. Bender, TRICARBOXYLIC ACID CYCLE, Encyclopedia of Food Sciences and Nutrition. (2003) 5851–5856. https://doi.org/10.1016/B0-12-227055-X/01363-8.

[32] H. Morrison, Pyruvate carboxylase, Enzyme Active Sites and Their Reaction Mechanisms. (2021) 179–186. https://doi.org/10.1016/B978-0-12-821067-3.00030-1.

[33] G. Lazzarino, A.M. Amorini, S. Signoretti, G. Musumeci, G. Lazzarino, G. Caruso, F.S. Pastore, V. di Pietro, B. Tavazzi, A. Belli, Pyruvate Dehydrogenase and Tricarboxylic Acid Cycle Enzymes Are Sensitive Targets of Traumatic Brain Injury Induced Metabolic Derangement, International Journal of Molecular Sciences. 20 (2019) 5774. https://doi.org/10.3390/IJMS20225774.

[34] R.P. Shank, G.S. Bennett, S.O. Freytag, G.L.M. Campbell, Pyruvate carboxylase: an astrocyte-specific enzyme implicated in the replenishment of amino acid neurotransmitter pools, Brain Research. 329 (1985) 364–367. https://doi.org/10.1016/0006-8993(85)90552-9.

[35] A.C.H. Yu, J. Drejer, L. Hertz, A. Schousboe, Pyruvate carboxylase activity in primary cultures of astrocytes and neurons, J Neurochem. 41 (1983) 1484–1487. https://doi.org/10.1111/J.1471-4159.1983.TB00849.X.

[36] M. Cesar, B. Hamprecht, Immunocytochemical examination of neural rat and mouse primary cultures using monoclonal antibodies raised against pyruvate carboxylase, J Neurochem. 64 (1995) 2312–2318. https://doi.org/10.1046/J.1471-4159.1995.64052312.X.

[37] B. Hassel, A. Bråthe, Neuronal Pyruvate Carboxylation Supports Formation of Transmitter Glutamate, Journal of Neuroscience. 20 (2000) 1342–1347. https://doi.org/10.1523/JNEUROSCI.20-04-01342.2000.

[38] American Diabetes Association, Classification and Diagnosis of Diabetes, Diabetes Care. 38 (2015) S8–S16. https://doi.org/10.2337/DC15-S005.

[39] A. Katsarou, S. Gudbjörnsdottir, A. Rawshani, D. Dabelea, E. Bonifacio, B.J. Anderson, L.M. Jacobsen, D.A. Schatz, A. Lernmark, Type 1 diabetes mellitus, Nature Reviews Disease Primers. 3 (2017) 1–18. https://doi.org/10.1038/nrdp.2017.16.

[40] R. Barnett, Type 1 diabetes, The Lancet. 391 (2018) 195. https://doi.org/10.1016/S0140-6736(18)30024-2.

[41] International Diabetes Federation, Worldwide toll of diabetes, IDF Diabetes Atlas. (2019). https://www.diabetesatlas.org/en/sections/worldwide-toll-of-diabetes.html (accessed February 20, 2021).

[42] M. Oresic, Metabolomics in the studies of islet autoimmunity and type 1 diabetes, Review of Diabetic Studies. 9 (2012) 236–247. https://doi.org/10.1900/RDS.2012.9.236.

[43] M. Karamanou, Milestones in the history of diabetes mellitus: The main contributors, World Journal of Diabetes. 7 (2016) 1. https://doi.org/10.4239/wjd.v7.i1.1.

[44] J. van der Greef, A.K. Smilde, Symbiosis of chemometrics and metabolomics: Past, present, and future, Journal of Chemometrics. 19 (2005) 376–386. https://doi.org/10.1002/cem.941.

[45] Diabetes Tests & Diagnosis | NIDDK, (n.d.). https://www.niddk.nih.gov/health-information/diabetes/overview/tests-diagnosis (accessed July 11, 2022).

[46] M.C. Moore, K.C. Coate, J.J. Winnick, Z. An, A.D. Cherrington, Thematic Review Series: Nutrient Control of Metabolism and Cell Signaling Regulation of Hepatic Glucose Uptake and Storage In Vivo, Adv. Nutr. (2012) 286–294. https://doi.org/10.3945/an.112.002089.

[47] M.J. Pagliassotti, L.C. Holste, M.C. Moore, D.W. Neal, A.D. Cherrington, Portal Signal and Liver Glucose Uptake Comparison of the Time Courses of Insulin and the Portal Signal on Hepatic Glucose and Glycogen Metabolism in the Conscious Dog, J. Clin. Invest. 97 (1996) 81–91.

[48] S.R. Myers, O.P. Mcguinness, D.W. Neal, A.D. Cherrington, Intraportal Glucose Delivery Alters the Relationship Between Net Hepatic Glucose Uptake and the Insulin Concentration, (n.d.).

[49] A. Vella, P. Shah, R. Basu, A. Basu, M. Camilleri, W.F. Schwenk, R.A. Rizza, Effect of enteral vs. parenteral glucose delivery on initial splanchnic glucose uptake in nondiabetic humans, Am J Physiol Endocrinol Metab. 283 (2002) 259–266. https://doi.org/10.1152/ajpendo.00178.2001.-To.

[50] J.-H. Hwang, G. Perseghin, D.L. Rothman, G.W. Cline, I. Magnusson, F. Petersen, G. 1 Shulman, Impaired Net Hepatic Glycogen Synthesis in Insulin-dependent Diabetic Subjects during Mixed Meal Ingestion A 13C Nuclear Magnetic Resonance Spectroscopy Study, J. Clin. Invest. 95 (1995) 783–787.

[51] M. Krssak, A. Brehm, E. Bernroider, C. Anderwald, P. Nowotny, C. Dalla Man, C. Cobelli, G.W. Cline, G.I. Shulman, W. Waldhä Usl, M. Roden, Alterations in Postprandial Hepatic Glycogen Metabolism in Type 2 Diabetes, Diabetes Association. 3048 DIABETES. 53 (2004). http://diabetesjournals.org/diabetes/article-pdf/53/12/3048/375599/zdb01204003048.pdf (accessed July 12, 2022).

[52] A. Basu, R. Basu, P. Shah, A. Vella, C.M. Johnson, K. Sreekumaran Nair, M.D. Jensen, W.F. Schwenk, R.A. Rizza, Effects of Type 2 Diabetes on the Ability of Insulin and Glucose to Regulate Splanchnic and Muscle Glucose Metabolism Evidence for a Defect in Hepatic Glucokinase Activity, 272 DIABETES. 49 (2000). http://diabetesjournals.org/diabetes/article-pdf/49/2/272/338016/10868944.pdf (accessed July 12, 2022).

[53] M.G. Bischof, M. Krssak, M. Krebs, E. Bernroider, H. Stingl, W. Waldhäusl, M. Roden, Effects of Short-Term Improvement of Insulin Treatment and Glycemia on Hepatic Glycogen Metabolism in Type 1 Diabetes, 392 DIABETES. 50 (2001). http://diabetesjournals.org/diabetes/article-pdf/50/2/392/646751/0500392.pdf (accessed July 12, 2022).

[54] J. Girard, Glucagon, a key factor in the pathophysiology of type 2 diabetes, (2017). https://doi.org/10.1016/j.biochi.2017.10.004.

[55] M. Hatting, C.D.J. Tavares, K. Sharabi, A.K. Rines, P. Puigserver, Insulin regulation of gluconeogenesis, Ann N Y Acad Sci. 1411 (2018) 21–35. https://doi.org/10.1111/nyas.13435.

[56] K. Falk Petersen, T.B. Price, R. Bergeron, Regulation of Net Hepatic Glycogenolysis and Gluconeogenesis during Exercise: Impact of Type 1 Diabetes, (2004). https://doi.org/10.1210/jc.2004-0408.

[57]   Y. Lee, M.Y. Wang, X.Q. Du, M.J. Charron, R.H. Unger, Glucagon Receptor Knockout Prevents Insulin-Deficient Type 1 Diabetes in Mice, Diabetes. 60 (2011) 391–397. https://doi.org/10.2337/DB10-0426.

[58]   L. Agius, M. Peak, Binding and translocation of glucokinase in hepatocytes, Biochem Soc Trans. 25 (1997) 145–150. https://doi.org/10.1042/BST0250145.

[59]   L. Agius, The physiological role of glucokinase binding and translocation in hepatocytes, Adv Enzyme Regul. 38 (1998) 303–331. https://doi.org/10.1016/S0065-2571(97)00001-0.

[60]   R.A. Haeusler, S. Camastra, B. Astiarraga, M. Nannipieri, M. Anselmino, E. Ferrannini, Decreased expression of hepatic glucokinase in type 2 diabetes, Molecular Metabolism. 4 (2015) 222. https://doi.org/10.1016/J.MOLMET.2014.12.007.

[61]   N. Bidemi Abdulrazaq, M.M. Cho, N.N. Win, R. Zaman, M.T. Rahman, Beneficial effects of ginger (Zingiber officinale) on carbohydrate metabolism in streptozotocin-induced diabetic rats, (n.d.). https://doi.org/10.1017/S0007114511006635.

[62]   P. Kishore, I. Gabriely, M.-H. Cui, J. di Vito, S. Gajavelli, J.-H. Hwang, H. Shamoon, Role of Hepatic Glycogen Breakdown in Defective Counterregulation of Hypoglycemia in Intensively Treated Type 1 Diabetes, (2006). http://diabetesjournals.org/diabetes/article-pdf/55/3/659/651233/zdb00306000659.pdf (accessed July 12, 2022).

[63]   D.C. Henly, J.W. Phillips, M.N. Berry, Suppression of Glycolysis Is Associated with an Increase in Glucose Cycling in Hepatocytes from Diabetic Rats*, THE JOURNAL OF BIOLOGICAL CHEMISTRY. 271 (1996) 11268–11271.

[64]   M. Chen, H. Zheng, M. Xu, L. Zhao, Q. Zhang, J. Song, Z. Zhao, S. Lu, Q. Weng, X. Wu, W. Yang, X. Fan, H. Gao, J. Ji, Changes in hepatic metabolic profile during the evolution of STZ-induced diabetic rats via an 1 H NMR-based metabonomic investigation, Bioscience Reports. (2019). https://doi.org/10.1042/BSR20181379.

[65]   L.S. Chow, R.C. Albright, M.L. Bigelow, G. Toffolo, C. Cobelli, K. Sreekumaran Nair, K.S. Nair, Mechanism of insulin's anabolic effect on muscle: measurements of muscle protein synthesis and breakdown using aminoacyl-tRNA and other surrogate measures, Am J Physiol Endocrinol Metab. 291 (2006) 729–736. https://doi.org/10.1152/ajpendo.00003.2006.-Despite.

[66]   K. Sreekumaran Nair, G.C. Ford, K. Ekberg, E. Femqvist-Forbes, J. Wahren, Protein Dynamics in Whole Body and in Splanchnic and Leg Tissues in Type I Diabetic Patients Key words: type I diabetes * protein synthesis * protein breakdown * splanch-Iic * muscle Introduction Patients with type I diabetes (IDDM)' typically were cachectic, J. Clin. Invest. 95 (1995) 2926–2937.

[67]   P. Zabielski, I.R. Lanza, S. Gopala, C.J.H. Heppelmann, H.R. Bergen, S. Dasari, K.S. Nair, Altered Skeletal Muscle Mitochondrial Proteome As the Basis of

Disruption of Mitochondrial Function in Diabetic Mice, Diabetes. 65 (2016) 561–573. https://doi.org/10.2337/DB15-0823.

[68]   A. Vaag, O. Hother-Nielsen, P. Skott, P. Andersen, E.A. Richter, H. Beck-Nielsen, Effect of acute hyperglycemia on glucose metabolism in skeletal muscles in IDDM patients, Diabetes. 41 (1992) 174–182. https://doi.org/10.2337/DIAB.41.2.174.

[69]   B. Feng, C. Banner, S.R. Max, Effect of diabetes on glutamine synthetase expression in rat skeletal muscles, American Journal of Physiology - Endocrinology and Metabolism. 258 (1990). https://doi.org/10.1152/ajpendo.1990.258.5.e762.

[70]   T. Dutta, H. Seng Chai, L.E. Ward, A. Ghosh, X.-M.T. Persson, G. Charles Ford, Y.C. Kudva, Z. Sun, Y.W. Asmann, J.-P.A. Kocher, K. Sreekumaran Nair, Concordance of Changes in Metabolic Pathways Based on Plasma Metabolomics and Skeletal Muscle Transcriptomics in Type 1 Diabetes, Diabetes. 61 (2012) 1004–1016. https://doi.org/10.2337/db11-0874.

[71]   G.A. Dienel, Brain glucose metabolism: integration of energetics with function, Physiol Rev. 99 (2019) 949–1045.

[72]   A.M.A. Brands, G.J. Biessels, E.H.F. de Haan, L.J. Kappelle, R.P.C. Kessels, The Effects of Type 1 Diabetes on Cognitive Performance A meta-analysis, 2005. http://care. (accessed February 20, 2021).

[73]   C. Tonoli, E. Heyman, B. Roelands, N. Pattyn, L. Buyse, M.F. Piacentini, S. Berthoin, R. Meeusen, Type 1 diabetes-associated cognitive decline: A meta-analysis and update of the current literature, Journal of Diabetes. 6 (2014) 499–513. https://doi.org/10.1111/1753-0407.12193.

[74]   M.J. Marzelli, P.K. Mazaika, N. Barnea-Goraly, T. Hershey, E. Tsalikian, W. Tamborlane, N. Mauras, N.H. White, B. Buckingham, R.W. Beck, K.J. Ruedy, C. Kollman, P. Cheng, A.L. Reiss, Neuroanatomical Correlates of Dysglycemia in Young Children With Type 1 Diabetes, Diabetes. 63 (2014) 343–353. https://doi.org/10.2337/db13-0179.

[75]   A. Gjedde, C. Crone, Blood-brain glucose Transfer: Repression in chronic hyperglycemia, Science (1979). 214 (1981) 456*457.

[76]   A.D. Mooradian, A.M. Morin, Brain uptake of glucose in diabetes mellitus: The role of glucose transporters, American Journal of the Medical Sciences. 301 (1991) 173–177. https://doi.org/10.1097/00000441-199103000-00004.

[77]   E.M. Cornford, S. Hyman, M.E. Cornford, M. Clare-Salzler, Down-regulation of blood-brain glucose transport in the hyperglycemic nonobese diabetic mouse, Neurochemical Research. 20 (1995) 869–873. https://doi.org/10.1007/BF00969700.

[78]   W.M. Pardridge, D. Triguero, C.R. Farrell, Downregulation of Blood-Brain Barrier Glucose Transporter in Experimental Diabetes, 39 (1990) 1039.

[79]   J. Dai, G.F.J.M. Vrensen, R.O. Schlingemann, Blood-brain barrier integrity is unaltered in human brain cortex with diabetes mellitus, Brain Res. 954 (2002) 311–316. https://doi.org/10.1016/S0006-8993(02)03294-8.

[80]   S.R. Ennis, A. Lorris Berz, Sucrose Permeability of the Blood-Retinal and Blood-Brain Barriers Effects of Diabetes, Hypertonicity, and Iodate, Investigative Ophthalmology & Visual Science. (1986).

[81]   W. Feldberg, D. Pyke, W.A. Stubbs, Hyperglycaemia: Imitating Claude Bernard's Piqûre with drugs, Journal of the Autonomic Nervous System. 14 (1985) 213–228. https://doi.org/10.1016/0165-1838(85)90111-0.

[82]   K.M. Alonge, D.A. D'Alessio, M.W. Schwartz, Brain control of blood glucose levels: implications for the pathogenesis of type 2 diabetes, Diabetologia. 64 (2021) 5–14. https://doi.org/10.1007/s00125-020-05293-3.

[83]   J.E. Gerich, A. Mitrakou, D. Kelley, L. Mandarino, N. Nurjhan, J. Reilly, T. Jenssen, T. Veneman, A. Consoli, Contribution of impaired muscle glucose clearance to reduced postabsorptive systemic glucose clearance in NIDDM, Diabetes. 39 (1990) 211–216. https://doi.org/10.2337/DIAB.39.2.211.

[84]   R.G. Firth, P.M. Bell, H.M. Marsh, I. Hansen, R.A. Rizza, Postprandial hyperglycemia in patients with noninsulin-dependent diabetes mellitus. Role of hepatic and extrahepatic tissues., The Journal of Clinical Investigation. 77 (1986) 1525–1532. https://doi.org/10.1172/JCI112467.

[85]   D.A. D'Alessio, T.J. Kieffer, G.J. Taborsky, P.J. Havel, Activation of the Parasympathetic Nervous System Is Necessary for Normal Meal-Induced Insulin Secretion in Rhesus Macaques, The Journal of Clinical Endocrinology & Metabolism. 86 (2001) 1253–1259. https://doi.org/10.1210/JCEM.86.3.7367.

[86]   H.J. Grill, Distributed Neural Control of Energy Balance: Contributions from Hindbrain and Hypothalamus, Obesity. 14 (2006) 216S-221S. https://doi.org/10.1038/OBY.2006.312.

[87]   J.M. Scarlett, M.W. Schwartz, Gut-brain mechanisms controlling glucose homeostasis, F1000Prime Rep. 7 (2015). https://doi.org/10.12703/P7-12.

[88]   M.W. Schwartz, R.J. Seeley, M.H. Tschöp, S.C. Woods, G.J. Morton, M.G. Myers, D. D'Alessio, Cooperation between brain and islet in glucose homeostasis and diabetes, Nature. 503 (2013) 59–66. https://doi.org/10.1038/nature12709.

[89]   M.W. Schwartz, S.C. Woods, D. Porte, R.J. Seeley, D.G. Baskin, Central nervous system control of food intake, Nature. 404 (2000) 661–671. https://doi.org/10.1038/35007534.

[90]   J.D. Deem, K. Muta, J.M. Scarlett, G.J. Morton, M.W. Schwartz, How Should We Think About the Role of the Brain in Glucose Homeostasis and Diabetes?, Diabetes. 66 (2017) 1758–1765. https://doi.org/10.2337/DBI16-0067.

[91]   S. Pitra, B.N. Smith, Musings on the wanderer: What's new in our understanding of vago-vagal reflexes? VI. Central vagal circuits that control glucose metabolism,

American Journal of Physiology - Gastrointestinal and Liver Physiology. 320 (2021) G175–G182. https://doi.org/10.1152/AJPGI.00368.2020.

[92] M. Carey, E. Lontchi-Yimagou, W. Mitchell, S. Reda, K. Zhang, S. Kehlenbrink, S. Koppaka, S.R. Maginley, S. Aleksic, S. Bhansali, D.M. Huffman, M. Hawkins, Central KATP Channels Modulate Glucose Effectiveness in Humans and Rodents, Diabetes. 69 (2020) 1140–1148. https://doi.org/10.2337/DB19-1256.

[93] J.W. Hill, C.F. Elias, M. Fukuda, K.W. Williams, E.D. Berglund, W.L. Holland, Y.R. Cho, J.C. Chuang, Y. Xu, M. Choi, D. Lauzon, C.E. Lee, R. Coppari, J.A. Richardson, J.M. Zigman, S. Chua, P.E. Scherer, B.B. Lowell, J.C. Brüning, J.K. Elmquist, Direct Insulin and Leptin Action on Pro-opiomelanocortin Neurons Is Required for Normal Glucose Homeostasis and Fertility, Cell Metabolism. 11 (2010) 286–297. https://doi.org/10.1016/j.cmet.2010.03.002.

[94] R.A. Travagli, L. Anselmi, Vagal neurocircuitry and its influence on gastric motility, Nat Rev Gastroenterol Hepatol. 13 (2016) 389–401. https://doi.org/10.1038/nrgastro.2016.76.

[95] R.A. Travagli, G.E. Hermann, K.N. Browning, R.C. Rogers, Brainstem Circuits Regulating Gastric Function, Annual Review of Physiology. 68 (2006) 279–305. https://doi.org/10.1146/annurev.physiol.68.040504.094635.

[96] J.B. Wean, B.N. Smith, Fibroblast Growth Factor 19 Increases the Excitability of Pre-Motor Glutamatergic Dorsal Vagal Complex Neurons From Hyperglycemic Mice, Frontiers in Endocrinology. 12 (2021) 1–12. https://doi.org/10.3389/fendo.2021.765359.

[97] C.R. Boychuk, K.C. Smith, L.E. Peterson, J.A. Boychuk, C.R. Butler, I.D. Derera, J.J. McCarthy, B.N. Smith, A hindbrain inhibitory microcircuit mediates vagally-coordinated glucose regulation, Scientific Reports. 9 (2019) 1–12. https://doi.org/10.1038/s41598-019-39490-x.

[98] E.M. Færgestad, O. Langsrud, M. Høy, K. Hollung, S. Sæbø, K.H. Liland, A. Kohler, L. Gidskehaug, J. Almergren, E. Anderssen, H. Martens, Analysis of Megavariate Data in Functional Genomics, Comprehensive Chemometrics. 4 (2009) 221–278. https://doi.org/10.1016/B978-044452701-1.00011-9.

[99] N. Zamboni, A. Saghatelian, G.J. Patti, Defining the Metabolome: Size, Flux, and Regulation, Molecular Cell. 58 (2015) 699–706. https://doi.org/10.1016/J.MOLCEL.2015.04.021.

[100] K. Burgess, N. Rankin, S. Weidt, Metabolomics, Handbook of Pharmacogenomics and Stratified Medicine. (2014) 181–205. https://doi.org/10.1016/B978-0-12-386882-4.00010-4.

[101] K.M. Sas, A. Karnovsky, G. Michailidis, S. Pennathur, Metabolomics and Diabetes: Analytical and Computational Approaches, Diabetes. 64 (2015) 718. https://doi.org/10.2337/DB14-0509.

[102] J.R. Bain, Targeted Metabolomics Finds Its Mark in Diabetes Research, Diabetes. 62 (2013). https://doi.org/10.2337/db12-1189.

[103] J.R. Bain, R.D. Stevens, B.R. Wenner, O. Ilkayeva, D.M. Muoio, C.B. Newgard, Metabolomics Applied to Diabetes Research: Moving From Information to Knowledge, Diabetes. 58 (2009) 2429–2443. https://doi.org/10.2337/DB09-0580.

[104] L.A. Filla, J.L. Edwards, Metabolomics in diabetic complications, 1090 | Mol. BioSyst. 12 (2016) 1090. https://doi.org/10.1039/c6mb00014b.

[105] A. Mediani, F. Abas, M. Maulidiani, A. Abu Bakar Sajak, A. Khatib, C.P. Tan, I.S. Ismail, K. Shaari, A. Ismail, N.H. Lajis, Metabolomic analysis and biochemical changes in the urine and serum of streptozotocin-induced normal- and obese-diabetic rats, Journal of Physiology and Biochemistry. 74 (2018) 403–416. https://doi.org/10.1007/S13105-018-0631-3.

[106] H.C. Williams, M.A. Piron, G.K. Nation, A.E. Walsh, L.E.A. Young, R.C. Sun, L.A. Johnson, Oral gavage delivery of stable isotope tracer for in vivo metabolomics, Metabolites. 10 (2020) 501.

[107] T.J. Wang, M.G. Larson, R.S. Vasan, S. Cheng, E.P. Rhee, E. McCabe, G.D. Lewis, C.S. Fox, P.F. Jacques, C. Fernandez, C.J. O'Donnell, S.A. Carr, V.K. Mootha, J.C. Florez, A. Souza, O. Melander, C.B. Clish, R.E. Gerszten, Metabolite Profiles and the Risk of Developing Diabetes, Nat Med. 17 (2011) 448. https://doi.org/10.1038/NM.2307.

[108] U. Sauer, Metabolic networks in motion: 13C-based flux analysis, Molecular Systems Biology. 2 (2006) 62. https://doi.org/10.1038/MSB4100109.

[109] J.M. Buescher, M.R. Antoniewicz, L.G. Boros, S.C. Burgess, H. Brunengraber, C.B. Clish, R.J. DeBerardinis, O. Feron, C. Frezza, B. Ghesquiere, E. Gottlieb, K. Hiller, R.G. Jones, J.J. Kamphorst, R.G. Kibbey, A.C. Kimmelman, J.W. Locasale, S.Y. Lunt, O.D.K. Maddocks, C. Malloy, C.M. Metallo, E.J. Meuillet, J. Munger, K. Nöh, J.D. Rabinowitz, M. Ralser, U. Sauer, G. Stephanopoulos, J. St-Pierre, D.A. Tennant, C. Wittmann, M.G. vander Heiden, A. Vazquez, K. Vousden, J.D. Young, N. Zamboni, S.M. Fendt, A roadmap for interpreting 13C metabolite labeling patterns from cells, Current Opinion in Biotechnology. 34 (2015) 189–201. https://doi.org/10.1016/j.copbio.2015.02.003.

[110] C. Jang, L. Chen, J.D. Rabinowitz, Metabolomics and Isotope Tracing, Cell. 173 (2018) 822–837. https://doi.org/10.1016/j.cell.2018.03.055.

[111] M. Grima-Reyes, A. Martinez-Turtos, I. Abramovich, E. Gottlieb, J. Chiche, J.E. Ricci, Physiological impact of in vivo stable isotope tracing on cancer metabolism, Molecular Metabolism. 53 (2021) 101294. https://doi.org/10.1016/j.molmet.2021.101294.

[112] I.Y. Kim, S.H. Suh, I.K. Lee, R.R. Wolfe, Applications of stable, nonradioactive isotope tracers in in vivo human metabolic research, Experimental and Molecular Medicine. 48 (2016). https://doi.org/10.1038/emm.2015.97.

[113] C. Choi, S.K. Ganji, R.J. DeBerardinis, K.J. Hatanpaa, D. Rakheja, Z. Kovacs, X.-L. Yang, T. Mashimo, J.M. Raisanen, I. Marin-Valencia, 2-hydroxyglutarate

detection by magnetic resonance spectroscopy in IDH-mutated patients with gliomas, Nat Med. 18 (2012) 624–629.

[114] E.A. Maher, I. Marin-Valencia, R.M. Bachoo, T. Mashimo, J. Raisanen, K.J. Hatanpaa, A. Jindal, F.M. Jeffrey, C. Choi, C. Madden, Metabolism of [U-13C] glucose in human brain tumors in vivo, NMR Biomed. 25 (2012) 1234–1244.

[115] M.E. Merritt, C. Harrison, C. Storey, F.M. Jeffrey, A.D. Sherry, C.R. Malloy, Hyperpolarized 13C allows a direct measure of flux through a single enzyme-catalyzed step by NMR, Proceedings of the National Academy of Sciences. 104 (2007) 19773–19777.

[116] M.K. Brewer, A. Uittenbogaard, G.L. Austin, D.M. Segvich, A. DePaoli-Roach, P.J. Roach, J.J. McCarthy, Z.R. Simmons, J.A. Brandon, Z. Zhou, Targeting pathogenic Lafora bodies in Lafora disease using an antibody-enzyme fusion, Cell Metabolism. 30 (2019) 689-705. e6.

[117] J. Duran, A. Hervera, K.H. Markussen, O. Varea, I. López-Soldado, R.C. Sun, J.A. del Río, M.S. Gentry, J.J. Guinovart, Astrocytic glycogen accumulation drives the pathophysiology of neurodegeneration in Lafora disease, Brain. 144 (2021) 2349–2360.

[118] R.C. Sun, L.E.A. Young, R.C. Bruntz, K.H. Markussen, Z. Zhou, L.R. Conroy, T.R. Hawkinson, H.A. Clarke, A.E. Stanback, J.K.A. Macedo, Brain glycogen serves as a critical glucosamine cache required for protein glycosylation, Cell Metabolism. 33 (2021) 1404-1417. e9.

[119] R.L. Friede, W.H. van Houten, Relations between post-mortem alterations and glycolytic metabolism in the brain, Experimental Neurology. 4 (1961) 197–204.

[120] A.J. Rauckhorst, N. Borcherding, D.J. Pape, A.S. Kraus, A. Diego, Mouse tissue harvest-induced hypoxia rapidly alters the in vivo metabolome , between-genotype metabolite level differences , and 13 C-tracing enrichments, (2022) 1–32.

[121] A.A. Shestov, X. Liu, Z. Ser, A.A. Cluntun, Y.P. Hung, L. Huang, D. Kim, A. Le, G. Yellen, J.G. Albeck, Quantitative determinants of aerobic glycolysis identify flux through the enzyme GAPDH as a limiting step, Elife. 3 (2014) e03342.

[122] N. Slavov, B.A. Budnik, D. Schwab, E.M. Airoldi, A. van Oudenaarden, Constant growth rate can be supported by decreasing energy flux and increasing aerobic glycolysis, Cell Rep. 7 (2014) 705–714.

[123] R.K. Suarez, J.F. Staples, J.R.B. Lighton, T.G. West, Relationships between enzymatic flux capacities and metabolic flux rates: nonequilibrium reactions in muscle glycolysis, Proceedings of the National Academy of Sciences. 94 (1997) 7065–7069.

[124] T.J. French, A.W. Goode, M.C. Sugden, Ischaemia and tissue pyruvate dehydrogenase activities in the rat: a comparison of the effects of cervical dislocation and pentobarbital anaesthesia, Biochemistry International. 13 (1986) 843–852.

[125] T. Zalewska, K. Domanska-Janik, Energy utilization and changes in some intermediates of glucose metabolism in normal and hypoxic rat brain after decapitation, Resuscitation. 7 (1979) 199–206.

[126] K.A. Overmyer, C. Thonusin, N.R. Qi, C.F. Burant, C.R. Evans, Impact of anesthesia and euthanasia on metabolomics of mammalian tissues: studies in a C57BL/6J mouse model, PLoS One. 10 (2015) e0117232.

[127] M. DiNuzzo, A.B. Walls, G. Öz, E.R. Seaquist, H.S. Waagepetersen, L.K. Bak, M. Nedergaard, A. Schousboe, State-dependent changes in brain glycogen metabolism, Brain Glycogen Metabolism. (2019) 269–309.

[128] J.P. O'Callaghan, K. Sriram, Focused microwave irradiation of the brain preserves in vivo protein phosphorylation: comparison with other methods of sacrifice and analysis of multiple phosphoproteins, J Neurosci Methods. 135 (2004) 159–168.

[129] N.J. English, J.M.D. MacElroy, Molecular dynamics simulations of microwave heating of water, J Chem Phys. 118 (2003) 1589–1592.

[130] C.P. Mayers, Histological fixation by microwave heating, Journal of Clinical Pathology. 23 (1970) 273.

[131] G.R. Login, Microwave fixation versus formalin fixation of surgical and autopsy tissue, The American Journal of Medical Technology. 44 (1978) 435–437.

[132] D.A. Andres, L.E.A. Young, S. Veeranki, T.R. Hawkinson, B.M. Levitan, D. He, C. Wang, J. Satin, R.C. Sun, Improved workflow for mass spectrometry-based metabolomics analysis of the heart, Journal of Biological Chemistry. 295 (2020) 2676–2686. https://doi.org/10.1074/jbc.RA119.011081.

[133] H.C. Williams, M.A. Piron, G.K. Nation, A.E. Walsh, L.E.A. Young, R.C. Sun, L.A. Johnson, Oral Gavage Delivery of Stable Isotope Tracer for In Vivo Metabolomics, Metabolites. 10 (2020) 1–18. https://doi.org/10.3390/METABO10120501.

[134] L.E.A. Young, C.O. Brizzee, J.K.A. Macedo, R.D. Murphy, C.J. Contreras, A.A. DePaoli-Roach, P.J. Roach, M.S. Gentry, R.C. Sun, Accurate and sensitive quantitation of glucose and glucose phosphates derived from storage carbohydrates by mass spectrometry, Carbohydrate Polymers. 230 (2020) 115651. https://doi.org/10.1016/j.carbpol.2019.115651.

[135] K. Johnston, P. Pachnis, A. Tasdogan, B. Faubert, L.G. Zacharias, H.S. Vu, L. Rodgers-Augustyniak, A. Johnson, F. Huang, S. Ricciardo, Isotope tracing reveals glycolysis and oxidative metabolism in childhood tumors of multiple histologies, Med. 2 (2021) 395-410. e4.

[136] A.K. Kaushik, R.J. DeBerardinis, Applications of metabolomics to study cancer metabolism, Biochimica et Biophysica Acta (BBA)-Reviews on Cancer. 1870 (2018) 2–14.

[137] S. Cunnane, S. Nugent, M. Roy, A. Courchesne-Loyer, E. Croteau, S. Tremblay, A. Castellano, F. Pifferi, C. Bocti, N. Paquet, Brain fuel metabolism, aging, and Alzheimer's disease, Nutrition. 27 (2011) 3–20.

[138] M. Suzanne, M. Tong, Brain metabolic dysfunction at the core of Alzheimer's disease, Biochem Pharmacol. 88 (2014) 548–559.

[139] L.F. McNair, R. Kornfelt, A.B. Walls, J. v Andersen, B.I. Aldana, J.D. Nissen, A. Schousboe, H.S. Waagepetersen, Metabolic characterization of acutely isolated hippocampal and cerebral cortical slices using [U-13C] glucose and [1, 2-13C] acetate as substrates, Neurochemical Research. 42 (2017) 810–826.

[140] D.C. Lee, H.A. Sohn, Z.-Y. Park, S. Oh, Y.K. Kang, K. Lee, M. Kang, Y.J. Jang, S.-J. Yang, Y.K. Hong, A lactate-induced response to hypoxia, Cell. 161 (2015) 595–609.

[141] S. Ganapathy-Kanniappan, J.-F.H. Geschwind, Tumor glycolysis as a target for cancer therapy: progress and prospects, Mol Cancer. 12 (2013) 1–11.

[142] K. Lee, J. Kim, J. Seo, T. Kim, J. Im, I. Baek, K. Kim, J. Lee, P. Han, Behavioral stress accelerates plaque pathogenesis in the brain of Tg2576 mice via generation of metabolic oxidative stress, J Neurochem. 108 (2009) 165–175.

[143] V. Bonhomme, P. Boveroux, P. Hans, J.F. Brichant, A. Vanhaudenhuyse, M. Boly, S. Laureys, Influence of anesthesia on cerebral blood flow, cerebral metabolic rate, and brain functional connectivity, Current Opinion in Anesthesiology. 24 (2011) 474–479.

[144] T.R. Hawkinson, L.E.A. Young, L.R. Conroy, H.A. Clarke, M.S. Gentry, R.C. Sun, In Situ Spatial Glycomic Imaging of Mouse and Human Alzheimerżs Disease Brains, Alzheimer's & Dementia. In Press (2021). https://doi.org/10.1002/alz.12523.

[145] M. Ximerakis, S.L. Lipnick, B.T. Innes, S.K. Simmons, X. Adiconis, D. Dionne, B.A. Mayweather, L. Nguyen, Z. Niziolek, C. Ozek, Single-cell transcriptomic profiling of the aging mouse brain, Nat Neurosci. 22 (2019) 1696–1708.

[146] S. Jiang, C.N. Chan, X. Rovira-Clavé, H. Chen, Y. Bai, B. Zhu, E. McCaffrey, N.F. Greenwald, C. Liu, G.L. Barlow, Combined protein and nucleic acid imaging reveals virus-dependent B cell and macrophage immunosuppression of tissue microenvironments, Immunity. (2022).

[147] L. Keren, M. Bosse, S. Thompson, T. Risom, K. Vijayaragavan, E. McCaffrey, D. Marquez, R. Angoshtari, N.F. Greenwald, H. Fienberg, MIBI-TOF: A multiplexed imaging platform relates cellular phenotypes and tissue structure, Sci Adv. 5 (2019) eaax5851.

[148] T.K.T. Lam, A. Pocai, R. Gutierrez-Juarez, S. Obici, J. Bryan, L. Aguilar-Bryan, G.J. Schwartz, L. Rossetti, Hypothalamic sensing of circulating fatty acids is required for glucose homeostasis, Nature Medicine. 11 (2005) 320–327. https://doi.org/10.1038/nm1201.

[149] J.P. German, J.P. Thaler, B.E. Wisse, S. Oh-I, D.A. Sarruf, M.E. Matsen, J.D. Fischer, G.J. Taborsky, M.W. Schwartz, G.J. Morton, Leptin activates a novel CNS mechanism for insulin-independent normalization of severe diabetic

hyperglycemia, Endocrinology. 152 (2011) 394–404.
https://doi.org/10.1210/en.2010-0890.

[150] A. Pocal, T.K.T. Lam, R. Gutierrez-Juarez, S. Obici, G.J. Schwartz, J. Bryan, L. Aguilar-Bryan, L. Rossetti, Hypothalamic KATP channels control hepatic glucose production, Nature. 434 (2005) 1026–1031. https://doi.org/10.1038/nature03439.

[151] S. Ritter, T.T. Dinh, Y. Zhang, Localization of hindbrain glucoreceptive sites controlling food intake and blood glucose, Brain Research. 856 (2000) 37–47. https://doi.org/10.1016/S0006-8993(99)02327-6.

[152] W.B. Laughton, T.L. Powley, Localization of efferent function in the dorsal motor nucleus of the vagus, American Journal of Physiology - Regulatory Integrative and Comparative Physiology. 252 (1987). https://doi.org/10.1152/ajpregu.1987.252.1.r13.

[153] J. Rossi, N. Balthasar, D. Olson, M. Scott, E. Berglund, C.E. Lee, M.J. Choi, D. Lauzon, B.B. Lowell, J.K. Elmquist, Melanocortin-4-receptors Expressed by Cholinergic Neurons Regulate Energy Balance and Glucose Homeostasis, Bone. 23 (2012) 1–7. https://doi.org/10.1016/j.cmet.2011.01.010.Melanocortin-4-receptors.

[154] B.M. Filippi, A. Bassiri, M.A. Abraham, F.A. Duca, J.T.Y.Y. Yue, T.K.T. Lam, Insulin signals through the dorsal vagal complex to regulate energy balance, Diabetes. 63 (2014) 892–899. https://doi.org/10.2337/db13-1044.

[155] R.J.W. Li, B. Batchuluun, S.Y. Zhang, M.A. Abraham, B. Wang, Y.M. Lim, J.T.Y. Yue, T.K.T. Lam, Nutrient infusion in the dorsal vagal complex controls hepatic lipid and glucose metabolism in rats, IScience. 24 (2021) 102366. https://doi.org/10.1016/j.isci.2021.102366.

[156] P.M. Gross, K.M. Wall, D.S. Wainman, S.W. Shaver, Subregional topography of capillaries in the dorsal vagal complex of rats: I. Morphometric properties, Journal of Comparative Neurology. 306 (1991) 73–82. https://doi.org/10.1002/cne.903060106.

[157] C.B. Blake, B.N. Smith, cAMP-dependent insulin modulation of synaptic inhibition in neurons of the dorsal motor nucleus of the vagus is altered in diabetic mice, American Journal of Physiology - Regulatory, Integrative and Comparative Physiology. 307 (2014) R711–R720. https://doi.org/10.1152/ajpregu.00138.2014.

[158] C.R. Boychuk, P. Gyarmati, H. Xu, B.N. Smith, Glucose sensing by GABAergic neurons in the mouse nucleus tractus solitarii, J Neuro-Physiol. 114 (2015) 999–1007. https://doi.org/10.1152/jn.00310.2015.-Changes.

[159] M. Ferreira, K.N. Browning, N. Sahibzada, J.G. Verbalis, R.A. Gillis, R. Alberto Travagli, Glucose effects on gastric motility and tone evoked from the rat dorsal vagal complex, Journal of Physiology. 536 (2001) 141–152. https://doi.org/10.1111/j.1469-7793.2001.t01-1-00141.x.

[160] K.W. Williams, A. Zsombok, B.N. Smith, Rapid inhibition of neurons in the dorsal motor nucleus of the vagus by leptin, Endocrinology. 148 (2007) 1868–1881. https://doi.org/10.1210/en.2006-1098.

[161] C.M. Lamy, H. Sanno, G. Labouèbe, A. Picard, C. Magnan, J.Y. Chatton, B. Thorens, Hypoglycemia-activated GLUT2 neurons of the nucleus tractus solitarius stimulate vagal activity and glucagon secretion, Cell Metabolism. 19 (2014) 527–538. https://doi.org/10.1016/j.cmet.2014.02.003.

[162] S. Wan, K.N. Browning, D-Glucose modulates synaptic transmission from the central terminals of vagal afferent fibers, American Journal of Physiology - Gastrointestinal and Liver Physiology. 294 (2008) 757–763. https://doi.org/10.1152/ajpgi.00576.2007.

[163] E.M. Swartz, K.N. Browning, R.A. Travagli, G.M. Holmes, Ghrelin increases vagally mediated gastric activity by central sites of action, Neurogastroenterology and Motility. 26 (2014) 272–282. https://doi.org/10.1111/nmo.12261.

[164] S. Wan, F.H. Coleman, R.A. Travagli, Glucagon-like peptide-1 excites pancreas-projecting preganglionic vagal motoneurons, American Journal of Physiology - Gastrointestinal and Liver Physiology. 292 (2007) 1474–1482. https://doi.org/10.1152/ajpgi.00562.2006.

[165] C.R. Boychuk, B.N. Smith, Glutamatergic drive facilitates synaptic inhibition of dorsal vagal motor neurons after experimentally induced diabetes in mice, Journal of Neurophysiology. 116 (2016) 1498–1506. https://doi.org/10.1152/jn.00325.2016.

[166] C.R. Boychuk, K.C. Smith, B.N. Smith, Functional and molecular plasticity of γ and α1 GABA a receptor subunits in the dorsal motor nucleus of the vagus after experimentally induced diabetes, Journal of Neurophysiology. 118 (2017) 2833–2841. https://doi.org/10.1152/jn.00085.2017.

[167] C.R. Boychuk, K.C. Halmos, B.N. Smith, Diabetes induces GABA receptor plasticity in murine vagal motor neurons, Journal of Neurophysiology. 114 (2015) 698–706. https://doi.org/10.1152/jn.00209.2015.

[168] E.C. Bach, K.C. Halmos, B.N. Smith, Enhanced NMDA receptor-mediated modulation of excitatory neurotransmission in the dorsal vagal complex of streptozotocin-treated, chronically hyperglycemic mice, PLoS ONE. 10 (2015) 1–21. https://doi.org/10.1371/journal.pone.0121022.

[169] A. Zsombok, M.D. Bhaskaran, H. Gao, A. v. Derbenev, B.N. Smith, Functional Plasticity of Central TRPV1 Receptors in Brainstem Dorsal Vagal Complex Circuits of Streptozotocin-Treated Hyperglycemic Mice, Journal of Neuroscience. 31 (2011) 14024–14031. https://doi.org/10.1523/JNEUROSCI.2081-11.2011.

[170] C.B. Blake, B.N. Smith, cAMP-dependent insulin modulation of synaptic inhibition in neurons of the dorsal motor nucleus of the vagus is altered in diabetic mice, American Journal of Physiology - Regulatory Integrative and Comparative Physiology. 307 (2014) R711–R720. https://doi.org/10.1152/ajpregu.00138.2014.

[171] K.N. Browning, S.R. Fortna, A. Hajnal, Roux-en-Y gastric bypass reverses the effects of diet-induced obesity to inhibit the responsiveness of central vagal motoneurones, Journal of Physiology. 591 (2013) 2357–2372. https://doi.org/10.1113/jphysiol.2012.249268.

[172] J.L. Gomez, J. Bonaventura, W. Lesniak, W.B. Mathews, P. Sysa-Shah, L.A. Rodriguez, R.J. Ellis, C.T. Richie, B.K. Harvey, R.F. Dannals, M.G. Pomper, A. Bonci, M. Michaelides, Chemogenetics revealed: DREADD occupancy and activation via converted clozapine, Physiol Behav. 176 (2016) 139–148. https://doi.org/10.1126/science.aan2475.Chemogenetics.

[173] T. Babic, K.N. Browning, R.A. Travagli, Differential organization of excitatory and inhibitory synapses within the rat dorsal vagal complex, American Journal of Physiology - Gastrointestinal and Liver Physiology. 300 (2011) 21–32. https://doi.org/10.1152/ajpgi.00363.2010.

[174] H. Gao, B.N. Smith, Tonic GABAa receptor-mediated inhibition in the rat dorsal motor nucleus of the vagus, Journal of Neurophysiology. 103 (2010) 904–914. https://doi.org/10.1152/jn.00511.2009.

[175] E. Bouairi, H. Kamendi, X. Wang, C. Gorini, D. Mendelowitz, Multiple types of GABAA receptors mediate inhibition in brain stem parasympathetic cardiac neurons in the nucleus ambiguus, Journal of Neurophysiology. 96 (2006) 3266–3272. https://doi.org/10.1152/jn.00590.2006.

[176] K. Yettefti, J.C. Orsini, T. el Ouazzani, T. Himmi, A. Boyer, J. Perrin, Sensitivity of nucleus tractus solitarius neurons to induced moderate hyperglycemia, with special reference to catecholaminergic regions, Journal of the Autonomic Nervous System. 51 (1995) 191–197. https://doi.org/10.1016/0165-1838(94)00130-C.

[177] R.H. Balfour, A.M.K. Hansen, S. Trapp, Neuronal responses to transient hypoglycaemia in the dorsal vagal complex of the rat brainstem, Journal of Physiology. 570 (2006) 469–484. https://doi.org/10.1113/jphysiol.2005.098822.

[178] Y. Mizuno, Y. Oomura, Glucose responding neurons in the nucleus tractus solitarius of the rat: In vitro study, Brain Research. 307 (1984) 109–116. https://doi.org/10.1016/0006-8993(84)90466-9.

[179] S. Wan, K.N. Browning, Glucose increases synaptic transmission from vagal afferent central nerve terminals via modulation of 5-HT3 receptors, American Journal of Physiology - Gastrointestinal and Liver Physiology. 295 (2008) 1050–1057. https://doi.org/10.1152/ajpgi.90288.2008.

[180] B.L. Roberts, M. Zhu, H. Zhao, C. Dillon, S.M. Appleyard, High glucose increases action potential firing of catecholamine neurons in the nucleus of the solitary tract by increasing spontaneous glutamate inputs, American Journal of Physiology - Regulatory Integrative and Comparative Physiology. 313 (2017) R229–R239. https://doi.org/10.1152/ajpregu.00413.2016.

[181] C. NamKoong, W.J. Song, C.Y. Kim, D.H. Chun, S. Shin, J.W. Sohn, H.J. Choi, Chemogenetic manipulation of parasympathetic neurons (DMV) regulates feeding

behavior and energy metabolism, Neuroscience Letters. 712 (2019) 134356. https://doi.org/10.1016/j.neulet.2019.134356.

[182] F. Erbsloh, A. Bernsmeier, H. Hillesheim, The glucose consumption of the brain & its dependence on the liver, Arch Psychiatr Nervenkr Z Gesamte Neurol Psychiatr. 196 (1958) 611–626. https://doi.org/10.1007/BF00344388.

[183] C.M. Díaz-García, G. Yellen, Neurons rely on glucose rather than astrocytic lactate during stimulation, J Neurosci Res. 97 (2019) 883–889.

[184] M. Nimgampalle, H. Chakravarthy, V. Devanathan, Glucose metabolism in the brain: An update, in: Recent Developments in Applied Microbiology and Biochemistry, Elsevier, 2021: pp. 77–88.

[185] R.C. Sun, T.W.-M. Fan, P. Deng, R.M. Higashi, A.N. Lane, A.-T. Le, T.L. Scott, Q. Sun, M.O. Warmoes, Y. Yang, Noninvasive liquid diet delivery of stable isotopes into mouse models for deep metabolic network tracing, Nat Commun. 8 (2017) 1–10.

[186] L.R. Conroy, T.R. Hawkinson, L.E.A. Young, M.S. Gentry, R.C. Sun, Emerging roles of N-linked glycosylation in brain physiology and disorders, Trends in Endocrinology & Metabolism. 32 (2021) 980–993.

[187] A. Telser, H.C. Robinson, A. Dorfman, The biosynthesis of chondroitin sulfate, Archives of Biochemistry and Biophysics. 116 (1966) 458–465.

[188] K. Sugahara, H. Kitagawa, Heparin and heparan sulfate biosynthesis, IUBMB Life. 54 (2002) 163–175.

[189] N.R. Sibson, G.F. Mason, J. Shen, G.W. Cline, A.Z. Herskovits, J.E.M. Wall, K.L. Behar, D.L. Rothman, R.G. Shulman, In vivo13C NMR measurement of neurotransmitter glutamate cycling, anaplerosis and TCA cycle flux in rat brain during [2-13C] glucose infusion, J Neurochem. 76 (2001) 975–989.

[190] J.Y. Jung, M.K. Oh, Isotope labeling pattern study of central carbon metabolites using GC/MS, J Chromatogr B Analyt Technol Biomed Life Sci. 974 (2015) 101–108. https://doi.org/10.1016/J.JCHROMB.2014.10.033.

[191] J.I. MacRae, L. Sheiner, A. Nahid, C. Tonkin, B. Striepen, M.J. McConville, Mitochondrial Metabolism of Glucose and Glutamine Is Required for Intracellular Growth of Toxoplasma gondii, Cell Host & Microbe. 12 (2012) 682–692. https://doi.org/10.1016/J.CHOM.2012.09.013.

[192] T. Kind, G. Wohlgemuth, D.Y. Lee, Y. Lu, M. Palazoglu, S. Shahbaz, O. Fiehn, FiehnLib – mass spectral and retention index libraries for metabolomics based on quadrupole and time-of-flight gas chromatography/mass spectrometry, Anal Chem. 81 (2009) 10038. https://doi.org/10.1021/AC9019522.

[193] O. Fiehn, Metabolomics by Gas Chromatography-Mass Spectrometry: Combined Targeted and Untargeted Profiling, Curr Protoc Mol Biol. 114 (2016). https://doi.org/10.1002/0471142727.MB3004S114.

[194] O. Fiehn, Metabolomics by Gas Chromatography-Mass Spectrometry: the combination of targeted and untargeted profiling, Current Protocols in Molecular Biology / Edited by Frederick M. Ausubel ... [et Al.]. 114 (2016) 30.4.1. https://doi.org/10.1002/0471142727.MB3004S114.

[195] M.J. Dagley, M.J. McConville, DExSI: a new tool for the rapid quantitation of 13C-labelled metabolites detected by GC-MS, Bioinformatics. 34 (2018) 1957–1958. https://doi.org/10.1093/BIOINFORMATICS/BTY025.

[196] L.E.A. Young, C.O. Brizzee, J.K.A. Macedo, R.D. Murphy, C.J. Contreras, A.A. DePaoli-Roach, P.J. Roach, M.S. Gentry, R.C. Sun, Accurate and sensitive quantitation of glucose and glucose phosphates derived from storage carbohydrates by mass spectrometry, Carbohydr Polym. 230 (2020) 115651. https://doi.org/10.1016/J.CARBPOL.2019.115651.

[197] P. Heinrich, C. Kohler, L. Ellmann, P. Kuerner, R. Spang, P.J. Oefner, K. Dettmer, Correcting for natural isotope abundance and tracer impurity in MS-, MS/MS- and high-resolution-multiple-tracer-data from stable isotope labeling experiments with IsoCorrectoR, Scientific Reports 2018 8:1. 8 (2018) 1–10. https://doi.org/10.1038/s41598-018-36293-4.

[198] A.M. Bolla, E. Butera, S. Pellegrini, A. Caretto, R. Bonfanti, R.A. Zuppardo, G. Barera, G.M. Cavestro, V. Sordi, E. Bosi, Expression of glucose transporters in duodenal mucosa of patients with type 1 diabetes, Acta Diabetol. 57 (2020) 1367–1373. https://doi.org/10.1007/s00592-020-01558-w.

[199] Y.K. Jiang, K.Y. Xin, H.W. Ge, F.J. Kong, G. Zhao, Upregulation Of Renal GLUT2 And SGLT2 Is Involved In High-Fat Diet-Induced Gestational Diabetes In Mice, Diabetes Metab Syndr Obes. 12 (2019) 2095–2105. https://doi.org/10.2147/DMSO.S221396.

[200] A.A. Wasik, S. Lehtonen, Glucose Transporters in Diabetic Kidney Disease-Friends or Foes?, Front Endocrinol (Lausanne). 9 (2018) 155. https://doi.org/10.3389/fendo.2018.00155.

[201] W.T. Cade, Diabetes-related microvascular and macrovascular diseases in the physical therapy setting, Phys Ther. 88 (2008) 1322–1335. https://doi.org/10.2522/ptj.20080008.

[202] M.E. Lacy, P. Gilsanz, A.J. Karter, C.P. Quesenberry, M.J. Pletcher, R.A. Whitmer, Long-term Glycemic Control and Dementia Risk in Type 1 Diabetes, Diabetes Care. 41 (2018) 2339–2345. https://doi.org/10.2337/DC18-0073.

[203] L.W. van Golen, M.C. Huisman, R.G. Ijzerman, N.J. Hoetjes, L.A. Schwarte, A.A. Lammertsma, M. Diamant, Cerebral blood flow and glucose metabolism measured with positron emission tomography are decreased in human type 1 diabetes, Diabetes. 62 (2013) 2898–2904.

[204] M.G. Bischof, M. Krssak, M. Krebs, E. Bernroider, H. Stingl, W. Waldhausl, M. Roden, Effects of short-term improvement of insulin treatment and glycemia on

hepatic glycogen metabolism in type 1 diabetes, Diabetes. 50 (2001) 392–398. https://doi.org/10.2337/diabetes.50.2.392.

[205] L. Mosconi, W.H. Tsui, K. Herholz, A. Pupi, A. Drzezga, G. Lucignani, E.M. Reiman, V. Holthoff, E. Kalbe, S. Sorbi, Multicenter standardized 18F-FDG PET diagnosis of mild cognitive impairment, Alzheimer's disease, and other dementias, Journal of Nuclear Medicine. 49 (2008) 390–398.

[206] Z. Walker, F. Gandolfo, S. Orini, V. Garibotto, F. Agosta, J. Arbizu, F. Bouwman, A. Drzezga, P. Nestor, M. Boccardi, Clinical utility of FDG PET in Parkinson's disease and atypical parkinsonism associated with dementia, European Journal of Nuclear Medicine and Molecular Imaging. 45 (2018) 1534–1545.

[207] O. Willmann, R. Wennberg, T. May, F.G. Woermann, B. Pohlmann-Eden, The contribution of 18F-FDG PET in preoperative epilepsy surgery evaluation for patients with temporal lobe epilepsy: a meta-analysis, Seizure. 16 (2007) 509–520.

[208] J.M. Pascual, R.L. van Heertum, D. Wang, K. Engelstad, D.C. de Vivo, Imaging the metabolic footprint of Glut1 deficiency on the brain, Annals of Neurology: Official Journal of the American Neurological Association and the Child Neurology Society. 52 (2002) 458–464.

[209] K. Monsorno, A. Buckinx, R.C. Paolicelli, Microglial metabolic flexibility: emerging roles for lactate, Trends in Endocrinology & Metabolism. (2022).

[210] X. Zhou, J. Liang, J. Wang, Z. Fei, G. Qin, D. Zhang, J. Zhou, L. Chen, Up-regulation of astrocyte excitatory amino acid transporter 2 alleviates central sensitization in a rat model of chronic migraine, Journal of Neurochemistry. (2019) 1–20. https://doi.org/10.1111/jnc.14944.

[211] V. Jakkamsetti, I. Marin-Valencia, Q. Ma, L.B. Good, T. Terrill, K. Rajasekaran, K. Pichumani, C. Khemtong, M.A. Hooshyar, C. Sundarrajan, Brain metabolism modulates neuronal excitability in a mouse model of pyruvate dehydrogenase deficiency, Sci Transl Med. 11 (2019) eaan0457.

[212] L. Muccioli, A. Farolfi, F. Pondrelli, G. d'Orsi, R. Michelucci, E. Freri, L. Canafoglia, L. Licchetta, F. Toni, R. Bonfiglioli, FDG-PET assessment and metabolic patterns in Lafora disease, European Journal of Nuclear Medicine and Molecular Imaging. 47 (2020) 1576–1584.

[213] S.M. Gray, R.I. Meijer, E.J. Barrett, Insulin Regulates Brain Function, but How Does It Get There?, Diabetes. 63 (2014) 3992. https://doi.org/10.2337/DB14-0340.

[214] A.J. Lutz, W.M. Pardridge, Insulin therapy normalizes GLUT1 glucose transporter mRNA but not immunoreactive transporter protein in streptozocin-diabetic rats, Metabolism. 42 (1993) 939–944. https://doi.org/10.1016/0026-0495(93)90004-8.

[215] G.A. Badr, J. Tang, F. Ismail-Beigi, T.S. Kern, Diabetes downregulates GLUT1 expression in the retina and its microvessels but not in the cerebral cortex or its

microvessels., Diabetes. 49 (2000) 1016–1021.
https://doi.org/10.2337/DIABETES.49.6.1016.

[216] L.P. Reagan, N. Gorovits, E.K. Hoskin, S.E. Alves, E.B. Katz, C.A. Grillo, G.G. Piroli, B.S. McEwen, M.J. Charron, Localization and regulation of GLUTx1 glucose transporter in the hippocampus of streptozotocin diabetic rats, Proc Natl Acad Sci U S A. 98 (2001) 2820–2825. https://doi.org/10.1073/PNAS.051629798/ASSET/047A8DA2-EF00-424C-A3A7-9F97F740B011/ASSETS/GRAPHIC/PQ0516297006.JPEG.

[217] L.P. Reagan, A.M. Magariños, B.S. McEwen, Neurological changes induced by stress in streptozotocin diabetic rats, Ann N Y Acad Sci. 893 (1999) 126–137. https://doi.org/10.1111/J.1749-6632.1999.TB07822.X.

[218] L. Mounien, N. Marty, D. Tarussio, S. Metref, D. Genoux, F. Preitner, M. Foretz, B. Thorens, Glut2-dependent glucose-sensing controls thermoregulation by enhancing the leptin sensitivity of NPY and POMC neurons, The FASEB Journal. 24 (2010) 1747–1758. https://doi.org/10.1096/fj.09-144923.

[219] B. Thorens, GLUT2, glucose sensing and glucose homeostasis, Diabetologia. 58 (2015) 221–232. https://doi.org/10.1007/s00125-014-3451-1.

[220] E. Stolarczyk, C. Guissard, A. Michau, P.C. Even, A. Grosfeld, P. Serradas, A. Lorsignol, L. Pénicaud, E. Brot-Laroche, A. Leturque, M. le Gall, Detection of extracellular glucose by GLUT2 contributes to hypothalamic control of food intake, American Journal of Physiology - Endocrinology and Metabolism. 298 (2010) 1078–1087. https://doi.org/10.1152/ajpendo.00737.2009.

[221] A. Alnahdi, A. John, H. Raza, Augmentation of Glucotoxicity, Oxidative Stress, Apoptosis and Mitochondrial Dysfunction in HepG2 Cells by Palmitic Acid, Nutrients. 11 (2019). https://doi.org/10.3390/NU11091979.

[222] A. Currais, M. Prior, D. Lo, C. Jolivalt, D. Schubert, P. Maher, Diabetes exacerbates amyloid and neurovascular pathology in aging-accelerated mice, Aging Cell. 11 (2012) 1017–1026. https://doi.org/10.1111/ACEL.12002.

[223] W. Li, E. Huang, S. Gao, Type 1 Diabetes Mellitus and Cognitive Impairments: A Systematic Review, Journal of Alzheimer's Disease. 57 (2017) 29–36. https://doi.org/10.3233/JAD-161250.

[224] K.C. Halmos, P. Gyarmati, H. Xu, S. Maimaiti, G. Jancsó, G. Benedek, B.N. Smith, Molecular and functional changes in glucokinase expression in the brainstem dorsal vagal complex in a murine model of type 1 diabetes, Neuroscience. 306 (2015) 115–122. https://doi.org/10.1016/j.neuroscience.2015.08.023.

[225] A.A. Dunn-Meynell, V.H. Routh, L. Kang, L. Gaspers, B.E. Levin, Glucokinase is the likely mediator of glucosensing in both glucose-excited and glucose-inhibited central neurons, Diabetes. 51 (2002) 2056–2065. https://doi.org/10.2337/DIABETES.51.7.2056.

[226] C.R. Boychuk, P. Gyarmati, H. Xu, B.N. Smith, Glucose sensing by GABAergic neurons in the mouse nucleus tractus solitarii, Journal of Neurophysiology. 114 (2015) 999–1007. https://doi.org/10.1152/jn.00310.2015.

[227] N. Sanders, What Do We Know After 50 Years? Article in Diabetes, (2004). https://doi.org/10.2337/diabetes.53.10.2521.

[228] J.Y. Chou, B.C. Mansfield, D.A. Weinstein, Renal Disease in Type I Glycogen Storage Disease, Genetic Diseases of the Kidney. (2009) 693–708. https://doi.org/10.1016/B978-0-12-449851-8.00041-3.

[229] J. Santo-Domingo, A.N. Galindo, O. Cominetti, U. de Marchi, P. Cutillas, L. Dayon, A. Wiederkehr, Glucose-dependent phosphorylation signaling pathways and crosstalk to mitochondrial respiration in insulin secreting cells, Cell Communication and Signaling. 17 (2019) 1–19. https://doi.org/10.1186/S12964-019-0326-6/FIGURES/6.

[230] S.R. Nelson, D.W. Schulz, J. v. Passonneau, O.H. Lowry, Control of Glycogen Levels in Brain, Journal of Neurochemistry. 15 (1968) 1271–1279. https://doi.org/10.1111/j.1471-4159.1968.tb05904.x.

[231] H.M. Sickmann, H.S. Waagepetersen, Effects of diabetes on brain metabolism – is brain glycogen a significant player?, Metabolic Brain Disease. 30 (2014) 335–343. https://doi.org/10.1007/s11011-014-9546-z.

[232] J.D. Huber, R.L. VanGilder, K.A. Houser, Streptozotocin-induced diabetes progressively increases blood-brain barrier permeability in specific brain regions in rats, Am J Physiol Heart Circ Physiol. 291 (2006). https://doi.org/10.1152/AJPHEART.00489.2006.

[233] S. Morgello, R.R. Uson, E.J. Schwartz, R.S. Haber, The human blood-brain barrier glucose transporter (GLUT1) is a glucose transporter of gray matter astrocytes, Glia. 14 (1995) 43–54. https://doi.org/10.1002/glia.440140107.

VITA

Education

B.A. in Biochemistry ………………………………...……….…..Earlham College, 2011-15

B.A. in Politics……………………………………...…………..Earlham College, 2011-15

Scientific Work Experience

2014-2015   Research Assistant, Department of Biology, Earlham College

2015-2017   Laboratory Technician, Lab of Dr. Kathryn Saatman, University of Kentucky

2018-2019   Laboratory Manager, Lab of Dr. Bret Smith, University of Kentucky

2021   Teaching Assistant, Department of Neuroscience, University of Kentucky

Awards and Honors

2009   Student of the year award, Gimnazija Cakovec, Croatia

2009   United World College international scholarship (Victoria, Canada, $66,000)

2011   Earlham College international scholarship (Richmond, Indiana, $250,000)

April 2014   J. Arthur Funston scholarship, Earlham College

April 2015   Russell M. Lawall in Biomedical Research award, Earlham College

May 2015   College honors and departmental honors, Earlham College, Richmond, IN

Publications

Juras JA*, Pitra MS* and Smith BN, Systemic glucose regulation by an inhibitory brainstem circuit in a mouse model of type 1 diabetes (In Preparation).

Juras JA., Webb MB., Young LEA., Markussen KH., Hawkinson TR., Buoncristiani MD., Bolton KE., Coburn PT., Williams MI., Sun LPY., Sanders WC., Bruntz RC., Conroy LR., Wang C., Gentry MS., Smith BN., & Sun RC. (2022). In Situ Microwave Fixation to Define the Terminal Rodent Brain Metabolome. *BioRxiv*, 2022.08.16.504166.
https://doi.org/10.1101/2022.08.16.504166

Kang Y-J*, Lee S-H*, Boychuk JA*, Butler CR, Juras JA, Cloyd RA, and Smith BN (2022) Adult born dentate granule cell mediated upregulation of feedback inhibition in a mouse model of traumatic brain injury. J Neurosci. 42:7077-7093.

B. Hubbard, *A. Juras,* B. Joseph, H. Vekaria, K. Saatman, and P. Sullivan, "Acute Mitochondrial Dysfunction after Mild Traumatic Brain Injury," J. Neurotrauma, v. 34, p.A-108, 2017.

Littlejohn EL, DeSana AJ, Williams HC, Chapman RT, Joseph B, *Juras JA*, Saatman KE. IGF1-Stimulated Posttraumatic Hippocampal Remodeling Is Not Dependent on mTOR.Front Cell Dev Biol. 2021 May 20,9:663456. doi: 10.3389/fcell.2021.663456. PMID: 34095131, PMCID: PMC8174097.